BioMetals **14:** 271–313, 2001.

Review

Zinc coordination sphere in biochemical zinc sites

David S. Auld
Center for Biochemical and Biophysical Sciences and Medicine and Department of Pathology, Harvard Medical School, Boston, Massachusetts 02115, USA (Fax: 617-566-3137; E-mail: David_Auld@hms.harvard.edu)

Received 15 April 2001; accepted 28 May 2001

Key words: crystal structure, metalloenzyme, NMR, protein sequence, X-ray crystallography, XAFS or X-ray absorption fine structure

Abstract

Zinc is known to be indispensable to growth and development and transmission of the genetic message. It does this through a remarkable mosaic of zinc binding motifs that orchestrate all aspects of metabolism. There are now nearly 200 three dimensional structures for zinc proteins, representing all six classes of enzymes and covering a wide range of phyla and species. These structures provide standards of reference for the identity and nature of zinc ligands in other proteins for which only the primary structure is known. Three primary types of zinc sites are apparent from examination of these structures: *structural, catalytic* and *cocatalytic*. The most common amino acids that supply ligands to these sites are His, Glu, Asp and Cys. In catalytic sites zinc generally forms complexes with water and any three nitrogen, oxygen and sulfur donors with His being the predominant amino acid chosen. Water is always a ligand to such sites. Structural zinc sites have four protein ligands and no bound water molecule. Cys is the preferred ligand in such sites. Cocatalytic sites contain two or three metals in close proximity with two of the metals bridged by a side chain moiety of a single amino acid residue, such as Asp, Glu or His and sometimes a water molecule. Asp and His are the preferred amino acids for these sites. No Cys ligands are found in such sites. The scaffolding of the zinc sites is also important to the function and reactivity of the bound metal. The influence of zinc on quaternary protein structure has led to the identification of a fourth type of zinc binding site, *protein interface*. In this case zinc sites are formed from ligands supplied from amino acid residues residing in the binding surface of two proteins. The resulting zinc site usually has the coordination properties of a catalytic or structural zinc binding site.

Abbreviations: ABC – ATP-binding cassette; AAP – *Aeromonas proteolytica* aminopeptidase; ADA – adenosine deaminase; ADAM – A disintegrin and metalloprotease domain; ADH – alcohol dehydrogenase; ALA – 5-aminolevulinic acid; ALAD – 5-aminolevulinic acid dehydratase; Apo2L or TRAIL – apoptosis-inducing ligand 2; BIR – baculovirus inhibitor of apoptosis repeat; BLAP – bovine lens leucine aminopeptidase; CA – carbonic anhydrase; CAM – γ-carbonic anhydrase; CPD A – carboxypeptidase A; CDA – cytidine deaminase; EDTA – ethylenediaminetetraacetic acid; eNOS or NOS-3 – endothelial nitric oxide synthase; FPP – farnesyl diphosphate; FTase – farnesyl transferase; H_4B – tetrahydrobiopterin; HIV – human immunodeficiency virus; GGPP – geranylgeranyl diphosphate; GSNO – S-nitrosoglutathione; HLA-DR – class II major histocompatibility molecule; huIFN – human interferon; IAP – inhibitor of apoptosis; iNOS or NOS-2 – inducible nitric oxide synthase; Im3 – *E. coli* immunity protein; IUB – International Union of Biochemistry; MEROPS – system for classification of peptidase sequences; MetAP-1 – methionine aminopeptidase-1; MetAP-2 – methionine aminopeptidase-2; MHC – major histocompatibility complex; MMP – matrix metalloproteinase; MPD – 2-methyl-2,4-pentanediol; NAD – nicotinamide adenine dinucleotide; NADH – reduced nicotinamide adenine dinucleotide; NADP – nicotinamide adenine dinucleotide phosphate; NGF – nerve growth factor; nNOS, NOS-1 – neuronal nitric oxide synthase; PAC – perturbed angular correlation of γ-rays; PAP – purple acid phosphatase; PBG – porphobilinogen;

PBGS – porphobilinogen synthase; Peptidase – enzyme acting on peptides; PLBP – periplasmic ligand-binding protein; PKC – protein kinase C; PMI – phosphomannose isomerase; PTS – signal transducing protein; PsaA – pneumococcal surface antigen; Proteinase – enzyme acting on proteins; SEA, B etc – staphylococcal enterotoxins type A, B etc; SPEA, C etc – streptococcal pyrogenic exotoxins type A, C etc; SMEZ – streptococcal mitogenic exotoxin; SOD – superoxide dismutase; TCR – T cell receptor; TL – thermolysin; TRAP – tartrate-resistant acid phosphatases; TNF – tumor necrosis factor; TACE – tumor necrosis factor-α-converting enzyme; TSST – toxic shock syndrome toxin; VanX – dipeptidase of vancomycin-resistant pathogenic *Enterococci*; XAFS – X-ray absorption fine structure.

Introduction

Zinc deficiency studies of microorganisms followed by those in plants and animals established the importance of zinc to growth and development in all forms of life (Vallee & Falchuk 1993). Technical advances in analytical methods that could detect the presence of zinc in minute amounts such as atomic absorption, fluorescence and microwave emission spectroscopy coupled with advances in the methodology for protein isolation and purification led to the establishment of zinc involvement in a wide variety of metabolic processes including carbohydrate, lipid, protein and nucleic acid synthesis and degradation (Vallee & Auld 1992a). Zinc is the only metal to have representatives in all six of the International Union of Biochemistry, IUB, classes of enzymes. The fact that it was demonstrated to be involved in transcription and translation of the genetic message gave new meaning to its known essentiality to life processes.

The molecular details of the participation of zinc in enzyme systems came first through replacing the spectroscopically silent zinc with the chromophoric metal cobalt. These studies in conjunction with kinetic studies of function gave information on the importance of the metal site to protein structure and function. Structural studies obtained by X-ray diffraction, NMR and X-ray absorption fine structure, XAFS, techniques gave detailed information of the metal ligands and the coordination geometry of the metal site and allowed formulation of mechanisms that could be tested by a combined approach using mutagenesis and kinetics (Auld 1997). Finally, the ability to determine primary protein structure through translation of DNA sequences now permits prediction of zinc binding sites and thereby enzyme function without even having an expressed protein (Auld 2001). This in turn heightens the awareness of the participation of zinc in metabolic processes.

The zinc ligands and coordination geometries of about *one and a half* dozen zinc enzymes led to the recognition of three types of zinc binding sites: *catalytic, cocatalytic* and *structural* (Figure 1) (Vallee & Auld 1990b, 1993a). Today there are about *fifteen* dozen zinc sites that have been reported, the great majority of which still fit into the original classification (see below). A new type of zinc binding site, *protein interface*, has also become apparent during the last few years (Auld 2001). In this case zinc binding sites are formed through ligands supplied from amino acid residues residing in the binding surface of two protein molecules.

Catalytic zinc sites

There are today about 7 dozen 3-dimensional structural references of *catalytic* zinc sites encompassing five of the six classes of enzymes (Table 1). The class III hydrolases has by far the greatest number of representatives. A catalytic zinc generally forms complexes with any three nitrogen, oxygen and sulfur donors of His, Glu, Asp and Cys with His being the predominant amino acid chosen. Histidine (usually the Nε2 nitrogen) may be chosen because of its capacity to disperse charge through H-bonding of its non-liganding nitrogen. The overall length of such sites can be as small as 11 amino acids as is observed in the astacin superfamily of zinc proteases and 5-aminolevulinic acid dehydratase (Table 1). The ligands are generally separated by short and long amino acid spacers. Short spacers of one and three are commonly found although spacers of 2, 4, 6 and 7 have also been observed (Table 1). The length of the short spacer is often dictated by the ligand support structure; 3 for an α-helix and 1 for a β-sheet. In the case of the alcohol dehydrogenase family the involvement of H-bonding interactions between residues in the short spacer (for example His47 and/or His51) and the cofactor NADH may have led to the extension of the 'short' spacer to 20 (versus a long spacer of about 106).

Table 1. Catalytic zinc sites[a].

Enzyme	PDB#	L_1	X	L_2	Y	L_3	Z	L_4	L_5	Ref.
				Class I: Oxidoreductases						
Alcohol dehydrogenase family										
Horse EE	8ADH & 3BTO	Cys_L	20	$His_{b\beta}$	106	Cys_L(C)	-	H_2O		(Cho *et al.* 1997; Colonna-Cesari *et al.* 1986; Eklund *et al.* 1981)
Mouse Class II	1E3E	Cys_L	20	$His_{b\beta}$	110	Cys_L(C)	-	H_2O		(Svensson *et al.* 2000)
Cod	1CDO	Cys_L	21	His_L	106	Cys_L	-	H_2O		(Ramaswamy *et al.* 1996)
Human $\beta_1\beta_1$	1HDZ	Cys_L	20	$His_{b\beta}$	106	Cys_L	-	H_2O		(Hurley *et al.* 1991)
Human $\beta_2\beta_2$	1HDY	Cys_L	20	$His_{b\beta}$	106	Cys_L	-	H_2O		(Hurley *et al.* 1994)
Human $\beta_3\beta_3$	1DEH	Cys_L	20	$His_{b\beta}$	106	Cys_L	-	H_2O		(Davis *et al.* 1996)
Human $\chi\chi$	1TEH	Cys_L	20	$His_{b\beta}$	106	$Cys_{2b\alpha}$	-	H_2O	Glu_β	(Yang *et al.* 1997)
Human $\sigma\sigma$	1AGN	Cys_L	20	$His_{b\beta}$	106	Cys_L	-	H_2O		(Xie *et al.* 1997)
Clostridium beijerinckii	1KEV	Cys_L	21	His_L	90	Asp_L(C)	-	H_2O	Glu_β	(Korkhin *et al.* 1998)
Thermoanaerobacter brockii	1YKF	Cys_L	21	$His_{b\beta}$	90	Asp_L	-	H_2O		(Korkhin *et al.* 1998)
				Class II: Transferases						
Rat farnesyl transferase	1FT1	Asp	1	Cys	62	His_α(C)	-	H_2O		(Park *et al.* 1997)
Rat Rab geranylgeranyltransferase	1DCE	$Asp_{b\alpha}$	1	Cys_α	49	His_α(C)	-	H_2O		(Zhang *et al.* 2000)
				Class III: Hydrolases						
Carboxypeptidase (CPD) family										
Bovine A	3CPA, 1CPX	His	2	$Glu_{2b\alpha}$	123	His_β(C)	-	H_2O		(Bukrinsky *et al.* 1998; Quiocho & Lipscomb 1971)
Bovine B	1CPB	His	2	Glu	123	His	-	H_2O		(Schmid & Herriott 1976)
Rat A_2		His	2	Glu	123	His	-	H_2O		(Faming *et al.* 1991)
Human A_2	1DTD	His	2	$Glu_{2b\alpha}$	124	His_β	-	H_2O		(Reverter *et al.* 2000)
Avian D	1QMU	His	2	$Glu_{2b\alpha}$	103	His_β	-	H_2O		(Gomis-Ruth *et al.* 1999)
Thermoactinomyces vulgaris T	1OBR	His	2	$Glu_{2b\alpha}$	131	His_β	-	H_2O		(Teplyakov *et al.* 1992)
Porcine PCPD A	1PCA	His	2	$Glu_{2b\alpha}$	123	His_β	-	H_2O		(Guasch *et al.* 1992)
Bovine PCPD A	1PYT	His	2	$Glu_{2b\alpha}$	123	His_β	-	H_2O		(Gomis-Ruth *et al.* 1995)
Porcine PCPD B	1NSA	His	2	$Glu_{2b\alpha}$	123	His_β	-	H_2O		(Coll *et al.* 1991)
Human PCPD A_2	1AYE	His	2	Glu	123	His_β	-	H_2O		(Garcia-Saez *et al.* 1997)

Table 1. Continued.

Enzyme	PDB#	L_1	X	L_2	Y	L_3	Z	L_4	L_5	Ref.
Thermolysin family										
Bacillus thermoproteolyticus	1LND	His_α	3	His_α	19	Glu_α(C)	-	H_2O		(Matthews *et al.* 1974)
Bacillus cereus	1ESP	His_α	3	His_α	19	Glu_α	-	H_2O		(Pauptit *et al.* 1988)
Pseudomonas aeruginosa	1EZM	His_α	3	His_α	19	Glu_α	-	H_2O		(Thayer *et al.* 1991)
Staphylococcus aureus	1BQB	His_α	3	His_α	19	Glu_α	-	H_2O		(Banbula *et al.* 1998)
Human leukotriene A_4 hydrolase	1HS6	His_α	3	His_α	18	Glu_α(C)	-	H_2O		(Thunnissen *et al.* 2001)
Human neutral endoprotease (Neprilysin)	1DMT	His_α	3	His_α	58	Glu_α(C)	-	H_2O		(Oefner *et al.* 2000)
Leishmania major surface proteinase	1LML	His_α	3	His_α	65	Glu_β(C)	-	H_2O		(Schlagenhauf *et al.* 1998)
Clostridium botulinum neurotoxin A	3BTA	His_α	3	His_α	34	Glu_L (C)	-	H_2O		(Lacy & Stevens 1999; Lacy *et al.* 1998)
Clostridium botulinum neurotoxin B	1EPW	His_α	3	His_α	33	Glu_α(C)	-	H_2O		(Swaminathan & Eswaramoorthy 2000)
Streptomyces albus G DD-CPD	1LBU	His	6	Asp_β	35	His_β (C)	-	H_2O		(Ghuysen 1988)
VanX D-Ala-D-Ala carboxypeptidase		His_α	6	Asp_β	60	His_β (C)	-	H_2O		(Bussiere *et al.* 1998)
Mouse Sonic Hedgehog	1VHH	His_α	6	Asp_β	34	His_β(C)	-	H_2O		(Hall *et al.* 1995)
Astacin superfamily	1AST	His_α	3	His_α	5	$His_{a\beta}$(C)	-	H_2O	Tyr	(Bode *et al.* 1992)
Serratia family										
Pseudomonas aeruginosa alkaline protease	1KAP	His_α	3	His_α	5	His(C)	-	H_2O	Tyr	(Baumann *et al.* 1993; Miyatake *et al.* 1995)
Serratia marcescens metalloprotease	1SAT	His_α	3	His_α	5	His	-	H_2O	Tyr	(Baumann *et al.* 1995)
Serratia sp. E-15 metalloprotease	1SRP	His_α	3	His_α	5	His	-	H_2O	Tyr	(Hamada *et al.* 1996)
Snake venom protease family										
Crotalus adamanteus or Adamalysin II	1IAG	His_α	3	His_α	5	His(C)	-	H_2O		(Gomis-Ruth *et al.* 1993a; Gomis-Ruth *et al.* 1994)
Trimeresurus flavoviridis H_2-Proteinase		His_α	3	His_α	5	His	-	H_2O		(Kumasaka *et al.* 1996)
Agkistrodon acutus, Acutolysin A	1BSW	His_α	3	His_α	5	His	-	H_2O		(Gong *et al.* 1998)
Agkistrodon acutus, Acutolysin C	1QUA	His_α	3	His_α	5	His	-	H_2O		(Zhu *et al.* 1999)
Human TNF-α-converting enzyme (TACE)	1BKC	His_α	3	His_α	5	His	-	H_2O		(Maskos *et al.* 1998)
Matrix metalloproteinase family										
Human fibroblast collagenase (MMP-1)	1CGL	His_α	3	His_α	5	His(C)	-	H_2O		(Lovejoy *et al.* 1994a)
Human fibroblast collagenase (MMP-1)	1AYK	His_α	3	His_α	5	His	-	H_2O		(Moy *et al.* 1999; Moy *et al.* 1998) NMR

Table 1. Continued.

Enzyme	PDB#	L_1	X	L_2	Y	L_3	Z	L_4	L_5	Ref.
Human matrilysin (MMP-7)	1MMP	His_{α}	3	His_{α}	5	His	-	H_2O		(Browner *et al.* 1995)
Human neutrophil collagenase (MMP-8)	1KBC	His_{α}	3	His_{α}	5	$His_{a\beta}$	-	H_2O		(Betz *et al.* 1997; Bode *et al.* 1994)
Human stromelysin-1 (MMP-3)	2SRT, 1BM6	His_{α}	3	His_{α}	5	His	-	H_2O		(Gooley *et al.* 1994; Li *et al.* 1998; Van Doren *et al.* 1995) NMR
Human stromelysin-1 (MMP-3)	1B3D	His_{α}	3	His_{α}	5	His	-	H_2O		(Chen *et al.* 1999; Dhanaraj *et al.* 1996)
Human prostromelysin-1 (MMP-3)	1SLM	His_{α}	3	His_{α}	5	His(C)	125	Cys_{β}(N)		(Becker *et al.* 1995)
Human collagenase-3 (MMP-13)	830C	His_{α}	3	His_{α}	5	His	-	H_2O		(Lovejoy *et al.* 1999)
Mouse collagenase-3 (MMP-13)	1CXV	His_{α}	3	His_{α}	5	His	-	H_2O		(Botos *et al.* 1999)
Human progelatinase 72kDa (MMP-2)	1CK7	His_{α}	3	His_{α}	5	His(C)	200	Cys_{β} (N)		(Morgunova *et al.* 1999)
Streptomyces caespitosus endopeptidase	1KUH	His_{α}	3	His_{α}	5	Asp(C)	-	H_2O		(Kurisu *et al.* 1997)
Murine adenosine deaminase	2ADA, 1A4L	His	1	His	196	His_{β}(C)	-	H_2O	Asp_L	(Wang & Quiocho 1998; Wilson *et al.* 1991)
Escherichia coli cytidine deaminase	1CTT	Cys_{α}	2	$Cys_{b\alpha}$	26	$His_{b\alpha}$(N)	-	H_2O		(Betts *et al.* 1994; Xiang *et al.* 1995)
Escherichia coli peptide deformylase	1BS4	His_{α}	3	His_{α}	41	Cys(N)	-	H_2O		(Becker *et al.* 1998; Chan *et al.* 1997; Meinnel *et al.* 1996)
E. coli colicin E7 (ColE7) DNase	7CEI	$His_{a\alpha}$	3	His_{α}	24	His_{β}(N)	-	H_2O		(Ko *et al.* 1999)
Human GTP cyclohydrolase I	1FB1	Cys_{β}	2	$His_{2b\beta}$	67	$Cys_{a\beta}$(C)	-	H_2O		(Auerbach *et al.* 2000)
S. cerevisiae π-Scei endonuclease	1EF0	Cys_{β}	1	His_{β}	372	Glu_{β} (N)	-	H_2O		(Poland *et al.* 2000)
Bacteriophage T7 lysozyme	1LBA	$Cys_{2b\beta}$	7	His_{β}	104	His_{β}(N)	-	H_2O		(Cheng *et al.* 1994)
β-Lactamase family										
Bacillus cereus	1BMC	$His_{2a\beta}$	1	His	60	His(C)	-	H_2O		(Carfi *et al.* 1998a; Carfi *et al.* 1995; Fabiane *et al.* 1998)
Bacteroides fraglis	1ZNB	His	1	His	60	His(C)	-	H_2O		(Concha *et al.* 1996)
Stenotrophomonas maltophilia	1SML	His	1	His	73	His(C)	-	H_2O		(Ullah *et al.* 1998)
Pseudomonas aeruginosa	1DD6	$His_{2a\beta}$	1	His	59	His (C)	-	H_2O		(Concha *et al.* 2000)
Escherichia coli alkaline phosphatase	1ALK	Asp_{α}	3	His_{α}	80	His(C)	-	H_2O		(Kim & Wyckoff 1991; Stec *et al.* 1998)
Bacillus cereus phospholipase C	1AH7	Glu_{α}	3	His_{α}	13	His_{α}(N)	-	H_2O		(Hough *et al.* 1989)
Penicillium citrinum P1 nuclease	1AK0	$Asp_{a\alpha}$	3	His_{α}	12	His(N)	-	H_2O		(Volbeda *et al.* 1991)
Escherichia coli Endonuclease IV	1QTW	His_{β}	3	$Asp_{b\beta}$	46	His_{α}(N)	-	H_2O		(Hosfield *et al.* 1999)
Hepatitis C virus proteinase	1AIQ, 1JXP	Cys	1	Cys	45	Cys_{β}(C)	-	H_2O		(Love *et al.* 1996; Yan *et al.* 1998)

Table 1. Continued.

Enzyme	PDB#	L_1	X	L_2	Y	L_3	Z	L_4	L_5	Ref.
Hepatitis C virus NS3 proteinase	1BT7	Cys	1	Cys	45	$Cys_{2a\beta}$(C)	-	H_2O		(Barbato *et al.* 1999) NMR
				Class IV: Lyases						
Carbonic anhydrase family										
Homo Sapiens CA I	2CAB	His_β	1	His_β	22	His_β(C)	-	H_2O		(Kannan *et al.* 1975)
Homo Sapiens CA II	1CA2	His_β	1	His_β	22	His_β(C)	-	H_2O		(Liljas *et al.* 1972)
Bovine CA III		His_β	1	His_β	22	His_β(C)	-	H_2O		(Eriksson & Liljas 1993)
Rattus Norvegius CA III	1FLJ	His_β	1	His_β	22	His_β(C)	-	H_2O		(Mallis *et al.* 2000)
Homo Sapiens membrane CA IV	1ZNC	His_β	1	His_β	22	His_β(C)	-	H_2O		(Stams *et al.* 1996)
Murine CA IV	2ZNC	His_β	1	His_β	22	His_β(C)	-	H_2O		(Stams *et al.* 1998)
Murine mitochrondrial CA V	1DMX	His_β	1	His_β	22	His_β(C)	-	H_2O		(Boriack-Sjodin *et al.* 1995)
Neisseria gonorrhoeae CA	1KOP	His_β	1	His_β	16	His_β(C)	-	H_2O		(Huang *et al.* 1998)
Pisum sativum β-CA	1EKJ	Cys_L	2	His_β	59	Cys_β(N)	-	Acetate		(Kimber & Pai 2000)
Porphyridium purpureum β-CA	1DDZ	Cys_L	2	His_β	55	Cys_β(N)	-	$Asp_{a\beta}$		(Mitsuhashi *et al.* 2000)
Methanosarcina thermophila β-CA	1G5C	Cys_L	2	His_β	54	Cys_β(N)	-	H_2O		(Strop *et al.* 2001)
Methanosarcina thermophila γ-CA	1THJ	His_β	4	$His_{\alpha\beta}$	35	His_β(N)	-	H_2O		(Kisker *et al.* 1996) see Table 4
Rat 6-pyruvoyl-tetrahydropterin synthase	1B6Z	His_β	1	His_β	24	His_β(N)	-	H_2O		(Burgisser *et al.* 1995; Ploom *et al.* 1999)
S. cerevisiae 5-aminolaevulinate dehydratase	1AW5,1QVN	Cys_β	1	$Cys_{a\beta}$	7	$Cys_{2b\beta}$(C)	-	H_2O		(Erskine *et al.* 2000; Erskine *et al.* 1997)
E. coli 5-aminolaevulinate dehydratase	1B4E	$Cys_{a\beta}$	1	Cys	7	Cys(C)	-	H_2O		(Erskine *et al.* 1999b)
E. coli fuculose 1-phosphate aldolase	4FUA,1DZU	His_β	1	$His_{\alpha\beta}$	60	$His_{b\beta}$(C)	-	H_2O	Glu_L	(Dreyer & Schulz 1993; Joerger *et al.* 2000)
				Class V: Isomerases						
Candida albicans phosphomannose isomerase	1PMI	Gln_β	1	$His_{a\beta}$	24	Glu_β	146	His_β	H_2O	(Cleasby *et al.* 1996)

[a]The amino acid spacer between ligands L_1 and L_2 is X; that between L_3 and nearest ligand L_1 or L_2 is Y and that between L_3 and L_4 is Z. The symbols N and C indicate that L_3 is located on the amino (N) or the carboxyl (C) side of L_2, respectively. The subscripts α, β, refer to the α-or 3_{10} helix and β-sheet structure which supplies the ligand. The letter subscript L denotes an amino acid sequence of ≤ 5 residues between two structural elements. The subscripts a and b indicate the ligand is either one (or two, 2) residues after or before the secondary structural element.

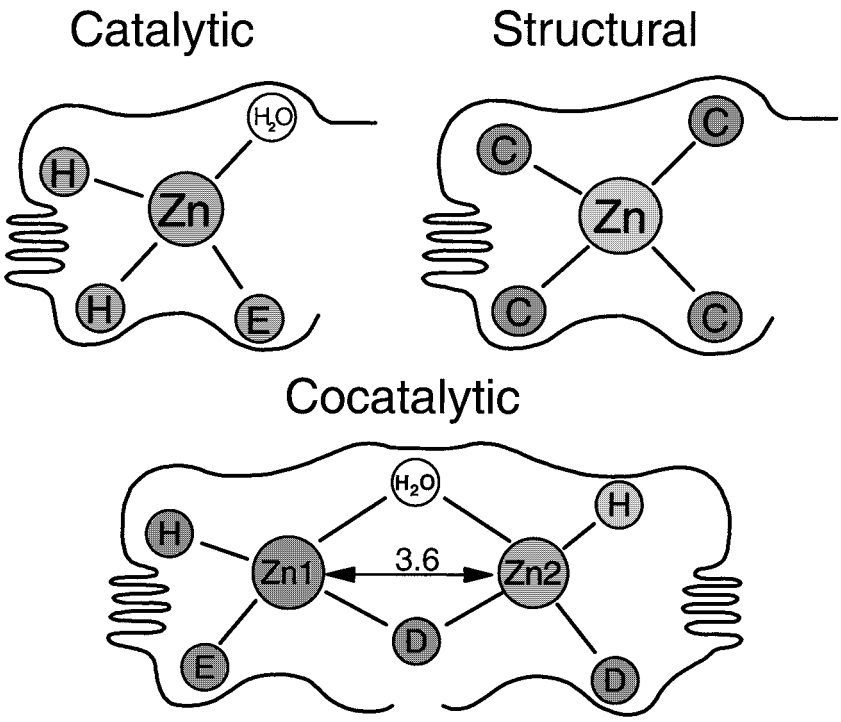

Fig. 1. Zinc binding sites in enzymes: catalytic (thermolysin (Matthews 1988)), structural (alcohol dehydrogenase (Eklund & Branden 1987)), cocatalytic (*Aeromonas proteolytica* aminopeptidase (Chevrier *et al.* 1994)). The letters D, E and H refer to the amino acids, aspartic acid, glutamic acid and histidine, respectively.

The coordination number for such sites is usually 4 or 5 and the geometry in the free state is frequently distorted-tetrahedral or trigonal-bipyramidal. Water is always a ligand to the catalytic zinc. The zinc-bound water is activated for ionization, polarization or displacement by the identity and arrangement of ligands coordinated to zinc (Vallee & Auld 1990a). Ionization of the activated water or its polarization brought about by a base form of an active-site amino acid provides hydroxide ions at neutral pH, and displacement of water or expansion of the coordination sphere results in Lewis acid catalysis by the catalytic zinc atom. The structure of the active site implies that the identity of the three protein ligands, their spacing and secondary interactions with neighboring amino acids in conjunction with the vicinal properties of the active center created by protein folding are all critical for the various mechanisms through which zinc can be involved in catalysis.

This group of zinc sites is too large for this perspective to comment on each individual zinc site. I will therefore generally restrict my comments to some of the larger and more well studied families.

Alcohol dehydrogenase

The dimeric alcohol dehydrogenases (ADH) (EC 1.1.1.1) contain both a catalytic and a structural zinc site (Tables 1 and 2). These zinc enzymes are NAD dependent and catalyze the reversible oxidation of alcohols to aldehydes. Seven human ADH genes have been identified and designated as ADH1 through ADH7 (Jornvall & Hoog 1995). The ADH1 to ADH5 and ADH7 encode 6 subunits of the ADH enzymes that are designated by the Greek letters, α, β, γ, π, χ and σ. The gene product of ADH6 has not been observed. Polymorphism occurs for the ADH2 (β) and ADH3(γ) loci resulting in nine distinct human subunits. These enzymes have also been classified, based on sequence identity and substrate specificity (Jornvall *et al.* 1987), as class I (α, β_1, β_2, β_3, γ_1, γ_2 containing isozymes), class II (π), class III (χ) and class IV (σ) ADHs. Class III ADH is also known as glutathione-dependent formaldehyde dehydrogenase (Yang *et al.* 1997). In addition, a protein that possesses the ability to metabolize S-nitrosoglutathione (GSNO) has been purified from *E. coli*, *S. cerevisiae* and mouse

macrophages and identified as class III (χ) ADH (Liu *et al.* 2001).

The first crystal structure reported for this family of enzymes was for the horse enzyme, denoted EE, and considered to be part of class I ADH (Eklund *et al.* 1974, 1976). The three dimensional structure of several human isozymes as well as those from cod liver and mouse have been reported (Tables 1 and 3). A great deal of the structural and mechanistic studies have been performed on the horse liver enzyme. Each subunit of the dimeric enzyme is divided into a coenzyme binding domain and a catalytic domain that are separated by a cleft containing a deep pocket (Eklund & Branden 1987). Both zinc ions reside in the catalytic domain.

The catalytic zinc is ligated to the sulfurs of Cys46 and Cys174, the Nε2 nitrogen of His67 and a water molecule in a tetrahedral coordination geometry. When the coenzyme binds it triggers a major change in conformation of the enzyme (Eklund 1989). The two coenzyme-binding domains have similar orientations while the two catalytic domains are rotated relative to each other. When NADH is bound the cleft between the catalytic and coenzyme binding domains 'closes' around the coenzyme (Eklund *et al.* 1981). In the absence of the coenzyme the cleft is considered open (Eklund *et al.* 1976). Solvent is accessible to the catalytic zinc and the fourth ligand is water in the open conformation. The conformational changes places the zinc-bound substrate in the proper orientation to the C4 position of the cofactor nicotinamide ring for optimal hydride transfer (Klinman 1981).

The major changes in conformation upon cofactor binding have made it difficult to assign the pK_a values of about 7 and 9 in the pH profiles of coenzyme binding to functional groups in the enzyme (LeBrun & Plapp 1999). Candidates for these groups are the imidazolium of His51, the amino group of Lys228 and the catalytic zinc-bound water. The induction of the closed form by coenzyme permits the displacement of the water by the alcohol or aldehyde substrate and places the zinc substrate complex in a more hydrophobic environment (Eklund & Branden 1987).

The displacement of the zinc-bound water by substrate and role of the zinc as a Lewis acid catalyst has been a generally accepted mechanism although expansion of the coordination sphere to allow both Lewis acid catalysis by zinc and acid/base chemistry for zinc-bound water has been considered. A 1 Å resolution structure of the native zinc and cadmium substituted horse liver enzyme complexed with the cofactor NADH and 2-methyl-2,4-pentanediol (MPD) combined with quantum chemical calculations has given support to the involvement of a metal-bound water in catalysis (Meijers *et al.* 2001). The results suggest that a metal-bound hydroxide is part of the activation process for hydride transfer from the reduced NADH cofactor in the LADH•NADH complex. In the proposed mechanism the zinc-bound water is displaced towards the NADH in order to allow the aldehyde substrate to become the fifth ligand.

Metalloproteases

The carboxypeptidase family of exopeptidases and the thermolysin family of endopeptidases are likely examples of polarization assisted zinc water catalysis. The zinc containing pancreatic exopeptidases carboxypeptidase A & B (CPD A & B) were two of the earliest identified and studied zinc metalloenzymes (Auld, 1998a, 1998b; Aviles & Vendrel 1998). The carboxypeptidases catalyze the degradation of food proteins leading to the formation of amino acids. These enzymes complement the actions of chymotrypsin, pepsin and trypsin by allowing the production of essential amino acids such as Phe, Trp, Lys and Arg (Riordan 1974). The reader is directed to the Handbook of Proteolytic Enzymes for a presentation of evolutionary relationship of carboxypeptidases (Barrett *et al.* 1998) as well as several chapters on individual carboxypeptidases. The human mast cell, E, M, N carboxypeptidases are believed to be involved in immune/inflammatory and hormone processing (Auld 1998a; Vallee & Auld 1990b).

Three dimensional structures are available for several members of the CPD family (Table 1). The catalytic zinc site of CPD A is comprised of His69 (Nδ1), Glu72 (Oε1 and Oε2), His196 (Nδ1) and a water molecule. The first two ligands, separated by a short spacer of two, reside in a seven amino acid loop region between a β-sheet and an α-helix while His196 is the last residue in a β-pleated sheet extending from amino acids 191 to 196 (Rees *et al.* 1983). This site is highly conserved throughout the extended carboxypeptidase family (Vallee & Auld 1990b). There are also several crystalline derived structures of the thermolysin family (Table 1). In this case the amino acid ligands His142 (Nε2) and His146 (Nε2), separated by a short spacer of three, reside in an α-helix extending from amino acid 137 to 152 (Matthews *et al.* 1974). The amino acid residue Glu143, proposed to function as the gen-

eral acid/general base in catalysis, resides within the short spacer (Holland *et al.* 1995; Matthews, 1988). The third ligand, Glu166 (Oε1), is supplied by a second α-helix extending from residue 160 to 180. The fourth ligand is water.

The immediate thermolysin family is composed of several bacterial endoproteases. However comparison of the properties of this zinc site to sequences of other proteins led to the prediction that the mono zinc aminopeptidases would also contain this same type of catalytic zinc site (Vallee & Auld 1990b). In addition these studies led to the prediction that human leukotriene A_4 hydrolase would be a zinc aminopeptidase with a thermolysin type zinc site. Both of these predictions have been confirmed (Haeggstrom *et al.* 1990; Medina *et al.* 1991; Thunnissen *et al.* 2001).

X-ray diffraction studies of the crystalline CPD A•inhibitor complexes (Christianson & Lipscomb 1989; Lipscomb & Strater 1996) in conjunction with spectroscopic studies on inhibitor and substrate binding on the cobalt substituted enzyme (Auld & Vallee 1987) and XAFS studies of the effect of pH and inhibitor bonding on the zinc coordination sphere (Auld 1997) have provided evidence for a mechanism involving the metal-bound water and a general acid/base role for Glu270 in catalysis assisted by Arg127 in the transition state (Auld 1987, 2001; Christianson & Lipscomb 1989; and references therein).

Astacin superfamily

This superfamily began with the identification of *Astacus* protease, or astacin, as a zinc protease in 1988 (Stocker *et al.* 1988). A potential zinc binding site signature existed within astacin, **H**ExxHxxGxx**H**, that was also present in a small number of proteases that would eventually make the four subclasses of this superfamily (Stocker *et al.* 1990) (Table 1). The recognition of the homology of both mouse kidney and human intestine meprin to *Astacus* protease resulted in the naming of the immediate astacin family of zinc proteases (Dumermuth *et al.* 1991). By 1992 the use of this putative zinc signature led to the identification of 33 proteases that defined four major groups of homologous proteins (Auld 1992). This discovery was rapidly followed by the X-ray crystallographic structure of astacin that confirmed the prediction of this new catalytic zinc site (Bode *et al.* 1992). Within two years the structures of a member of each of the astacin subfamilies was determined, i.e., matrix metalloproteinase-1 (Lovejoy *et al.* 1994b), the snake venom protease, adamalysin II (Gomis-Ruth *et al.* 1993a) and the alkaline protease of *Pseudomonas aeruginosa* (Baumann *et al.* 1993). As of Mar. of 2001 the MEROPS data base file lists 441 members of this superfamily (Barrett & Rawlings 2001) and there are 19 reported structures of individual members (Table 1). The human class of snake venom like proteases have been given the name ADAM, which stands for A disintegrin and metalloprotease domain. The tumor necrosis factor-α-converting enzyme or TACE is a member of this sub-group (Maskos *et al.* 1998). The involvement of these proteases in remodeling the extracellular matrix makes them targets of diseases that require these processes such as tumor progression, metastasis, arthritis and heart tissue instability.

The zinc binding site in this superfamily is the smallest site known since all zinc ligands and the presumed catalytic glutamate residue are supplied from an eleven amino acid segment (Table 1). The first two His ligands (Nε2) are part of a long (12 to 15 amino acids) α-helix in all members of this superfamily. This helix is broken by the highly conserved glycine residue residing three residues after the second His. The break in the helix allows the third His (Nε2) to complete the zinc binding site.

The role for the glutamate in catalysis is generally believed to be the same as in the carboxypeptidase A and thermolysin families. However comparison of the structures of matrilysin, thermolysin (TL) and carboxypeptidase A reveals both similarities and differences in their active sites (Auld 1997). A common feature is a catalytic zinc atom that is coordinated by three protein ligands and a nearby ionizable carboxylate group of a Glu residue that is considered to act as a nucleophile or general base. The fourth ligand is water in the active enzyme. However, the type of the ligand and the scaffolding of the zinc site is not the same. The catalytic zinc of matrilysin is made up of three His residues whereas the zinc atom of thermolysin and CPD-A contains 2 His and 1 Glu (Table 1). Furthermore, the secondary interactions of the zinc ligands with adjacent side chain carboxylate groups observed in TL and CPD-A is not observed in matrilysin. Mutagenesis studies of the proposed Glu residue in matrilysin suggest this residue may play a different role in catalysis in the MMPs (Cha & Auld 1997).

β-Lactamases

The majority of β-lactamases utilize an active site serine in the hydrolysis of the β-lactam ring. However there are now new pathogenic bacteria that have a metallo-β-lactamase that contains zinc. Several X-ray structures have recently appeared on this class of zinc enzymes from *Bacillus cereus* (Carfi *et al.* 1995, 1998a; Fabiane *et al.* 1998), *Bacteroides fragilis* (Carfi *et al.* 1998b; Concha *et al.* 1996), *Stenotrophomonas maltophilia* (Ullah *et al.* 1998) and *Pseudomonas aeruginosa* (Concha *et al.* 2000). These structures are similar in the presence of at least one zinc site that has the characteristics of a catalytic zinc site. The first structure of the *B. cereus* enzyme had one zinc coordinated by three histidines 86 (Nε2), 88 (Nδ1) and 149 (Nε2) and a water molecule in a tetrahedral arrangement (Carfi *et al.* 1995). These histidine residues are conserved in all members of this class of enzymes. These crystals were grown at pH 5.6 in 0.1 M $ZnSO_4$ in a citrate, cacodylate buffer. At this pH the binding constant for a second zinc is 29 mM (Baldwin *et al.* 1978). Growing the crystals at pH 7.0 in the presence of 0.5 mM $ZnSO_4$ in Tris buffer yields an enzyme with two zincs bound (Fabiane *et al.* 1998). The second zinc binds to Asp90, Cys168, and His210 and two water molecules in a trigonal bipyramidal coordination geometry. There is considerable variation in the ligand properties of the second zinc site raising questions about its role in catalysis (Auld 2001) (see below, cocatalytic sites).

Carbonic anhydrases

The class IV lyase carbonic anhydrase (CA) is likely the best example of an ionization activated zinc-bound water mechanism. This superfamily of enzymes, involved in the physiology of CO_2 transport, has been assigned to three independent gene families α, β and γ (Hewett-Emmett & Tashian 1996). The α-class contains all mammalian, as well as some CAs from algae and bacteria. Several distinct forms exist in mammals: three cytosolic forms, (CA I, II and III); two membrane-bound forms (CA IV and CA VII); a mitochondrial form (CA V) and a secreted salivary form (CA VI). Crystal structures of five different forms of the α-enzyme class (Table 1) has shown the catalytic zinc is located in a 15 Å deep active center cavity near the middle of the enzyme molecule. One part of the cavity is dominated by hydrophobic residues while another segment has a more hydrophilic nature (Silverman & Lindskog 1988). The catalytic zinc is tetrahedrally coordinated to the Nε2 of His94 and His96 supplied from a β-strand encompassing residues 88 to 108 and a Nδ1 of His119 from a second β-strand extending from 113 to 126 (Liljas *et al.* 1972) and a water molecule. The amino acid ligands and adjacent amino acids are highly conserved throughout this class of CAs.

The β-class has a strikingly different catalytic zinc coordination site (Table 1). This class includes CAs from plants, algae, bacteria and archaea (Hewett-Emmett & Tashian 1996; Smith & Ferry 2000). The higher plant and unicellular green algae use the β-CAs for photosynthetic CO_2 fixation. The crystal structures *Pisum sativum* β-CA (Kimber & Pai 2000), *Porphyridium purpureum* β-CA (Mitsuhashi *et al.* 2000) and *Methanosarcina thermophila* β-CA (Strop *et al.* 2001) have been reported recently. In all cases the catalytic zinc is coordinated by two Cys and a His as was anticipated by XAFS studies of the spinach CA (Bracey *et al.* 1994; Rowlett *et al.* 1994). Two of the ligands, His87 (Nε2) and Cys90, are supplied by a loop region and a β-sheet, respectively and are separated by a short spacer of two (Table 1). The third ligand, Cys32 (*M. thermophila* β-CA numbering), is supplied by a β-sheet from the N-terminal side. The reported structure for the *P. purpureum* β-CA (Mitsuhashi *et al.* 2000) also has an Asp coordinated to the zinc with no bound water molecules. It was therefore proposed that this β-CA and possible the γ-class does not use a zinc hydroxide mechanism in their function (Mitsuhashi *et al.* 2000). However in the other two reported structures the fourth ligand is a solvent molecule (acetate) for *P. sativum* β-CA (Kimber & Pai 2000) and a water molecule for *M. thermophila* β-CA (Strop *et al.* 2001). The potential Asp ligand exists in all three enzymes in a highly conserved loop region C-terminal to the third Cys ligand (CysXAs pSerArg). In the enzymes where the Asp is not a ligand the Arg guanidinium group is hydrogen-bonded to the Asp carboxyl group preventing it from coordinating the zinc (Strop *et al.* 2001). The zinc coordinated water molecule in the *M. thermophila* β-CA has therefore been displaced either by an acetate carboxylate in the *P. sativum* β-CA or the carboxylate of Asp151 in the *P. purpureum* β-CA. Further studies will be needed to determine what is the function of the Asp residue in question. However comparison of the α- and β-CA catalytic zinc sites is of interest in this regard. The positive charge on the zinc in the β-CAs should be re-

duced by the replacement of two His imidazole ligands by Cys sulfur ligands. The ionization of the zinc bound water molecule might therefore need the assistance of a neighboring carboxyl group as is postulated in metalloproteases (Auld 1987, 1997). A role for Asp151 in catalysis rather than zinc binding could be inferred from the results of a mutation of this residue to an Asn in spinach β-CA. The resulting enzyme still binds zinc but retains little CO_2 hydratase activity (Mitsuhashi *et al.* 2000).

The γ-class of CAs has one structural representative from *Methanosarcina thermophila* (Iverson *et al.* 2000; Kisker *et al.* 1996). While it retains three His ligands as in the α-class the spacing characteristics change (Table 1). The resulting trimeric enzyme forms a zinc site from the interface of its subunits (See protein interface and Table 4).

The α-class of enzymes is one of the best studied from the point of mechanism of action. The role of the zinc ligands, its bound water molecule, the 'gatekeeper' residue, Thr199 and orientating residues such as Glu106 and proton shuttle residues such as His64 have been carefully investigated (See reviews by Christianson & Cox 1999; Christianson & Fierke 1996; Coleman 1998; Lindskog & Liljas 1993; Silverman & Lindskog 1988).

Other catalytic zinc sites containing Cys ligands

While the predominant ligand found in these sites is His there are a number of sites that contain from one to three Cys residues. Several catalytic sites now exist where there is one Cys ligand in combination with two His or one His and an Asp or Glu residue (Table 1). In the likely best studied single Cys containing zinc site, the protein prenyltransferases catalyze the formation of a sulfur ether linkage between either the isoprenoid units of farnesyl diphosphate (FPP) or geranylgeranyl diphosphate (GGPP) and the cysteine residues of protein acceptor substrates such as Ras thereby attaching these proteins to the cell membrane (Zhang & Casey 1996). Since a number of human cancers are linked to Ras mutations, inhibition of these enzymes is a potential target for antitumor chemotherapy (Gibbs & Oliff 1997). In both the rat farnesyl transferase (FTase) and the Rab geranylgeranyl transferase the zinc site is found in the β-subunit coordinated to a Cys sulfur and an Asp carboxylate oxygen separated by one amino acid (Park *et al.* 1997; Zhang *et al.* 2000). The Nε2 nitrogen of a His residue and a water molecule complete the tetrahedral zinc site. Spectral kinetic studies on the cobalt substituted FTase (Huang *et al.* 1997) and an x-ray structure of a ternary complex containing a Cys peptide (Strickland *et al.* 1998) indicate that the Cys peptide thiol group displaces the metal-bound water. These results suggest the role of zinc in these enzymes is to activate the cysteine thiol of the protein substrate for nucleophilic attack on the C1 position of the FPP substrate.

The deamination mechanism of *E. coli* cytidine deaminase (CDA) is believed to be similar to that of *E. coli* adenosine deaminase (ADA) (Betts *et al.* 1994; Wang & Quiocho 1998). However the zinc binding site of ADA contains 3 His residues while that of CDA contains two Cys and one His residue (Table 1). Examination of the structures of transition state analogs show that the inhibitor complex is stabilized by a zinc hydroxide and an adjacent carboxyl group of an Asp or Glu residue in the active site. The differences in zinc ligands and tertiary structures of ADA and CDA has led to the proposal that the common features in the transition state stabilization has arisen from convergent evolution (Betts *et al.* 1994). The variation in the zinc binding site nature in this functional class of enzymes is also evident in the *Bacillus subtilis* cytidine deaminase. Sequence alignment has led to the proposal that the tetrameric *B. subtilis* enzyme has three Cys ligands, Cys89, Cys86 and Cys53 coordinated to the catalytic zinc (Carlow *et al.* 1999).

A three Cys ligated catalytic zinc site has been proposed for the 5-aminolevulinic acid dehydratase (ALAD) of *E. coli* (Erskine *et al.* 1999b) and *Saccharomyces cerevisiae* (Erskine *et al.* 1997). All ligands reside in a short amino acid sequence of eleven amino acids with the first two Cys ligands being separated by a spacer of one. ALAD or porphobilinogen synthase (PBGS) catalyzes the condensation of two 5-aminolevulinic acid (ALA) molecules to form the pyrrole porphobilinogen (PBG), one of the initial steps in the biosynthesis of tetrapyrroles. The zinc site lies next to the lysine residue in the active site that is believed to form a Schiff base with 5-aminolevulinic acid (Erskine *et al.* 1999a). The zinc ion is postulated to coordinate the C4 carbonyl of ALA. A water molecule is bound to the zinc in the *E. coli* enzyme (Erskine *et al.* 1999b) on the side of the two active site Lys residues. While the same tetrahedral geometry is found in the *S. cerevisiae* enzyme the fourth site is vacant on the Lys side (Erskine *et al.* 1997).

The biochemistry of this enzyme has received particular attention due an inactivating mutation in the

human enzyme that is responsible for an inherited disease, porphyria (Doss *et al.* 1979) and the marked inhibition by lead ions, 70 fM (Simons 1995). Both lead and mercury have been shown to displace the active site zinc by the use of multiwavelength anomalous diffraction analysis (Erskine *et al.* 2000). The ligands involved in binding the zinc are not conserved in a number of plant species (Jaffe 2000). The three Cys ligands are replaced by either two Asp and an Ala or some combination of Asp and Cys residues. This finding has lead to the postulate that Mg may replace Zn in the plants. However the *Pseudomonas aeruginosa* ALAD (two Asp residues and an Ala) contains neither a Zn or Mg at this site (Frankenberg *et al.* 1999). Other binding sites for both zinc and magnesium have been observed in this class of enzymes (Jaffe 2000).

Another potential three Cys containing zinc site may exist in the NS3 protease from hepatitis C virus. This enzyme has a zinc site on the protein surface composed of Cys97, Cys99, Cys145 and a Zn-bound water molecule (Love *et al.* 1996). The zinc-bound water is further H-bonded to His149 in two of the three monomers in the asymmetrical unit cell. The His imidazole ring isolates the Zn site from solution. NMR studies of the enzyme also suggest a water or hydroxyl group is directly bound to the zinc and that the His imidazole nitrogen may H-bond to this water (Barbato *et al.* 1999; Urbani *et al.* 1998). This type of hydrogen bonding interaction is often seen in catalytic zinc sites but the zinc binding site in NS3 protease is assumed to play a structural role since it is 23 Å removed from the serine proteinase active site (Yan *et al.* 1998). The bound zinc can not be removed by chelators at pH values > 7 and its removal at lower pH values leads to protein unfolding and aggregation of the enzyme (De Francesco *et al.* 1996). However the k_{cat}/K_m value for the His149Ala mutant is decreased by 15,000-fold, suggesting there is some relationship between the coordination geometry of the metal site and catalytic activity (Urbani *et al.* 1998). The processing of the precursor protein NS2-NS3 is cleaved intramolecularly by an autocatalytic action that is chelator and zinc dependent (Pieroni *et al.* 1997). If this zinc site should be involved in the autoprocessing activity it may be more properly classified as a catalytic site.

Function of a fourth protein ligand

A fourth protein ligand has been observed in a few crystal structures of catalytic zinc sites. A highly conserved Cys is found in the zymogen form of the matrix metalloproteinases, MMPs, with no bound water molecule (Becker *et al.* 1995; Morgunova *et al.* 1999) (Table 1). The replacement of the water by the Cys residue was proposed to be cause of the lack of activity of the enzyme (Springman *et al.* 1990; Vallee & Auld 1990b). Upon activation, this metal site is converted into one that contains three protein ligands and a bound water, characteristic of a catalytic zinc site (Table 1). The only other example of a proposed catalytic zinc site lacking a water molecule is the *Porphyridium purpureum* β-carbonic anhydrase (Mitsuhashi *et al.* 2000). However other members of the β-carbonic anhydrases have 3 protein ligands and a solvent molecule bound to the zinc (see section on carbonic anhydrase).

Water is still bound to the site in a number of cases where a fourth protein ligand is found (Table 1). In these cases it appears that one ligand may dissociate from the zinc before or during catalysis. Thus the Oδ2 of the Asp295 carboxylate is 2.3 Å from the zinc in an adenosine deaminase inhibitor complex in which a zinc-activated water (hydroxide) binds to the metal (Wilson & Quiocho 1993). Conversion of this Asp residue to a Glu through mutagenesis results in the displacement of the metal-bound water by the γ-carboxyl group of Glu and inactivation of the enzyme (Sideraki *et al.* 1996). The role of the side chain carboxyl group Asp295 in catalysis is therefore not likely in binding to the zinc but rather in stabilizing the charge of the hydrate intermediate or orienting the zinc bound hydroxide oxygen for addition to the C6 position of adenosine (Wang & Quiocho 1998). The functionally similar zinc enzyme, cytidine deaminase, has a catalytic zinc bound to 3 protein ligands and a water or hydroxide ion (Betts *et al.* 1994) (Table 1).

In *Clostridium beijerinckii* alcohol dehydrogenase a Glu residue adjacent to the second catalytic zinc ligand is also bound to the zinc in the NADP free form of the enzyme (Korkhin *et al.* 1998). However, the distance between the carboxylate oxygen and the zinc increases from 2.35 to 3.94 Å upon binding the coenzyme. In the human $\chi\chi$ alcohol dehydrogenase, ADH, the equivalent residue, Glu68 is observed 2.9 Å and 2.0 Å from the catalytic zinc in the A and B subunits respectively (Yang *et al.* 1997). In other human and horse ADHs the carboxylate oxygens are at least 4.7 Å from the catalytic zinc atom. The binding of the Glu to the zinc in this case may be a reflection of the involvement of Glu68 in the displacement of water in a late step in catalysis as predicted by mole-

cular dynamics calculations (Ryde 1995; Yang *et al.* 1997). This unusual binding of Glu to the metal may also be reflected in the presence of a pH independent band at 562 nm in Co(II) substituted $\chi\chi$ ADH (Maret 1989). Such an absorption band had been assigned to an anion binding in studies of horse EE ADH (Bertini *et al.* 1987; Maret & Zeppezauer 1986). The Glu68-carboxylate coordinated to zinc would be consistent with such a zinc-bound 'anion' species (Yang *et al.* 1997).

In *Escherichia coli* fuculose aldolase, both of the carboxylate oxygens of Glu73 bind to the zinc in the resting state (Dreyer & Schulz 1993). Upon binding of a transition state analog phosphoglycolohydroxamate, Glu73 rotates away providing room for the hydroxamate oxygen to bind to the zinc (Dreyer & Schulz 1996). In astacin, the gram-negative bacterium *Serratia marcescens* proteinase and the alkaline protease from *Pseudomonas aeruginosa* a conserved tyrosine residue following the Met turn in these proteins acts as a fourth protein zinc ligand with phenolic oxygen to Zn distances of 2.54 Å (Gomis-Ruth *et al.* 1993b), 2.75 Å (Baumann 1994; Hamada *et al.* 1996), and 3.01 Å (Miyatake *et al.* 1995) respectively, resulting in a trigonal-bipyramidal coordination sphere in the free enzymes. Binding of a phosphinic peptide inhibitor to astacin increases the distance between the phenolic oxygen and the zinc from 2.5 Å to 5.0 Å (Grams *et al.* 1996). Movement of the tyrosine away from the zinc has also been observed in inhibited forms of the *Serratia* protease (seralysin) (Baumann *et al.* 1995) and in the alkaline protease from *Pseudomonas aeruginosa* (Baumann *et al.* 1993; Miyatake *et al.* 1995).

The zinc binding site in *Candida albicans* phosphomannose isomerase, PMI, contains 4 protein ligands and a water molecule arranged in a distorted trigonal bipyramid (Cleasby *et al.* 1996). All the ligands are on three β-strands in the catalytic domain. Gln111 and His113 (Nε2) are on the same β-strand. The site is unusual for a catalytic zinc site in that one of the ligands is Gln, a residue found in cocatalytic sites but not previously in a catalytic zinc site. Gln111, Glu168 (Oε1), and His285 (Nε2) form the equatorial ligands and His113 and water the axial ligands. The pH dependence of PMI on activity was originally suggested to be due to a His residue on the basis of diethyl pyrocarbonate modification experiments (Cleasby *et al.* 1996). In view of some of the other 4 protein ligand sites the axial ligand His113 or one of the equatorial ligands, His285 or Glu168 may be displaced by the substrate in order to participate in the reversible isomerization of fructose-6-phosphate and mannose 6-phosphate.

In a number of the cases cited above the fourth protein ligand bonding distance is 2.3 to 3 Å which is long for inner sphere oxygen-zinc ligation. Such a distance maybe an indicator for an amino acid that dissociates from the zinc upon substrate binding and plays a role in catalysis.

Structural zinc sites

Structural zinc sites have 4 protein ligands and no bound water molecule. The first zinc enzymes recognized to have a structural zinc site were horse alcohol dehydrogenase (Eklund *et al.* 1974) and the regulatory subunit of aspartate carbamoyltransferase (Honzatko *et al.* 1982). In both cases the zinc is bound to four cysteines in a relatively short linear sequence of 15 to 33 amino acids with the ligands separated by 2, 2 and 7 or 4, 23 and 2 amino acids, respectively. There are today about 41/2 dozen zinc sites with representatives in five of the six IUB enzyme classes (Table 2). The overall length of these sites can vary from 15 to 209 but the majority are in the range of 20 to 40 amino acids. There is at least one short spacer, generally containing two amino acids, in the great majority of these sites. While Cys is still by far the preferred ligand for such sites other ligands are also found. The second most prevalent ligand is His which is usually found in combination with Cys. The presence of His and Cys in the same zinc binding site frequently gets some form of a 'zinc finger' nomenclature. Based on only 'loose' criteria some of the sites listed here are still referred as zinc finger domains even if they do not fit the criteria of having DNA binding properties or of the ligand nature (2His/2Cys), sequence length ($\sim$30 amino acids) and presence of both α-helix and β-sheets in the zinc binding site associated with a classical zinc finger (Vallee *et al.* 1991).

His and Asp/Glu sites

There are only a few examples where Asp and Glu in combination with His residues are found (Table 2). The matrix metalloproteinase class of enzymes contain such a non-Cys structural zinc site. Early metal analyses of the matrix metalloproteinases indicated that these enzymes contained a zinc site in addition to

Table 2. Structural zinc sites[a].

Enzyme	PDB#	L_1	X	L_2	Y	L_3	Z	L_4	Ref.
				Class I: Oxidoreductases					
Alcohol dehydrogenase									
Horse EE	8ADH & 3BTO	Cys	2	$Cys_{b\alpha}$	2	Cys_{α}	7	Cys	(Eklund *et al.* 1981)
Cod	1CDO	Cys	2	$Cys_{b\alpha}$	2	Cys_{α}	7	Cys	(Ramaswamy *et al.* 1996)
Mouse Class II	1E3E	Cys	2	$Cys_{b\alpha}$	2	Cys_{α}	7	Cys	(Svensson *et al.* 2000)
Human $\beta_1\beta_1$	1HDZ	Cys	2	$Cys_{b\alpha}$	2	Cys_{α}	7	Cys	(Hurley *et al.* 1991)
Human $\beta_2\beta_2$	1HDY	Cys	2	$Cys_{b\alpha}$	2	Cys_{α}	7	Cys	(Hurley *et al.* 1994)
Human $\beta_3\beta_3$	1DEH	Cys	2	$Cys_{b\alpha}$	2	Cys_{α}	7	Cys	(Davis *et al.* 1996)
Human $\chi\chi$	1TEH	Cys	2	$Cys_{b\alpha}$	2	Cys_{α}	7	Cys	(Yang *et al.* 1997)
Human $\sigma\sigma$	1AGN	Cys	2	$Cys_{b\alpha}$	2	Cys_{α}	7	Cys	(Xie *et al.* 1997)
Bovine heart cytochrome c oxidase	1OCC	Cys_{β}	1	$Cys_{2a\beta}$	19	Cys_{β}	2	Cys_{L}	(Karlin *et al.* 1998)
				Class II: Transferases					
Aspartate carbamoyltransferase	1AT1	Cys	4	$Cys_{2b\alpha}$	23	Cys_{β}	2	Cys_{L}	(Honzatko *et al.* 1982)
Human Bruton's tyrosine kinase	1BTK	$His_{a\beta}$	10	$Cys_{a\beta}$	0	$Cys_{2a\beta}$	9	$Cys_{b\beta}$	(Hyvonen & Saraste 1997)
Bacillus stearothermophilus adenylate kinase	1ZIP	Cys_{β}	2	Cys_{L}	16	Cys_{β}	2	Cys_{L}	(Berry & Phillips 1998)
Protein kinase family									
Human casein kinase, CK2β	1QF8	Cys_{β}	4	Cys_{L}	22	Cys_{β}	2	$Cys_{2b\beta}$	(Chantalat *et al.* 1999)
Rat C-α Cys-rich domain		Cys	2	Cys	21	His	2	Cys	(Hommel *et al.* 1994) NMR
Rat C-α		His	29	Cys	2	Cys	15	Cys	(Hommel *et al.* 1994)
Rabbit C-α Cys-rich domain		Cys_{β}	2	$Cys_{\alpha\beta}$	21	His_{β}	2	Cys_{α}	(Ichikawa *et al.* 1995) NMR
Rabbit C-α		$His_{b\beta}$	29	Cys_{β}	2	$Cys_{b\beta}$	15	Cys	(Ichikawa *et al.* 1995)
Mouse C-δ activator-binding domain	1PTQ	Cys_{β}	2	$Cys_{2b\beta}$	21	$His_{a\beta}$	2	Cys	(Zhang *et al.* 1995)
Mouse C-δ	1PTQ	$His_{b\beta}$	29	Cys_{β}	2	Cys_{L}	15	Cys	(Zhang *et al.* 1995)
Human Raf-1	1FAQ	Cys_{β}	2	Cys_{L}	17	$His_{a\beta}$	2	Cys	(Mott *et al.* 1996) NMR
Human Raf-1	1FAQ	His	25	Cys_{β}	2	Cys	15	Cys	(Mott *et al.* 1996)
Thermococcus celer RNA polymerase II RPB9	1QYP	Cys_{β}	2	$Cys_{b\beta}$	24	Cys_{β}	2	Cys_{L}	(Wang *et al.* 1998) NMR
Methanobacterium Thermautotrophicum RNA polymerase subunit RPB10	1EF4	Cys	2	Cys	33	Cys_{α}	0	Cys_{α}	(Mackereth *et al.* 2000) NMR
Thermus aquaticus RNA polymerase	1DDQ	$Cys_{a\alpha}$	81	Cys	6	$Cys_{b\alpha}$	2	Cys_{α}	(Zhang *et al.* 1999)
E. coli DNA polymerase III δ' subunit	1A5T	$Cys_{a\alpha}$	8	Cys	2	$Cys_{b\alpha}$	2	Cys_{α}	(Guenther *et al.* 1997)

Table 2. Continued.

Enzyme	PDB#	L_1	X	L_2	Y	L_3	Z	L_4	Ref.
Galactose-1-phosphate uridylyltransferase	1GUP	Cys	2	Cys	59	His	48	$His_{b\beta}$	(Geeganage & Frey 1999; Thoden *et al.* 1997)
Bacillus stearothermophilus DNA primase	1D0Q	$Cys_{2a\beta}$	2	His	17	Cys_{β}	2	Cys_{L}	(Pan & Wigley 2000)
Human O6-Alkylguanine-DNA alkyltransferase	1EH6	Cys	18	Cys_{β}	4	Cys_{β}	55	Cys	(Daniels *et al.* 2000)
				Class III: Hydrolases					
Matrix metalloproteinase family									
Human fibroblast collagenase (MMP-1)	1CGL	His	1	Asp	12	His_{β}	12	His_{β}	(Lovejoy *et al.* 1994a; Moy *et al.* 1998)
Human fibroblast collagenase (MMP-1)	3AYK	His	1	Asp	12	His_{β}	12	His_{β}	(Moy *et al.* 1999; Moy *et al.* 1998) NMR
Human matrilysin (MMP-7)	1MMP	His	1	Asp	12	His_{β}	12	His_{β}	(Browner *et al.* 1995)
Human neutrophil collagenase (MMP-8)	1KBC	His	1	Asp	12	His_{β}	12	His_{β}	(Betz *et al.* 1997; Bode *et al.* 1994)
Human stromelysin-1 (MMP-3)	2SRT, 1BM6	His	1	Asp	12	His_{β}	12	His_{β}	(Gooley *et al.* 1994; Li *et al.* 1998; Van Doren *et al.* 1995) NMR
Human stromelysin-1 (MMP-3)	1B3D	His	1	Asp	12	His_{β}	12	His_{β}	(Chen *et al.* 1999; Dhanaraj *et al.* 1996)
Human prostromelysin-1 (MMP-3)	1SLM	His	1	Asp	12	His_{β}	12	His_{β}	(Becker *et al.* 1995)
Human collagenase-3 (MMP-13)	830C	His	1	Asp	12	His_{β}	12	His_{β}	(Lovejoy *et al.* 1999)
Mouse collagenase-3 (MMP-13)	1CXV	His	1	Asp	12	His_{β}	12	His_{β}	(Botos *et al.* 1999)
Human progelatinase 72 kDa (MMP-2)	1CK7	His	1	Asp	12	His_{β}	12	His_{β}	(Morgunova *et al.* 1999)
Bacteriophage T4 endonuclease VII	1EN7	Cys_{β}	2	Cys_{L}	31	$Cys_{b\alpha}$	2	Cys_{α}	(Raaijmakers *et al.* 1999)
E. coli DNA mismatch endonuclease	1VSR	Cys_{α}	4	$Cys_{2a\alpha}$	1	Cys	42	Cys_{α}	(Tsutakawa *et al.* 1999)
Human picornavirus endoprotease 2A	2HRV	Cys	1	$Cys_{b\beta}$	57	Cys_{β}	1	His_{L}	(Petersen *et al.* 1999)
Thermus thermophilus HB8 MutM	1EE8	Cys_{β}	2	Cys_{L}	16	$Cys_{a\beta}$	2	Cys	(Sugahara *et al.* 2000)
				Class V: Isomerases					
Escherichia coli rhamnose isomerase	1DE5	Glu_{β}	32	Asp_{β}	26	His_{β}	39	Asp_{β}	(Korndorfer *et al.* 2000)
				Class VI: Ligases					
tRNA synthetase family									
Escherichia coli MetRS	1QQT	Cys_{β}	2	$Cys_{2b\beta}$	9	Cys_{β}	2	$Cys_{2b\beta}$	(Fourmy *et al.* 1993a; Fourmy *et al.* 1993b) NMR, (Mechulam *et al.* 1999)
Thermus thermophilus HB8 MetRS	1A8H	Cys_{β}	2	$Cys_{2b\beta}$	13	Cys	2	His	(Sugiura *et al.* 2000)

Table 2. Continued.

Enzyme	PDB#	L_1	X	L_2	Y	L_3	Z	L_4	Ref.
Thermus thermophilus HB8 ProRS		Cys	4	Cys_{α}	25	Cys	2	Cys	(Yaremchuk *et al.* 2000)
Thermus thermophilus IsoleucylRS	1ILE	Cys_{β}	2	$Cys_{2a\beta}$	37	Cys_{β}	1	$Cys_{2b\beta}$	(Nureki *et al.* 1998)
Thermus thermophilus IsoleucylRS		Cys_{β}	2	$Cys_{2b\beta}$	204	Cys_{β}	2	$Cys_{2b\beta}$	
Thermus thermophilus ValRS	1GAX	Cys_{β}	2	$Cys_{2a\beta}$	17	Cys	2	Cys	(Fukai *et al.* 2000)
		Cys_{β}	2	$Cys_{2b\beta}$	164	Cys_{β}	2	$Cys_{2b\beta}$	
Escherichia coli IsoleucylRS	1QU2	Cys_{β}	2	$Cys_{2b\beta}$	16	$Cys_{b\alpha}$	2	Cys_{α}	(Silvian *et al.* 1999)
HIV-1 Integrase	1WJA	His	3	His_{α}	33	$Cys_{2b\beta}$	2	Cys_{α}	(Cai *et al.* 1997) NMR
HIV-2 Integrase	1AUB	His_{α}	3	$His_{2\alpha}$	33	$Cys_{a\alpha}$	2	Cys	(Eijkelenboom *et al.* 1997; Eijkelenboom *et al.* 2000) NMR
Thermus filiformis DNA ligase	1DGS	Cys_{β}	2	Cys_{L}	12	Cys_{β}	4	Cys	(Lee *et al.* 2000)

[a]See footnote in Table 1 for other definitions.

the catalytic one proposed for the entire astacin family (Soler *et al.* 1994). This site is highly conserved in all the matrix metalloproteinases (Sang & Douglas 1996; Soler *et al.* 1995) and contains three His and an Asp residue in a linear sequence spanning 28 amino acids (Table 2). Thus in matrilysin the zinc is bound to His168 (Nε2), Asp170 (Oδ1), His183 (Nε2) and His196 (Nδ1). This zinc site has the characteristics of a structural zinc site since it is has four protein ligands, no bound water molecules and a relatively short sequence of the protein provides all four zinc ligands (Vallee & Auld 1990b). While this zinc site and the catalytic zinc of the MMPs (Table 1) are 12.5 Å apart several of the conserved amino acids adjacent to the third and fourth His ligands of the structural zinc site (e.g., Ala182,-184,-195 and Phe197) form the environment surrounding the predicted catalytic residue Glu219 (Auld 1997). The properties of the 'structural' zinc site in the MMPs and in other similar sites may therefore influence function indirectly through effects on local conformation or local environment.

The crystal structure of *Escherichia coli* rhamnose isomerase (Korndorfer *et al.* 2000) shows zinc bound to a 'structural' site formed from the amino acid sequence Glu (Oε1)-32X-Asp (Oδ1)-26X-His (Nδ1)-39X-Asp (Oδ1) (Table 2). In the presence of substrate a second 'catalytic' Mn binding site is found in close proximity to this zinc binding site. The catalytic site appears to be occupied only when the substrate is present suggesting the true substrate is the Mn bound form of it. Two very similar metal binding sites are observed in *Streptomyces rubiginsous* xylose isomerase (Whitlow *et al.* 1991) although the overall identity to rhamnose isomerase is only 13% (Korndorfer *et al.* 2000). Both metals are identified as Mn in the case of xylose isomerase (Whitlow *et al.* 1991). The structural site for xylose isomerase is made up of two Asp and two Glu ligands. It may be that a site composed of multiple Glu and Asp residues only is too flexible for zinc and leads to weak binding constants due to fast dissociation rates of the zinc from such sites. The usual presence of Ca^{2+} and Mg^{2+} in such acidic ligand sites does correlate with the weak binding constants of such ions for protein binding sites and fast off rate constants for such metals.

Thus far the amino acid residues Asp and Glu have not been found in combination with Cys residues in structural zinc binding sites. The zinc binding site in adenylate kinases is of interest in this regard. The *Bacillus stearothermophilus* adenylate kinase contains a zinc binding site composed of four Cys ligands a in linear 24 amino acid span (Berry & Phillips 1998). The adenylate kinase from *Bacillus subtilis* also contains a structural zinc site (Perrier *et al.* 1994). Sequence alignment and mutagenic studies suggest the fourth Cys has been replaced by an Asp residue in this structural zinc site. Based on the knowledge gained on these systems it was also possible to genetically engineer a structural zinc binding site equivalent to the *B. stearothermophilus* into the *E. coli* adenylate kinase that does not normally bind zinc (Perrier *et al.* 1998). The incorporation of the zinc site into the *E. coli* enzyme improved its thermal stability while not adversely affecting its catalytic properties.

Interwoven zinc binding site

An interwoven zinc site occurs in the protein kinase C, PKC, family. In this case one zinc site is formed from residues residing within the two long spacers of the other zinc site. These enzymes are Ser/Thr protein kinases that depend on phospholipids and diacyl glycerol and are known to play crucial roles in intracellular signal transduction events elicited by various extracellular signal transduction events summoned by extracellular stimuli such as growth factors, hormones and neurotransmitters (Quest *et al.* 1992) Rat brain PKC is a zinc metalloenzyme in which zinc is bound within the lipid binding domain (Quest *et al.* 1992). NMR studies indicate that the regulatory domain of rat PKC contains two Cys rich independent subdomains in which two zinc atoms each are bound in a C3H coordination (Hommel *et al.* 1994). This study is in agreement with an XAFS study (Hubbard *et al.* 1991) that favored 3S/1N ligand sites without bridging zinc sites. The metal ligands from the two zinc sites are interwoven. The ligands in site I are Cys26, Cys29, His51, Cys54 while those in site II are His13, Cys43, Cys46, Cys62. Thus the C2C ligation spacer of site I is contained within the first 29 amino acid spacer of site II while the H2C ligation spacer of site I resides within the last 15 amino acid spacer for site II. This type of site has been observed also in the solution structures of Raf-1 protein kinase (Mott *et al.* 1996) and rabbit PKC-α (Ichikawa *et al.* 1995) and the crystal structure of the cysteine rich activator domain of murine PKC-δ (Zhang *et al.* 1995). The zinc ligands are conserved in C1 domains of protein kinases encompassing a wide range of organisms (Hurley *et al.* 1997).

The role of the structural zinc sites in general is to maintain the structure of the protein in its immediate

vicinity. These sites can have indirect effects on activity by affecting the chemical environment of the active center and/or influencing the alignment of active site residues for catalysis.

Cocatalytic zinc sites

While it was known for many years that a number of zinc enzymes required two or three metals for full activity the location of these metals relative to one another was often in debate. Prior to the X-ray structure analyses these metal atoms were referred to as 'modulating' or 'regulatory' (Vallee & Auld 1992a; 1993b). As the first three-dimensional structures of these enzymes became available it became apparent that the metals were in close proximity.

A novel feature of these sites is the bridging of two of the metal sites by a side chain moiety of a single amino acid residue, usually Asp and sometimes a water molecule (Vallee & Auld 1993a). In principle any sp^2 center containing two nucleophilic atoms should have a bridging potential. Thus the ring nitrogens of His and the carboxylate oxygens of Asp, Glu, $LysCO_2^-$ have been found to bridge such sites (Table 3). Such an interaction would of course require the metals to be in close proximity to each other. The distance between the metals in these sites depends on the bridging amino acid. In the case of an Asp or Glu it is generally between 3 and 4 Å apart (Table 3). In the case of His the distance increases to about 6 Å.

There are 3 dozen representatives of this type of zinc site with the great majority belonging to the Class III hydrolases (Table 3). Asp and His predominate as ligands in cocatalytic zinc sites where the frequency is Asp $\cong$ His $>$ Glu. These sites also contain unusual zinc ligands such as amide carbonyls provided by Asn, Gln, and the peptide backbone; hydroxyl groups from Ser, Thr, and Tyr and the amine nitrogen of Lys or the N-terminal amino acid of the protein. With the possible exception of the β-lactamases (see below) there are no Cys ligands. The absence of Cys in this type of zinc site is perhaps surprising since there are bridging sulfur ligands in the zinc Cys clusters of metallothionein and fungal transcription factors such as GAL4 (Vallee *et al.* 1991). The ligands to these sites often come from nearly the entire length of the protein. The metals in these sites may therefore be important to the overall fold of the protein as well as catalytic function. The ligands are often part of a β-sheet or are provided by amino acids 1 or 2 residues before or after a β-sheet.

The bridging amino acids and H_2O could have critical roles in catalysis. Thus, their dissociation from either metal atom during catalysis could change the charge on the metal promoting its action as a Lewis acid or allowing interaction with an electronegative atom of the substrate. Alternatively, the bridging ligand might participate transiently in the reaction as a nucleophile or general acid/base catalyst. The flexibility of the arm supplying the bridging ligands (e.g., one C for Asp *vs* 5 C/N for $LysCO_2^-$) would be expected to influence the stability and reactivity of the two metal sites. In this manner the metal atoms and their associated ligands would play specific roles in each step of the reaction that works to bring about catalysis.

Only a few of these sites contain only zinc ions. Several contain zinc in combination with Cu, Fe or Mg. Zn/Mg are seen in alkaline phosphatase and lens aminopeptidase; Fe(III)/Zn in the purple acid phosphatase family and Cu(II)/Zn in the superoxide dismutase, SOD, family (Table 3).

Superoxide dismutases

This group of cocatalytic containing copper/zinc enzymes plays a critical role in the physiological control of oxygen radicals by catalyzing the dismutation of the superoxide anion into molecular oxygen and hydrogen peroxide (Bannister *et al.* 1987). There are x-ray structures available for several eukaryotic and bacterial sources of this enzyme (Table 3). This is the only cocatalytic site that has a bridging His residue thus far. The zinc site is composed of three His residues coordinated by their Nδ1 nitrogens and the Oδ1 oxygen of Asp81 while the Cu site has three His residues coordinated by their Nε2 nitrogens and only the first by Nδ1 (His44). Coordination by Nδ1 is not often observed in zinc sites and therefore maybe involved in fine tunning the function of the zinc. The role of zinc in the SOD family is generally considered supportive to that of the copper which undergoes oxidation/reduction during catalysis. However, zinc may be important to substrate specificity. Thus the zinc deficient SOD has been proposed to participate in both sporadic and familial amyotrophic lateral sclerosis by an oxidative mechanism involving nitric oxide (Estevez *et al.* 1999).

Phosphatases

Several of the zinc enzymes that catalyze phosphomonoester hydrolysis have cocatalytic zinc sites con-

Table 3. Cocatalytic zinc sites[a].

Enzyme	PDB#	metal	R,Å	L_1	X	L_2	Y	L_3	Z	L_4	L_5	Ref.
						Class I: Oxidoreductases						
Superoxide dismutase family												
Bovine	2SOD	Cu(II)	6.2	His_β	1	His_β	14	***His***$_\beta$	56	His_β(C)	Solv	(Tainer *et al.* 1982)
		Zn		***His***$_\beta$	7	His	8	His	2	$Asp_{2b\beta}$(C)	-	
Human	1SPD	Cu(II)	5.5	His_β	1	His_β	14	***His***	56	His_β(C)	-	(Parge *et al.* 1992)
		Zn		***His***	7	His	8	His	2	$Asp_{2b\beta}$(C)	-	
Frog (*Xenopus laevis*)	1XSO	Cu(II)	6.0	His_β	1	His_β	14	***His***$_\beta$	56	His_β(C)	Solv	(Carugo *et al.* 1994)
		Zn		***His***$_\beta$	7	His	8	His	2	$Asp_{2b\beta}$(C)	-	
Spinach (*Spinacia oleracea*)	1SRD	Cu(II)	6.0	His_β	1	His_β	14	***His***$_\beta$	56	His_β(C)	-	(Kitagawa *et al.* 1991)
		Zn		***His***$_\beta$	7	His	8	$His_{2b\beta}$	2	Asp_β(C)	-	
Yeast (*S. cerevisiae*)	1SDY	Cu(II)	6.1	His_β	1	His_β	14	***His***$_\beta$	56	His_β(C)	Solv	(Djinovic *et al.* 1992)
		Zn		***His***$_\beta$	7	His	8	$His_{2b\beta}$	2	Asp_β(C)	-	
Yeast (*Candida albicans*)	1YSO	Cu(I)	6.5	His_β	1	His_β	14	His_β	56	His_β(C)	Solv	(Ogihara *et al.* 1996)
		Zn		His_β	7	His	8	$His_{2b\beta}$	2	Asp_β(C)	-	
Escherichia coli	1ESO	Cu(II)	6.5	His_β	1	His_β	14	***His***$_\beta$	56	His_β(C)	-	(Pesce *et al.* 1997)
		Zn		***His***$_\beta$	7	His	8	$His_{2b\beta}$	2	Asp_β(C)	-	
Salmonella tryphimurium	1EQW	Cu(II)	6.5	His_β	1	His_β	14	***His***$_\beta$	56	His_β(C)	-	(Pesce *et al.* 2000)
		Zn		***His***$_\beta$	7	His	8	$His_{2b\beta}$	2	Asp_β(C)	-	
Photobacterium leiognathi	1YAI	Cu(II)	6.2	His_β	1	His_β	22	***His***$_\beta$	54	His_β(C)	-	(Bourne *et al.* 1996)
		Zn		***His***$_\beta$	8	His	8	$His_{2b\beta}$	2	Asp_β(C)	-	
Brucella abortus		Cu(II)		His	1	His	22	***His***	54	His(C)	-	(Chen *et al.* 1995) NMR
		Zn		***His***	8	His	7	His (C)	-	?		
Actinobacillus pleuropneumoniae	2APS	Cu(II)	6.4	His_β	1	His_β	22	***His***$_\beta$	55	His_β(C)	-	(Forest *et al.* 2000)
		Zn		***His***$_\beta$	8	His	8	$His_{2b\beta}$	2	Asp_β(C)	-	
						Class III: Hydrolases						
E. coli alkaline phosphatase	1ALK	Zn2	3.9	His	0	$Asp_{2a\beta}$	266	$Ser_{b\alpha}$	50	***Asp***$_\beta$(N)	-	
		Mg		***Asp***$_\beta$	103	Thr_α	166	Glu_β (C)	-	H_2O		(Kim & Wyckoff 1991; Stec *et al.* 1998)

Table 3. Continued.

Enzyme	PDB#	metal	R,Å	L_1	X	L_2	Y	L_3	Z	L_4	L_5	Ref.
B. cereus Phospholipase C1	AH7	Zn2	3.3	$\boldsymbol{Asp}_{a\alpha}$	3	His_{α}	48	His	13	$Asp_{a\alpha}$(N)	-	(Hough *et al.* 1989)
		Zn3		$Trp_{b\beta}$	12	His_{α}	107	$\boldsymbol{Asp}_{a\alpha}$(C)	-	H_2O		
P. citrinium P1 nuclease	1AK0	Zn2	3.2	$\boldsymbol{Asp}_{\alpha}$	3	His_{α}	55	$His_{a\alpha}$	14	Asp_{α}(N)		(Volbeda *et al.* 1991)
		Zn3		Trp	4	His_{α}	113	$\boldsymbol{Asp}_{\alpha}$(C)	-	H_2O		
E. coli Endonuclease IV	1QTW	Zn2	3.4	$\boldsymbol{Glu}_{\beta}$	33	Asp_{β}	36	His_{β}	44	$Glu_{\alpha\beta}$(C)	$\boldsymbol{H_2O}$	(Hosfield *et al.* 1999)
		Zn3		$\boldsymbol{Glu}_{\beta}$	35	$His_{\alpha\beta}$	39	His_{β} (N)	-	$\boldsymbol{H_2O}$		
Phosphotriesterase family												
Pseudomonas diminuta	1DPM	Zn1	3.3	$His_{2a\beta}$	1	His	111	$\boldsymbol{Lys}_{\beta}\boldsymbol{CO_2^-}$	131	$Asp_{2a\beta}$(C)	$\boldsymbol{OH}$	
		Zn2		$\boldsymbol{Lys}_{\beta}\boldsymbol{CO_2^-}$	31	His_{β}	28	His_{β} (C)	-	$\boldsymbol{OH}$		(Benning *et al.* 1994; Vanhooke *et al.* 1996)
Escherichia coli	1BP6	Zn1	3.35	$His_{2a\beta}$	1	His	110	$\boldsymbol{Glu}_{b}\beta$	117	$Asp_{2a\beta}$ (C)	$\boldsymbol{Unk}$	(Buchbinder *et al.* 1998)
		Zn2		$\boldsymbol{Glu}_{b}\beta$	32	His_{β}	27	$His_{\alpha\beta}$ (C)	-	$\boldsymbol{Unk}$		
Clostridium perfringens α-toxin	1QM6	Zn1	3.2	$\boldsymbol{Asp}_{\alpha}$	3	His_{α}	57	His	11	Asp(N)		(Naylor *et al.* 1999)
		Zn2		Trp	10	His_{α}	118	$\boldsymbol{Asp}_{\alpha}$ (C)	-	H_2O		
Purple acid phosphatase family												
Kidney bean	1KBP	Fe(III)	3.3	Asp_{β}	28	$\boldsymbol{Asp}_{\beta}$	2	$Tyr_{2a\beta}$	157	$His_{2a\beta}$(C)		
		Zn		$\boldsymbol{Asp}_{\beta}$	36	$Asn_{b\alpha}$	84	$His_{a\beta}$	36	$His_{2a\beta}$(C)	H_2O	(Klabunde *et al.* 1996; Strater *et al.* 1995)
Rat	1QFC	Fe(III)	3.1	$Asp_{2a\beta}$	37	$\boldsymbol{Asp}_{2a\beta}$	2	Tyr	167	$His_{b\beta}$(C)	H_2O	
		Fe(II)		$\boldsymbol{Asp}_{2a\beta}$	38	$Asn_{b\alpha}$	94	$His_{a\beta}$	34	$His_{2a\beta}$(C)	H_2O	(Lindqvist *et al.* 1999; Uppenberg *et al.* 1999)
Porcine (uteroferrin)	1UTE	Fe(III)	3.3	$Asp_{2a\beta}$	37	$\boldsymbol{Asp}_{2a\beta}$	2	Tyr	167	$His_{b\beta}$(C)	$\boldsymbol{OH}$	(Guddat *et al.* 1999)
		Fe(II)		$\boldsymbol{Asp}_{2a\beta}$	38	Asn_{α}	94	$His_{a\beta}$	34	$His_{2a\beta}$(C)	$\boldsymbol{OH}$	
Human protein phosphatase I		Fe(III)	3.5-4.0	Asp	1	His	25	$\boldsymbol{Asp}$	179	Tyr(C)	$\boldsymbol{H_2O}$	(Egloff *et al.* 1995)
		Mn		$\boldsymbol{Asp}$	31	Asn	48	His	74	His(C)	$\boldsymbol{H_2O}$	
Human brain calcineurin	1AUI	Fe(III)	3.1	Asp	1	His	25	$\boldsymbol{Asp}_{2a\beta}$ (C)		H_2O	$\boldsymbol{H_2O}$	
		Zn		$\boldsymbol{Asp}_{2a\beta}$	31	Asn	48	$His_{\alpha\beta}$	81	$His_{2a\beta}$(C)	$\boldsymbol{H_2O}$	(Griffith *et al.* 1995; Kissinger *et al.* 1995)
Escherichia coli UDP-sugar hydrolase	1USH	Zn1	3.3	$Asp_{2a\beta}$	1	His	40	$\boldsymbol{Asp}_{2a\beta}$	169	$Gln_{b\beta}$(C)	$\boldsymbol{CO_2^-}$ or $\boldsymbol{H_2O}$	(Knofel & Strater 1999)
		Zn2		$\boldsymbol{Asp}_{2a\beta}$	31	Asn_{L}	100	His_{β}	34	$His_{a\beta}$(C)	$\boldsymbol{CO_2^-}$ or $\boldsymbol{H_2O}$	

Table 3. Continued.

Enzyme	PDB#	metal	R,Å	L_1	X	L_2	Y	L_3	Z	L_4	L_5	Ref.
Pseudomonas sp. CPD G_2	1CG2	Zn1	3.3	***Asp***$_{2b\beta}$	34	$Glu_{a\alpha}$	208	His (C)	-	***H$_2$O***		(Rowsell *et al.* 1997)
		Zn2		His_{β}	28	***Asp***$_{2b\beta}$	58	His_{β} (C)	-	***H$_2$O***		
Aminopeptidase family												
bovine lens	1BLL	Zn1	2.9	***Glub***$_{\alpha}$	1	Asp	76	***Asp***$_{2a\beta}$(N)	-	***H$_2$O***		(Burley *et al.* 1992)
		Zn2		Lys_{β}	4	***Asp***$_{2a\beta}$	17	$Asp_{2b\beta}$	60	**Glu**$_{b\alpha}$(C)	***H$_2$O***	
Aeromonas proteolytica	1AMP	Zn1	3.5	***Asp***$_{2b\beta}$	34	Glu	104	His (C)	-	***H$_2$O***		(Chevrier *et al.* 1994)
		Zn2		His_{β}	19	***Asp***$_{2b\beta}$	61	$Asp_{a\beta}$(C)	-	***H$_2$O***		
Streptomyces griseus	1JXO, 1QQ9	Zn1	3.6	***Asp***$_{2b\beta}$	34	Glu	114	His (C)	-	***H$_2$O***		
		Zn2		His_{β}	11	***Asp***$_{2b\beta}$	62	$Asp_{a\beta}$ (C)	-	***H$_2$O***		(Gilboa *et al.* 2000; Greenblatt *et al.* 1997)
Escherichia coli methionine-1	1MAT	Co1	2.9	Asp_{β}	10	***Asp***$_{\beta}$	126	***Glu***$_{b\beta}$ (C)	-			
		Co2		***Asp***$_{\beta}$	62	His_{β}	32	$Glu_{\alpha\beta}$	30	***Glu***$_{b\beta}$(C)		(Lowther *et al.* 1999; Roderick & Matthews 1993)
Pyrococcus furiosus methionine-2	1XGM	Co1	2.8	Asp_{β}	10	***Asp***$_{\beta}$	186	***Glu***$_{\beta}$ (C)	-	***H$_2$O***		(Tahirov *et al.* 1998a)
		Co2		***Asp***$_{\beta}$	59	His_{β}	33	$Glu_{\alpha\beta}$	92	***Glu***$_{\beta}$ (C)	***H$_2$O***	
Human methionine-2	1B59	Co1	3.2	Asp_{β}	10	***Asp***$_{a\beta}$	196	***Glu***$_{\beta}$ (C)	-	H_2O		(Liu *et al.* 1998)
		Co2		***Asp***$_{a\beta}$	68	His_{β}	32	Glu_{β}	94	***Glu***$_{\beta}$ (C)	***H$_2$O***	
Human Glyoxalase II	1QH3,1QH5	Zn1	3.3-3.5	$His_{2a\beta}$	1	His	53	His	23	***Asp***$_{b\beta}$(C)	***H$_2$O***	(Cameron *et al.* 1999b)
		Zn2		Asp	0	His	74	***Asp***$_{b\beta}$	38	His_{β}(C)	***H$_2$O***	
β-lactamase family												
Bacteroides fragilis	1ZNB	Zn1	3.5	His	1	His	60	His(C)	-	***H$_2$O***		
		Zn2		Asp	77	$Cys_{2a\beta}$	41	His(C)	-	***H$_2$O***	H_2O	(Carfi *et al.* 1998b; Concha *et al.* 1996)
Bacillus cereus	1BC2	Zn1	3.7-4.4	$His_{2a\beta}$	1	$His_{b\alpha}$	60	His (C)	-	H_2O		
		Zn2		Asp	77	Cys	41	His (C)	-	H_2O	H_2O	(Carfi *et al.* 1998a; Fabiane *et al.* 1998)
Stenotrophomonas maltophilia	1SML	Zn1	3.4	His	1	His	73	His (C)	-	***H$_2$O***		(Ullah *et al.* 1998)
		Zn2		Asp	0	His	135	His (C)	-	***H$_2$O***	H_2O	
Pseudomonas aeruginosa	1DD6	Zn1	3.5	$His_{2a\beta}$	1	His	59	His (C)	-	***H$_2$O***		(Concha *et al.* 2000)
		Zn2		Asp	76	$Cys_{2a\beta}$	38	His (C)	-	***H$_2$O***	H_2O	

[a]The amino acid residue which bridges the two metal sites is shown *in italic bold face*. R is the distance between the metal atoms. See footnote in Table 1 for other definitions. Unk is an unknown bound molecule.

taining two or three metal atoms in close proximity (Tables 1 and 3). *E. coli* alkaline phosphatase is the best studied representative of this group. It has a cocatalytic zinc site in both of its subunits composed of two zinc atoms and one magnesium that form a nonequilateral triangle with the metals as the apices (Kim & Wyckoff 1991). The ligands to these metals and the adjacent amino acids are highly conserved for a large family made up of representatives from bacteria, yeast and mammalian sources (Vallee & Auld 1993a). One metal site has the properties of a catalytic zinc site being formed from two ligands, Asp327 (Oδ1) and His331 (Nε2) supplied from a short α-helix, a third protein ligand His412 (Nε2) supplied by a β-strand and a water molecule (Table 1). The second zinc, Zn2, and the Mg are bridged by Asp51 (Table 3). This was the first zinc site where a reactant amino acid in catalysis, Ser102, was found to be a ligand to a metal (Zn2) in the resting state. The serine is reported to be bound as an alkoxide since the oxygen-Zn distance is 1.91 Å (Stec *et al.* 2000). A hydroxide bound to the Mg may be responsible for aiding in deprotonating the zinc-bound serine. Several other phosphate hydrolyzing enzymes also have cocatalytic sites resembling *E. coli* alkaline phosphatase (Tables 1 and 3).

A combination of X-ray crystallographic, NMR and kinetic studies on the Cd and Co substituted enzymes have aided in deciphering the mechanism of action of the *E. coli* enzyme (Coleman 1992; Kim & Wyckoff 1991; Vallee & Galdes 1984). The rate determining step is strongly pH dependent. In the alkaline pH region the release of the non covalently bound product phosphate (E•P $\rightarrow$ E + P) is rate limiting while in the acidic pH region the breakdown of the covalent phosphoryl intermediate (E-P $\rightarrow$E•P) is postulated to be rate limiting. Ser102, a ligand to Zn2, is the nucleophile in the first step of the reaction.

The breakdown of the Ser phosphoryl intermediate, E-P, is believed to be through a zinc-bound water/hydroxide on the catalytic zinc in the proposed mechanism. The enzyme•vanadate complex has been proposed to mimic the transition state complex (Holtz *et al.* 1999). The vanadate ion is bound in a trigonal bipyramidal geometry with the active site Ser102 and water molecule in opposite apical positions. The equatorial oxygens are stabilized by interaction with the guanidinium group of Arg166. Mutation of the catalytic zinc ligand, His331Gln yields an enzyme in which the covalent phosphate intermediate can be observed in the crystal structure (Murphy *et al.* 1997). The structure shows the zinc-bound water on the catalytic zinc is in a position for apical attack on the Ser102 phosphoryl bond.

In the E•P complex the phosphate ion is coordinated to both Zn and Zn2 and with two of its oxygens to the guanidinium group of Arg166. The phosphate is further hydrogen bonded to the amide of Ser102 and a water molecule that is coordinated to the Mg (Kim & Wyckoff 1991). Mutation of Ser102 to Gly, Ala or Cys decreases activity 10^4 to 10^5 fold with only the Cys mutant having an effect on the position of the phosphate (Stec *et al.* 1998).

The purple acid phosphatases are a group of nonspecific phosphomonoesterases that have been found in animal, plant and fungal sources (Klabunde & Krebs 1997). The characteristic purple color of this subclass of acid phosphatases comes from a Tyr phenolate-Fe(III) charge-transfer transition at 560 nm. The presence of Fe(III) is universally found in these enzymes. The 35 kDa mammalian purple acid phosphatases, PAP, or tartrate-resistant acid phosphatases, TRAP, contain a Fe(III)-Fe(II) iron center (Uppenberg *et al.* 1999) in contrast to the Fe(III)-Zn(II) center found in the 110 kDa kidney bean enzyme (Klabunde *et al.* 1996). The Ser/Thr human protein phosphatase 1 and calcineurin also contain a very similar cocatalytic Fe(III)-M(II) (where M is Zn or Mn) site to that of the PAPs (Egloff *et al.* 1995; Kissinger *et al.* 1995). In this case there is no Tyr-Fe(III) interaction but the general ligand nature, the distance between metals, and the presence of a bridging Asp residue, is common to all of these enzymes (Table 3). A mechanism has been proposed for the PAPs in which the phosphate ester binds to the Zn (II) site and the phosphate bond undergoes nucleophilic attack by an Fe (III)-coordinated hydroxide ion (Klabunde & Krebs 1997).

Aminopeptidases

Aminopeptidases containing two metals catalyze the hydrolysis of a wide variety of N-terminal peptides and amino acid derivatives. These enzymes are widely distributed in bacteria, yeast, plant and animal sources. The structures of several aminopeptidases containing cocatalytic zinc sites have been reported (Table 3). In addition, a cocatalytic zinc site has also been observed in a bacterial carboxypeptidase (Rowsell *et al.* 1997).

While several of the aminopeptidases have been characterized as the zinc or cobalt complex the native metal is sometimes still in question. The *E. coli* methionine aminopeptidase-1, MetAP-1, (Roderick

& Matthews 1993), the hyperthermophile *Pyrococcus furiosus* methionine aminopeptidase-2, MetAP-2 (Tahirov *et al.* 1998b) and human methionine aminopeptidase-2 (Liu *et al.* 1998) have been isolated as di-cobalt enzymes. The physiological metal for these enzymes is still not certain. Zinc works as well as cobalt in the yeast aminopeptidase-1 (Walker & Bradshaw 1998) and recent studies of the *E. coli* MetAP-1 indicate it functions as an Fe(II) enzyme (D'Souza & Holz 1999).

The cocatalytic zinc sites of two of the best studied aminopeptidases, bovine lens leucine aminopeptidase (BLAP) and *Aeromonas proteolytica* aminopeptidase (AAP) differ in several details (Chevrier *et al.* 1996; Strater & Lipscomb 1995). His ligands are bound to both sites in AAP while no His residues are involved in BLAP (Table 3). AAP uses both an Asp carboxylate and a water molecule as bridging ligands while BLAP uses the carboxylate oxygens of a Glu residue, one oxygen of an Asp residue and a bridging water molecule. BLAP uses a Lys residue to bind Zn at the tightly bound site. These combinations of ligands as well as the difference in interatomic distances of the two zinc atoms could lead to differences in the charge on the zinc that in turn could influence catalysis. The reader is directed to several reviews on this class of enzymes for more detailed comments on their mechanism of action (Auld 2001; Kim & Lipscomb 1994; Lipscomb & Strater 1996; Taylor 1993).

β-Lactamases

The first reported β-lactamase structure that contained two zinc sites was for the *B. fragilis* enzyme (Concha *et al.* 1996). This enzyme was crystallized at pH 7.0 in a 10 μM $ZnCl_2$, Hepes buffer. It is not yet clear if this is a true cocatalytic zinc site. If so it will be the first cocatalytic zinc site in which there is no bridging amino acid. The importance of the second zinc site to catalytic activity is still not clear. The second zinc site is not conserved in the few enzymes that have been examined. Thus the *Stenotrophomonas maltophilia* β-lactamase has no Cys in the second zinc site (Ullah *et al.* 1998). The mono zinc *B. cereus* enzyme is active and the *Aeromonas hydrophila* AE06 enzyme is inhibited by Zn with a K_i of 46 μM (Hernandez Valladares *et al.* 1997) while the catalytic zinc binds to the enzyme with a dissociation constant lower than 20 nM.

The kinetic parameters for the mono and di-zinc *B. fragilis* enzyme differ only slightly for 4 substrates (Paul-Soto *et al.* 1998). The mutation of Cys168 to Ser in the *B. fragilis* enzyme eliminates the second zinc site (Li *et al.* 1999c). The k_{cat} values for this enzyme are reduced 140 to 1,500 fold while the k_{cat}/K_m values are reduced 970 to 3,700 fold dependent on the substrate used (Yang *et al.* 1999). This reduction in activity could be due to the loss of a residue that played a role in the transition state in catalysis.

The mutant Cys168Ser *B. cereus* enzyme can bind a second zinc weakly (Paul-Soto *et al.* 1999). The results of kinetic, metal binding and XAFS studies of this enzyme indicates the mono-zinc enzyme is dependent on the Cys for optimal activity while the di-zinc enzyme is not. Thus, in summation, all the β-lactamases are dependent on the presence of one zinc that has the characteristics of a catalytic zinc site while the second zinc is not universally important to the activity of the β-lactamases.

Protein interface zinc sites

Zinc may also influence the quaternary structure of proteins. Thus zinc binding to ligands supplied from two protein molecules at their interface contact surface has been observed in increasing numbers in the last few years (Auld 2001). These interactions can lead to dimers or trimers of the same protein or link two different proteins through the intermolecular ligands. The amino acid residues His, Glu and Asp primarily supply the ligands to these sites but Cys containing sites are also found (Table 4). The ligands are generally contributed by some form of secondary structure with β-sheets predominating. The resulting sites can function like catalytic zinc sites as in γ-carbonic anhydrase (Iverson *et al.* 2000) or structural-like sites as in the proposed superantigen-MHC class II complexes (Papageorgiou & Acharya 1997) (Figure 2).

Protein interface catalytic zinc sites

The first member of the γ-class of carbonic anhydrases, CAM, was isolated and characterized from the methanogenic archaeon *Methanosarcina thermophila* (Alber & Ferry 1994). The trimeric enzyme catalyzes the interconversion of CO_2 and HCO_3^- with turnover numbers about 20-fold lower than the fastest of the α-class of carbonic anhydrases (Alber *et al.* 1999). Both classes of enzymes have three histidine ligands supplied by β-sheet secondary structures in the catalytic zinc site (Tables 1 and 4). However they differ in the length of their short spacers (one versus four). This

Table 4. Protein interface zinc sites.

Enzyme/Protein	PDB#	Class	L_1	X	L_2	Y	L_3	L'_1	Z	L'_2	Ref.
Nitric oxide synthase family		I									
Bovine endothelial	1NSE		Cys_{β}	4	Cys			Cys_{β}	4	Cys	(Raman *et al.* 1998)
Human endothelial	3NOS		Cys_{β}	4	Cys			Cys_{β}	4	Cys	(Fischmann *et al.* 1999)
Human inducible	1NSI		Cys	4	Cys			Cys	4	Cys	(Fischmann *et al.* 1999; Li *et al.* 1999b)
Mouse inducible	1DWV		Cys	4	Cys			Cys	4	Cys	(Ghosh *et al.* 1999)
Sulfolobus solfactaricus Cytochrome P450	1F4T	I	$Glu_{2b\alpha}$	39	$His_{a\alpha}$			$Glu_{2b\alpha}$	39	$His_{a\alpha}$	(Yano *et al.* 2000)
E. coli signal transducing protein, PTS IIA^{Glc}	1F3Z	II	His_{β}	14	His_{β}			Glu_{β}		H_2O	(Feese *et al.* 1997)
E. coli PTS IIA^{Glc}/glycerol kinase	1GLC	II	His_{β}	14	His_{β}			Glu_{α}		H_2O	(Feese *et al.* 1994)
Rat tonin	1TON	III	His	1	His	39	His (N)	Glu			(Fujinaga & James 1987)
Mouse 7S nerve growth factor	1SGF	III	Glu	6	His_{β}			$His_{\alpha\beta}$	4	Glu	(Bax *et al.* 1997)
Human glyoxalase I	1FRO	IV	Gln_{β}	65	Glu_{β}	-	H_2O	His_{β}	45	Glu_{β}	(Cameron *et al.* 1997)
E. coli glyoxalase I	1F9Z	IV	His_{β}	50	Glu_{β}	-	H_2O	His_{β}	47	Glu_{β}	(He *et al.* 2000)
Methanosarcina thermophila γ-CA	1THJ	IV	His_{β}	-	H_2O	-	H_2O	His_{β}	40	His_{β}	(Iverson *et al.* 2000)
Superantigen family											
Staphylococcus aureus enterotoxin (SEC2)	1STE		His	3	His_{β}	34	Asp_{β}(N)	Asp			(Papageorgiou *et al.* 1995)
Staphylococcus aureus enterotoxin (SEA)	1ESF		H_2O		His_{β}	27	Asp_{β}(N)	$Glu_{a\beta}$			(Schad *et al.* 1997)
Staphylococcus aureus enterotoxin (SEA)	1SXT		Asp_{β}	1	His_{β}	37	His_{β} (N)	His or H_2O			(Sundstrom *et al.* 1996b)
Staphylococcus aureus enterotoxin (SED)			Asp_{β}	1	His_{β}	37	Asp_{β} (N)	His_{β}			(Sundstrom *et al.* 1996a)
Staphylococcus aureus enterotoxin (SED)			His_{β}	3	Glu_{β}			His	3	Lys	(Sundstrom *et al.* 1996a)
Staphylococcus aureus enterotoxin (SEH)	1EWC		Asp_{β}	1	His_{β}			H_2O		H_2O	(Hakansson *et al.* 2000)
Streptococcus pyogenes exotoxin (SPE-C)	1AN8		Asp_{β}	1	His_{β}	33	His_{β} (N)	$His_{b\beta}$			(Roussel *et al.* 1997)
Staphylococcus aureus TSST-1	4TSS		His	60	His_{β}			His	60	His_{β}	(Prasad *et al.* 1997)
Human psoriasin (S100A7)	3PRS		His_{α}	3	$His_{a\alpha}$			Asp	6	His_{α}	(Brodersen *et al.* 1999)
Human interferon-$\alpha_{2\beta}$ dimer			Glu_{α}	0	Glu_{α}			Glu_{α}	0	Glu_{α}	(Radhakrishnan *et al.* 1996)
Human interferon β dimer	1AUI		His_{α}	3	His_{α}			$His_{b\alpha}$		H_2O	(Karpusas *et al.* 1997)
Human prolactin receptor/growth hormone	1BP3		Asp_{β}	0	$His_{a\beta}$			His_{α}	155	Glu_{α}	(Somers *et al.* 1994)
Mouse survivin	1F3H		Glu_{β}	3	$His_{2a\beta}$			Glu_{β}	3	$His_{2a\beta}$	(Muchmore *et al.* 2000)
Shaw T1 tetramer	3KVT		$Cys_{2b\beta}$	0	Cys	26	His (N)	$Cys_{b\beta}$			(Bixby *et al.* 1999)
Human Apo21L/TRAIL	1DG6		$(Cys_{a\beta})_3$		Solv						(Hymowitz *et al.* 2000)
E. coli colicin 3 immunity protein	3EIP		$Cys_{b\beta}$					$Cys_{b\beta}$			(Li *et al.* 1999a)

L'_1 and L'_2 are the second subunit or protein zinc ligands and Z is the spacer for these ligands. See footnote in Table 1 for other definitions.

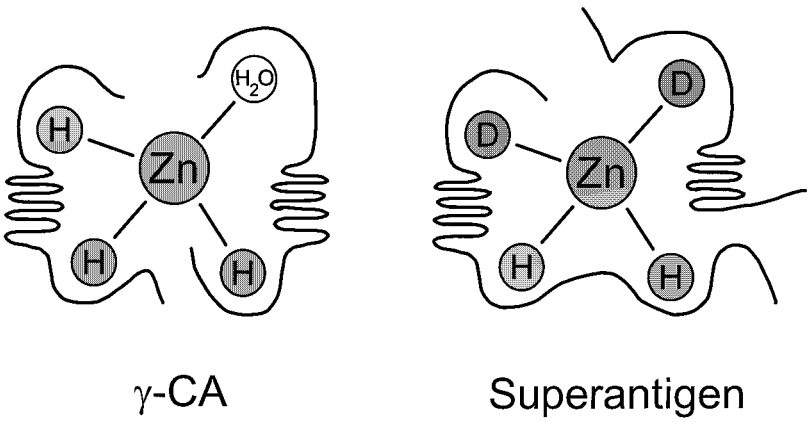

Fig. 2. Protein interface zinc binding sites: γ-CA, γ-carbonic anhydrase (Iverson *et al.* 2000), Superantigen, staphyloccus enterotoxin C2 (Papageorgiou *et al.* 1995)

in turn allows the second His of the CAM enzyme to become part of the zinc binding site in an adjacent monomer rather than bind to its own active site zinc. The crystal structures of the native zinc enzyme and the cobalt substituted enzyme show the metal binding site is formed from His81 (Nδ1) and His122 (Nε2) of one monomer and His117 (Nε2) of another monomer (Iverson *et al.* 2000; Kisker *et al.* 1996). In contrast to the tetrahedral zinc site observed in the α-class of enzymes that have only one zinc bound water molecule (Table 1), the zinc CAM contains two water molecules in a trigonal bipyramidal coordination geometry while the cobalt CAM contains three bound waters in an octahedral geometry. Both of these crystalline geometries are consistent with results obtained from XAFS studies performed in the solution state (Alber *et al.* 1999).

Another remarkable catalytic zinc site is found in human glyoxalase I where the C-terminal domain of one monomer interacts with the N-terminal domain of a second monomer to form two zinc binding sites at the interface of the subunits (Cameron *et al.* 1997). The active site zinc is coordinated by four protein residues and one water molecule in a square pyramidal coordination geometry. The base of the pyramid is formed from Gln33 and Glu 99 of one subunit, Glu172 from the second subunit and a water molecule. The apex of the pyramid uses His126 from the second subunit. Such a geometry could be viewed as octahedral with one axial ligand missing. Both EPR and XAFS studies suggest a distorted octahedral coordination in solution for the cobalt and zinc enzymes respectively (Garcia-Iniguez *et al.* 1984; Sellin *et al.* 1983). The sixth site may be a water molecule. Another remarkable feature of this metalloenzyme is that while zinc binds tighter than Mg (3×10^{-11} *vs* 1×10^{-6} M) the Mg enzyme is fully active (Sellin & Mannervik 1984). The octahedral metal coordination geometry and the functional replacement of Zn by Mg is unusual for catalytic zinc sites. These results raise the possibility that Mg or another metal is the functional metal *in vivo*. Nickel is believed to be the native metal in the *E. coli* glyoxalase I enzyme (Clugston *et al.* 1998). The nickel is bound octahedrally to His5 (Nε2) and Glu56 (Oε1) from one monomer and His74 (Nε2) and Glu122 (Oε1) from the other and two water molecules (He *et al.* 2000). Thus the human and *E. coli* enzymes do not have the identical protein ligands, even while they have homologous amino acid sequences and similar three-dimensional structures. Structure/function studies of *E. coli* glyoxalase I have shown that the nickel, cobalt and cadmium but not zinc enzymes are active (He *et al.* 2000). All of the former enzymes have an octahedral geometry as is observed in the human enzyme while the zinc *E. coli* glyoxalase I has a trigonal bipyramidal coordination.

Mutagenic studies of the zinc ligands of the human enzyme suggest that the metal ligand Glu172 may be directly involved in catalysis (Ridderstrom *et al.* 1998). Thus both the E172Q and Q33EE172Q double mutants still bind zinc but the catalytic ac-

tivity is decreased by 10^5 and 10^8 fold, respectively. Crystallographic results of the enzyme complexed with a transition state analog S-(N-hydroxy-N-p-iodophenylcarbamoyl) glutathione that mimics the enediolate intermediate that should form along the reaction pathway are consistent with this hypothesis (Cameron *et al.* 1999a). In this structure the two oxygen atoms of the hydroxycarbamoyl moiety displace two zinc-bound water molecules that are observed in a non-transition state complex. In addition the Glu172 carboxylate oxygen-Zn distance has increased from 2.0 Å to 3.3 Å in the complex. The zinc ion is envisioned to play a Lewis acid role in catalysis by directly coordinating the enediol intermediate and the freed zinc ligand Glu172 is proposed to facilitate proton transfer between the adjacent carbon atoms of the substrate (Cameron *et al.* 1999a).

Zinc binding sites in superantigens

Staphylococcus aureus and *streptococcus pyogenes* secrete a number of enterotoxins, SE and pyrogenic exotoxins, SPE respectively. These toxins are known as superantigens, since they simultaneously form complexes with the major histocompatibility class II (MHC-II) molecules and T cell receptors (TCRs) enabling them to activate a number of T cell lymphocytes (Fraser *et al.* 2000; Papageorgiou & Acharya 1997; Proft *et al.* 1999). Thus superantigens stimulate up to 20% of the T cells while only 0.0001% to 0.001% T cells are stimulated upon normal antigen presentation. The massive T cell activation leads to cytokine release and systemic shock. The staphylococcal enterotoxins (SE) A, B, C1-C3, D and E, toxic shock syndrome toxin (TSST-1), the streptococcal pyrogenic exotoxins (SPE-) A, B, Cs, G, and H, the streptococcal mitogenic exotoxins, SMEZ and SMEZ-2 are the best structurally studied superantigens thus far (Tables 4 and 5).

Zinc is believed to be an important factor in the mechanism of T cell activation. Thus binding of staphylococcal enterotoxin A and enterotoxin E to HLA-DR1 is completely abolished by low concentrations of EDTA (Fraser *et al.* 1992). This binding is completely restored by the addition of a 2 μM excess of Zn^{2+} but not by Ca^{2+}, Mg^{2+} or other metal ions. Recent studies using EDTA $\pm$ $ZnCl_2$ show zinc dependent binding of SPE-C, SPE-G, SPE-H and the streptococcal mitogenic exotoxins, SMEZ and SMEZ-2, to the MHC class II molecule HLA-DR1 (affinities of 15 to 36 nM) (Proft *et al.* 1999). Based on this criteria the superantigens, SEB and the toxic shock syndrome toxin, TSST, do not show zinc dependent binding to the MHC class II molecule.

The first crystal structures of the superantigens indicated zinc could bind at the interface of two protein molecules in the crystalline state (Table 4). The first potential zinc binding site in superantigens was found in the cadmium substituted *Staphylococcus aureus* enterotoxin type A (SEA) that has a metal binding site composed of Ser1, His187, His225 and Asp227 (Schad *et al.* 1995). The amino acids involved in binding the Cd ion are arranged in an octahedral coordination geometry. An approximate square plane is formed from the α-amino group and γO of Ser1, and nitrogens of His187 and His225. Asp227 ligates from beneath the plane and a water from above. Mutations of the His and Asp ligands indicate this site is important to the binding of MHC class II molecules (Abrahmsen *et al.* 1995). Crystals of the zinc containing protein revealed Zn binding between two molecules in an asymmetric unit (Sundstrom *et al.* 1996b) (Table 4). In this case His187 (Nδ1), His225 (Nε2) and Asp227 (Oδ2) bind to the zinc in a tetrahedral geometry. The fourth ligand is His61 (Nε2) from a neighboring SEA molecule.

The finding of zinc binding at the interface of two enterotoxin molecules in several of the superantigens (Table 4) could mean that zinc influences the function by forming dimer forms of the superantigen. SED crystallizes as a Zn^{2+} dependent dimer with two high affinity zinc sites located between the C-terminal β-sheets of the two monomers (Sundstrom *et al.* 1996a). Each zinc is tetrahedrally coordinated by His118 from one SED molecule and Asp182, His220 and Asp222 from the other. Thus in the case of SED it has been suggested that zinc binding could induce dimer formation and each monomer could bind to the MHC class II molecule (Sundstrom *et al.* 1996a).

Two distinct zinc binding sites are apparent from the reported structures of the superantigens during the last five years (Tables 4 and 5). Both sites contain at least three protein ligands with each site having short and long spacers. The third ligand comes from the N-terminal side of the second ligand. In one case the short spacer is one (Asp (Oδ1)-X-His (Nε2)) with both ligands coming from a β-sheet, located in the C-terminal side of the protein. The third ligand is either an Asp or His residue located 33 to 39 amino acids away. SEA (Schad *et al.* 1995; Sundstrom *et al.* 1996b), SED (Sundstrom *et al.* 1996a) and SEH

(Hakansson *et al.* 2000) (partial) and SPE-C (Roussel *et al.* 1997), SPE-H and SMEZ-2 (Arcus *et al.* 2000) all contain this type of zinc binding site (Tables 4 and 5). The second type of zinc binding site has a short spacer of 3 and contains two His ligands in the N-terminal side of the superantigen with the third ligand located 27 to 34 amino acids away. SEC2 (Papageorgiou *et al.* 1995), SEA (Schad *et al.* 1997) (2nd Zn site) and SPEA and SPEA1 (Earhart *et al.* 2000; Papageorgiou *et al.* 1999) contain this type of site. The fourth ligand in these sites is quite variable. It may come from a neighboring protein molecule, from within the same molecule or be a bound water molecule. The variability in the fourth ligand could be due to the fact that this ligand should come from the MHC class II molecule. His81 of the β chain of the DR1 molecule has been proposed to be this ligand based on the fact that mutation of this ligand disrupts HLA-DR1 binding to SEA but not SEB or TSST-1 that do not bind zinc strongly (Karp & Long 1992).

A zinc binding site at a protein interface, somewhat similar to the superantigen sites, was observed in crystals of rat submaxillary gland tonin that had been grown in a zinc containing mother liquor (Fujinaga & James 1987). The zinc binds to the Nε2 nitrogens of His97, His99 and the catalytic His57 of one molecule and Glu148 of an adjacent one. The presence of zinc was reported to inhibit the enzyme at pH 6.5. The structure of the zinc binding sites in the dimeric form of psoriasin (S100A7) also contains three His and one Asp ligand (Brodersen *et al.* 1999). This 22.7 kDa homodimeric protein belongs to the S100 class of calcium binding EF-hand proteins. Two zinc binding sites occur per dimer through the formation of a tetrahedral site consisting of the N-terminal His17 (Nε2) and Asp24 (Oδ1) of one monomer and His86 (Nε2) and His90 (Nε2) of the other. This binding site is apparently weak since it is reported to have a dissociation constant of 100 μM.

Zinc-His/Glu sites at protein interfaces

There are several His/Glu combinations that lead to zinc binding at the interface of proteins (Table 4). In crystals of the high molecular weight form of nerve growth factor, 7S NGF a zinc is tetrahedrally bound between His82 (Nε2) and Glu75 (Oε1) of the α-subunit and His217 (Nε2) and Glu222 (Oε1) of the γ-subunit (Bax *et al.* 1997). The binding of zinc to this interface is consistent with the observation that zinc enhances the stability of the 7S complex.

A number of these zinc sites are symmetry related. Thus zinc binds between Glu139 (Oε1) and His178 (Nε2) in one molecule of the asymmetric crystal unit of the 4 phenylimidazole-bound *Sulfolobus solfataricus* cytochrome P450 and their symmetry residues in another molecule (Yano *et al.* 2000). The functional importance of a dimer and zinc's contribution to its stability is not known. However no zinc was added in the crystallization procedure. A His/Glu site with a short spacer of 3 is observed in the dimer interface of mouse survivin (Table 4) (Muchmore *et al.* 2000). The human survivin does not form a similar intermolecular zinc site (Verdecia *et al.* 2000).

An asymmetric dimer observed for human interferon β, huIFN-β, is obtained under conditions where no zinc is added to the crystallization buffer (Karpusas *et al.* 1997). His ligands 93(Nε2) and 97(Nε2) reside on an α-helix in one monomer. The second monomer provides His121 (Nε2) and a water molecule to complete the 4-coordinate zinc site. However gel permeation experiments in the presence of zinc do not show any evidence of a dimer in solution. The dimers form in the crystal on contact surfaces opposite to those found in the IFN-α_{2B} crystal structure. The residue Glu43, which H-bonds to zinc ligand His121 has been identified as part of the binding site of monoclonal antibodies (Redlich & Grossberg 1990). The presence of zinc might therefore modulate this interaction.

High zinc concentrations are used in the crystallization procedure in some of these cases making it more difficult to ascertain physiologically significance of the site. Thus crystals of the human interferon-α_{2B} dimers, huIFN-α_{2B}, obtained in the presence of 40 mM zinc acetate (Radhakrishnan *et al.* 1996), show that the most extensive interactions occur in the vicinity of the zinc binding site. This site is formed from adjacent Glu residues 41 and 42 located on a 3_{10} helix. A distorted tetrahedral zinc coordination sphere is completed by the identical glutamates from a 2-fold symmetry related molecule. However, gel permeation studies indicate huIFN-α_{2B} is a monomer up to 50 μM and the presence of 1 mM Zn does not shift the equilibrium toward a dimer (Radhakrishnan *et al.* 1996).

A tetrahedral zinc binding site is observed in the crystal form of the *E. coli* signal transducing protein PTS IIA^{Glc} (Feese *et al.* 1997) and in its complex with glycerol kinase (Feese *et al.* 1994). In both cases the signal transducing protein supplies two His residues

with a spacer arm of 14 and the third Glu ligand comes from either a neighboring molecule in the crystal or the glycerol kinase. The fourth ligand in both cases is a water molecule (Table 4). The site is said to be geometrically equivalent to the zinc binding site in thermolysin (Table 1). If this site contained a suitable acid/base catalyst it might display hydrolytic activity. Although the biochemical effect of 0.01 mM zinc on the inhibition of glycerol kinase by PTS IIA^{Glc} has been demonstrated, the physiological role for zinc ions in PTS and protein interactions remains to be established (Feese *et al.* 1997).

Zinc-Cys protein interface sites

While His, Glu and Asp appear to be the predominate residues in forming these protein interface sites, Cys containing sites are also observed. A novel Cys site is found in the nitric oxide synthase enzymes (Table 4). In endothelial nitric oxide synthase, eNOS or NOS-3, a zinc ion is tetrahedrally coordinated to pairs of symmetry-related Cys residues near the bottom of the dimer interface (Raman *et al.* 1998) (Table 4). The Cys ligands, Cys96 and Cys101, are part of a small three-stranded antiparallel β-sheet that orientates the Cys ligands in the same direction directly across the antiparallel strands. The zinc site is further stabilized by H-bonds between the Cys ligands and the backbone amide NH of Leu102 and Gly103 as well as a H-bond of the amide NH of Cys101 to the carbonyl of Asn468. The zinc is positioned equidistant from each heme (21.6 Å) and each tetrahydrobiopterin, H_4B (12 Å). Ser104, 2 amino acids removed from one of the Cys ligands, H-bonds directly to the pterin side chain hydroxyl group. The metal center is believed to act in a structural capacity to maintain the integrity of the pterin-binding site. It is also centered in the most electropositive region of eNOS. It could therefore provide a binding site for the electronegative reductase domain. In addition, if one of the Cys ligands has nucleophilic capacity it could undergo S-nitrosylation (Stamler 1994). A precedent for this is the DNA repair protein *Escherichia coli* Ada in which a zinc bound Cys can be methylated irreversibly in the DNA complex (Myers *et al.* 1994). The nitrosylated Cys might then release zinc which may be controlled by the redox status in situ (Maret & Vallee 1998).

The crystal structure of the *E. coli* expressed human endothelial, eNOS, and the inducible form iNOS or NOS-2 also have this same zinc binding site (Fischmann *et al.* 1999). An independent study of human iNOS expressed in *E. coli* found the zinc site was not present after refolding (Li *et al.* 1999b), similar to an earlier study on the murine inducible, iNOS or NOS-2, where a disulfide was found (Crane *et al.* 1998). However in the presence of zinc and reducing agents the $Zn(Cys)_4$ site readily formed (Li *et al.* 1999b). These Cys residues are conserved in 20 mammalian e, i and n NOS enzymes suggesting the site may occur in all forms of NOS (Raman *et al.* 1998).

A highly conserved zinc protein interface Cys/His site occurs in the N-terminal, cytoplasmic tetramerization domain (T1) of voltage-gated K^+ channels (Bixby *et al.* 1999). The crystal structure of the *Shaw* T1 tetramers reveals a four-layered protein scaffolding. Within layer 4 on the proposed membrane side of the tetramer, there are 4 zinc ions coordinated by a His and two Cys from one monomer and one Cys from another. The zinc is tetrahedrally coordinated by Cys102 and Cys103 from layer 4 and His75 (Nδ1) from layer 3 of one monomer and Cys81 from layer 3 of another monomer. This site ($CysCysX_{20}CysX_5$His of one monomer) is conserved for 62 members of the *Shaw, Shab* and *Shal* T1 domain sequences but not for the *Shaker* T1 domain (Bixby *et al.* 1999). The physiological function of this zinc site is unknown.

The apoptosis-inducing ligand 2 protein (Apo2L or TRAIL), a member of the trimeric tumor necrosis factor (TNF) superfamily, is a type-II transmembrane protein that can be cleaved at the cell surface to form a soluble protein (Mariani *et al.* 1997). The cell killing properties of these cytokines have made them particularly attractive for the design of drugs that might selectively kill tumor cells. Recent structural studies of Apo2L revealed a homotrimeric protein with a zinc ion binding at the interface of the three monomers to three symmetry-related Cys ligands, one each from the three monomers (Hymowitz *et al.* 2000). The fourth ligand appears to be a solvent molecule, possibly chloride. Removal of the bound metal by dialysis against chelating agents or replacement of the Cys by Ala results in about a 100-fold decrease in apoptotic activity. Further studies show that the zinc is important to the stability of the native protein. Other members of the TNF superfamily do not have this zinc binding site. The Apo2L appears to be unique among TNF-related cytokines in that it selectively induces apoptosis in tumor cells while not affecting normal tissue (Hymowitz *et al.* 2000). The relationship of this specific activity and the unique zinc binding site is not known.

The antibiotic-like protein colicin E3 of *E. coli* acts as an RNase that specifically cleaves 16S rRNA (Li *et al.* 1999a). *E. coli* is protected from the action of this enzyme by forming a tight complex with an immunity protein, Im3. The crystal structure of Im3 shows the residue that is considered the most important determinant to the formation of the colicin complex, Cys47 is bound covalently to zinc at the interface of two monomers. It is unclear at present whether this zinc mediated dimer of Im3 has biological significance. However if the zinc concentration in *E. coli* should allow this zinc mediated dimer of Im3 to form it would negate the protective action of Im3 inactivating the host colicin E3.

Zinc binding sites in other proteins

Structural studies in recent years have revealed a number of zinc binding sites in proteins of diverse function. In compiling Table 5 the large number of identified DNA binding transcription factors or zinc fingers is purposely left out since they have been reviewed in detail elsewhere (Berg & Shi 1996; Klug 1999; Laity *et al.* 2001; Mackay & Crossley 1998).

The great majority of these zinc sites are formed from four protein side chain ligands to yield a tetrahedral binding site (Table 5). Their function may therefore be related to the local and/or overall structure since the sites span from 22 to 227 amino acids. The vast majority of the sites contain at least one short spacer. The residues generally are supplied from β-sheets or reside within one or two residues of such a secondary structure (Table 5). The amino acids, His and Cys, are the predominate suppliers of ligands but several sites are made up of combinations of His, Asp and Glu residues.

A zinc binding site containing His and Asp ligands was recently discovered in the crystalline state dimers of the 20-kDa human endostatin, the angiogenesis inhibitor, that is produced by proteolytic processing of the C-terminal globular domain of the collagen-like protein XVIII (Ding *et al.* 1998). The tetrahedral zinc site is formed by His132 (Nδ1), His134 (Nε2), His142 (Nε2) and Asp207 (Oδ1) (precursor protein numbering) (Table 5). Atomic absorption spectrometry indicates this site also exists in the solution state of human and mouse endostatin. No dimer contacts are observed in the crystalline form of mouse endostatin (Hohenester *et al.* 2000). However two mouse crystal forms are obtained which bind zinc in the N-terminal region of the protein but with different ligand compositions. One crystal form uses the same zinc ligands as the human endostatin while the other form substitutes Asp136 for His132, and retains His134, His142 and Asp207 as the other ligands. The effects of mutating either His132 or Asp136 or both on zinc binding to the protein are consistent with the different zinc binding modes. Thus mutants His132Ala and Asp136Ala still bind zinc while the double mutation does not. In addition mutation of Asp207Ala leads to loss of zinc binding. A number of conditions are different (pH, PEG types, presence or absence of oligosaccharide and zinc) in the production of the two crystal forms (Hohenester *et al.* 2000). It is not known whether any one of these conditions alone could account for the different zinc binding modes. Since the site is immediately adjacent to the precursor cleavage site the zinc may be involved in the antiangiogenic activity of endostatin or regulation of it (Ding *et al.* 1998). However, the structural diversity observed in the zinc binding site has led to the conclusion that zinc is not likely involved in the anti-tumor activity of the protein (Hohenester *et al.* 2000).

A somewhat similar His/Asp zinc binding site is conserved in the thermoacidophilic archaea ferredoxin family where the zinc is tetrahedrally bound to His16, His19, His34 and Asp76 (Iwasaki *et al.* 1997). This zinc site is found in the unusually long N-terminal extension region of these proteins that at present has no known function.

Both the periplasmic zinc binding protein TroA from the human parasite *Treponema pallidum* (Lee *et al.* 1999) and pneumococcal surface antigen PsaA (Lawrence *et al.* 1998) contain zinc sites that span a great distance in the protein (Table 5). These sites are very similar. The bound zinc ion is coordinated by the Nε2 nitrogens of His68, His133, His199 and both oxygens of Asp279 in TroA and His67 (Nε2), His139 (Nε2), Glu205 (Oε1) and one oxygen of Asp280 (Oδ1) in PsaA. The resulting coordination geometries are described as tetrahedral for PsaA and distorted square pyramidal in TroA due to the interaction of both oxygens of Asp279. The apex of the pyramid is occupied by the nitrogen of His199 while the other His ligands and the two oxygens of Asp 279 make up the square plane. These metal-binding proteins are believed to be the ligand binding component of an ATP-binding cassette (ABC) transport system (Lee *et al.* 1999). The function of the proteins is presumed to be similar to that of members of the

Table 5. Miscellaneous zinc binding proteins.

Protein	Classification	PDB#	L_1	X	L_2	Y	L_3	Z	L_4	Ref.
Human endostatin	Angiogenesis Inhib.	1BNL	His	1	His	7	His_{β}	64	$Asp_{b\beta}$	(Ding *et al.* 1998)
Mouse endostatin	Angiogenesis Inhib.	1DY0	His	1	His	7	His_{β}	64	$Asp_{b\beta}$	(Hohenester *et al.* 2000)
			His	3	Asp	5	His_{β}	64	$Asp_{b\beta}$	
Staphylococcus aureus A (SEA)	Enterotoxin	1ESF	Asp_{β}	1	His_{β}	37	His_{β}	185	Ser (N)	(Schad *et al.* 1995)
Streptococcus pyogenes (SPE-H)	Exotoxin	1EU3	Asp_{β}	1	His_{β}	39	His_{β} (N)		H_2O	(Arcus *et al.* 2000)
Streptococcus pyogenes (SMEZ-2)	Exotoxin	1EU4	Asp_{β}	1	His_{β}	37	Asp_{β} (N)		H_2O	(Arcus *et al.* 2000)
Streptococcus pyogenes A(SPE-A1)	Exotoxin	1B1Z	His_{β}	3	His_{β}	28	Asp_{β} (N)		H_2O	(Papageorgiou *et al.* 1999)
Streptococcus pyogenes A(SPE-A)	Exotoxin	1FNU	His_{β}	3	His_{β}	28	Asp_{β}	43	Glu_{β} (N)	(Earhart *et al.* 2000)
Sulfolobus Sp. ferredoxin	Electron transport	1XER	His_{β}	2	His_{β}	14	His_{β}	41	Asp_{β}	(Fujii *et al.* 1996)
Treponema pallidum Troa A	Zn binding protein	1TOA	His	64	$His_{2a\beta}$	65	His_{L}	79	Asp	(Lee *et al.* 1999)
S. Pneumoniae surface antigen Psaa	Immune system	1PSZ	His	71	$His_{2a\beta}$	65	Glu_{L}	74	Asp	(Lawrence *et al.* 1998)
Human survivin	Apoptosis	1F3H	Cys_{β}	2	Cys_{L}	16	His_{α}	6	Cys_{L}	(Verdecia *et al.* 2000)
Mouse survivin	Apoptosis		Cys	2	Cys	16	His	6	Cys	(Muchmore *et al.* 2000)
Xenopus laevis Xnf7 Bbox	Development	1FRE	Cys_{β}	2	His	18	Cys	5	His	(Borden *et al.* 1995) NMR
Thermus thermophilus chain D	Ribosomal protein	1FJF	$Cys_{b\alpha}$	2	Cys_{α}	13	Cys	4	Cys	(Wimberly *et al.* 2000)
ARF-GAP domain PYK2-associated protein β		1DCQ	Cys_{β}	2	Cys_{L}	16	$His_{b\alpha}$	2	Cys_{α}	(Mandiyan *et al.* 1999)
Thermus thermophilus L36	Ribosomal protein	1DGZ	Cys	2	$Cys_{b\beta}$	12	$Cys_{a\beta}$	4	$His_{2b\beta}$	(Hard *et al.* 2000)
E. coli DnaJ protein	Chaperone	1EXK	Cys_{β}	2	Cys	49	Cys_{β}	2	Cys	
			Cys_{β}	2	Cys	18	Cys_{β}	2	Cys	(Martinez-Yamout *et al.* 2000)
E. coli ADA	Repair		Cys	3	Cys	26	Cys	2	Cys	(Myers *et al.* 1994)
E. coli threonyl-tRNA synthetase	Descriminating	1EVK	Cys_{α}	50	His_{β}	125	His_{β}		H_2O	(Sankaranarayanan *et al.* 2000; Sankaranarayanan *et al.* 1999)
Human Sex hormone-binding globulin	Signaling protein	1F5F	Asp_{β}	17	$His_{a\beta}$	52	$His_{b\beta}$		?	(Avvakumov *et al.* 2000)

periplasmic ligand-binding protein (PLBP) family that function as ligand binding receptors for active transport and chemotaxis. However these proteins do not have the flexible interdomain β-strands of the PLBPs. An argument has been proposed for a more rigid hinge (in this case a backbone α-helix) if the purpose of these proteins is 'small' metal ion transport (Lee *et al.* 1999). Thus since the free energy of zinc in solution and bound to a protein is considered to be small (Lipscomb & Strater 1996), the binding of zinc to a protein can not incur the large entropy changes that would be associated with the ordering of a very mobile hinge region.

The steroid-binding specificity of the human sex hormone-binding globulin may also be influenced through a zinc binding site (Avvakumov *et al.* 2000). In this case zinc binding to both oxygens of Asp65, His83 (Nε2) and His136 (Nε2) prevents Asp65 from interaction with steroid 17β-hydroxyl group and further disorders the binding site. Since this site is observed when soaking the crystals with 2.5 mM $ZnCl_2$ further experiments are needed to evaluate the physiological significance of this finding.

A number of multi Cys zinc binding sites, several of which contain one or two His ligands, have also been reported. Survivin is a relatively small, 16 kDa, protein that is an inhibitor of apoptosis, IAP. Both the human and mouse proteins contain a zinc binding site in the N-terminal, BIR-like (baculovirus IAP repeat) domain (Muchmore *et al.* 2000; Verdecia *et al.* 2000). Survivin as well as caspase-3 localize to the microtubule organization centers during mitosis (Verdecia *et al.* 2000). The zinc binds to Cys57, Cys60, His77 (Nε2) and Cys84 in both human and mouse proteins. No direct interaction of this region with caspase-3 is observed (Verdecia *et al.* 2000). However since free zinc inhibits caspase-3 with a K_i less than 10 nM (Maret *et al.* 1999) the effect could be indirect if some agent should cause release of the zinc from the survivin protein. Survivin's high expression in a number of malignant tissues makes it a novel target for cancer therapy (Verdecia *et al.* 2000). A somewhat similar zinc binding site (in terms of spacing, Table 5) has been proposed by a NMR structural analysis of a *Xenopus* nuclear factor XNF7 regulating early *Xenopus* development (Borden *et al.* 1995). In this case the zinc is bound to Cys6, His9 (Nε2), Cys28 and His34 (Nε2).

Zinc binding sites of varying length (Table 5) that are likely involved in protein structure are found in the ARF-GAP domain of the PYK2-associated protein (Mandiyan *et al.* 1999), the *Thermus thermophilus* ribsome proteins (Hard *et al.* 2000; Wimberly *et al.* 2000), and the cysteine-rich domain of the *E. coli* chaperone protein DnaJ (Martinez-Yamout *et al.* 2000).

Some zinc sites have evolved to perform some unusual functions. In response to the threat posed by aberrant methylation of DNA, organisms express proteins that recognize and repair the resulting lesions (Lindahl 1993). Studies of how the DNA repair proteins might function have revealed a unique function of zinc. The solution structure of the DNA methyl phosphotriester repair domain of *E. coli* Ada contains a zinc bound to Cys38, Cys42, Cys69 and Cys72 (Myers *et al.* 1994). The acceptor residue of the repair protein appears to be the zinc-ligated Cys69. Since this is an irreversible transfer the protein performs a suicide role. Upon methyl transfer, Ada acquires the ability to bind to a DNA sequence-specifically and thereby induce genes that confer resistance to methylating agents (Myers *et al.* 1994).

A zinc binding site in the *E. coli* threonyl tRNA synthetase is also a unique zinc site not seen in any of the other synthetase family members. In this case the zinc binds in the active site to Cys334, His385 (Nε2), His511 (Nδ1) and a water molecule (Sankaranarayanan *et al.* 1999). The zinc ion is directly involved in the threonine recognition/discrimination. Upon binding threonine the zinc coordination changes from tetrahedral to a square pyramidal pentacoordinate intermediate by replacing the zinc bound water with both the amino and side chain hydroxyl groups of threonine (Sankaranarayanan *et al.* 2000). This binding mode permits other H-bonding interactions with amino acid residues in the active site. Amino acid activation experiments show no activation with the isosteric valine and a 1000-fold decreased activation with serine.

Support structure of zinc binding sites

The secondary support and scaffolding in combination with the direct ligands of the zinc allows fine tuning of the role of the zinc and its neighboring amino acids in the function of the enzyme. The following of observations are made about the structural properties of zinc binding sites observed in enzymes and other biological zinc sites (Tables 1–5): (1) Nearly all the sites contain at least one secondary structural element; (2) β-sheets

supply ligands to a wide variety of zinc binding sites; (3) Ligands frequently come from the first, last or 1 or 2 amino acids before or after a β-sheet or α-helix. This may allow more flexiblity in forming the zinc site. (4) Small loop regions (≤ 5 amino acids) between two types of secondary structure can also supply the ligands; (5) Short spacers of one generally use a β-sheet to supply the ligands while a spacer of three uses an α-helix; (6) An α-helix is used to supply the short spacer ligands most frequently in hydrolytic enzymes (in particular the metalloproteases). Overall this suggests that the stability of biological zinc sites requires some form of secondary structural support. However, the fact that short spacers are supplied by a variety of support types indicate this maybe one level of fine tuning the functional properties of such sites.

The stability and the function of the metal site is also likely influenced by the second shell of residues in the vicinity of the metal binding site. The secondary interactions of the ligands with hydrogen-bonding groups of the side chain groups of the amino acid residues or the carbonyl oxygen of the back-bone peptide chain may be critical to the formation and stabilization of the zinc sites containing oxygen, sulfur and nitrogen ligands. Comparative structural studies of four of the first known zinc enzymes, carbonic anhydrase, carboxypeptidase A, alcohol dehydrogenase and thermolysin led to the identification of carbonyl and carboxyl 'orienters' (Argos *et al.* 1978).

The interaction between a carboxylate anion orienter and a zinc-ligated histidine could have multiple effects on the reactivity and stability of the zinc site. Thus the negatively charged carboxylate could reduce the charge on the zinc which in turn could fine-tune the ability of the zinc to act as a Lewis acid or make it more difficult for zinc bound water to ionize. On the other hand the interaction would place constraints on the rotation of the His residue and might thus make zinc bind tighter and/or distort the geometry of the zinc site. Recent studies have shown some agents such as the drug D-pencillamine can facilitate the release of zinc, likely by disrupting stabilizing interactions between orienters and ligands (Chong & Auld 2000). Examination of the effect of the orienters or indirect ligands on catalysis has been most thoroughly examined in the carbonic anhydrase α-class of enzymes (Christianson & Cox 1999; Christianson & Fierke 1996). In addition the local environment provided by highly conserved residues surrounding the zinc and its ligands will likely be important to the function and stability of the zinc site. In the case of carbonic anhydrase, conserved hydrophobic residues are believed to be important to positioning the zinc ligands in a distorted tetrahedron (Hunt *et al.* 1999). The surrounding amino acids may also influence the off rate constants for the metal, thus influencing the stability of the metal site.

Concluding remarks

Information on zinc binding sites in metalloenzymes and related proteins has become increasingly available as the interest in how zinc affects biological function has accelerated. This is particularly apparent over the last decade. Zinc binding site motifs can be highly conserved, not only in the identity of the ligands and their spacing but in the neighboring amino acids in the linear sequence. This leads to the formation of a family of zinc enzymes that may have a similarity in their overall primary structure (sometimes low) and some biological function in common.

The availability of structural standards of reference for the types of zinc sites coupled with prediction of protein sequences from DNA sequencing has resulted in an explosion of information on potential biological zinc sites. In 1992 the number of zinc enzymes was estimated to be 300, based on the original criteria of determining the metal content and its relationship to the function of an enzyme (Vallee & Auld 1992a). If one now broadens the definition of zinc enzymes to include those proteins who likely will bind zinc due to the presence of zinc binding motifs found in zinc reference sites the number of zinc enzymes will be in the thousands. Thus the number of zinc proteases based on this criteria has increased from about 100 in 1989 to 2,169 (Barrett & Rawlings 2001) in March 2001. As the number of sequenced genomes increases this number will also increase. Of course the number of unique functional zinc sites that is used by the majority of species and phyla should be much smaller.

The challenge still remains to understand how these zinc sites function in detail. Future mechanistic studies of zinc metalloenzymes will continue to benefit from a combined use of structural, mutagenic, and transient state kinetics approaches to examine the system. Analyses of zinc proteins using methods that give both global structural information (e.g., X-ray diffraction and NMR) and dynamic local structural information (e.g., electronic absorption, XAFS and NMR) performed on specifically modified enzymes is

beginning to reveal the manner in which the protein modulates the zinc to achieve both catalytic efficiency and specificity. These studies have established zinc as an integral component of numerous functional proteins involved in a multiplicity of tasks, thus accounting for its fundamental role in metabolism, growth and development.

There are likely a number of features that zinc possesses that make it suitable for such a wide variety of functions. Chief among this is the fact that it is a stable metal ion species in a biological medium whose redox potential is in constant flux. The filled d-shell of zinc prevents it from undergoing oxidation or reduction in contrast to some of its neighboring transition metal ions such as Cu and Fe where their oxido-reductive properties are essential to their function (Vallee & Auld 1992b). Redox changes in neighboring transition metals are major sources of change in coordination geometry and rate of ligand exchange. Zinc is amphoteric, existing in both hydrate and hydroxide forms even at neutrality. It has Lewis acid properties. It ligates nitrogen and oxygen compounds as readily as sulfur. While zinc can have coordination numbers from 2 to 8 in zinc complex ions, 4, 5 and 6 are most frequently found in biological systems. Its stereochemical flexibility likely contributes to catalysis since it can transiently accept different coordination geometries without impeding catalysis. This property allows expansion of the coordination sphere of the zinc at one step of catalysis and its contraction at another step.

Beyond the challenge of how zinc functions in detail in any given protein is the goal to understand how it is delivered and removed from proteins *in vivo*. The next frontier will likely begin to bring answers to how zinc is stored, transported and distributed and how does it influence the earliest stages of development.

References

Abrahmsen L, Dohlsten M, Segren S, Bjork P, Jonsson E, Kalland T. 1995 Characterization of two distinct MHC class II binding sites in the superantigen staphylococcal enterotoxin A. *EMBO J* **14**, 2978–2986.

Alber BE, Colangelo CM, Dong J, Stalhandske CM, Baird TT, Tu C, Fierke CA, Silverman DN, Scott RA, Ferry JG. 1999 Kinetic and Spectroscopic Characterization of the Gamma-Carbonic Anhydrase from the Methanoarchaeon *Methanosarcina thermophila*. *Biochemistry* **38**, 13119—13128.

Alber BE, Ferry JG. 1994 A carbonic anhydrase from the archaeon *Methanosarcina thermophila*. *Proc Natl Acad Sci USA* **91**, 6909–6913.

Arcus VL, Proft T, Sigrell JA, Baker HM, Fraser JD, Baker EN. 2000 Conservation and variation in superantigen structure and activity highlighted by the three-dimensional structures of two new superantigens from *Streptococcus pyogenes*. *J Mol Biol* **299**, 157–168.

Argos P, Garavito RM, Eventoff W, Rossmann MG, Branden CI. 1978 Similarities in active center geometries of zinc-containing enzymes, proteases and dehydrogenases. *J Mol Biol* **126**, 141–158.

Auerbach G, Herrmann A, Bracher A, Bader G, Gutlich M, Fischer M, Neukamm M, Garrido-Franco M, Richardson J, Nar H, Huber R, Bacher A. 2000 Zinc plays a key role in human and bacterial GTP cyclohydrolase I. *Proc Natl Acad Sci USA* **97**, 13567–13572.

Auld DS. 1987 Acyl group transfer- metalloproteinases. In: Page MI, Williams A, ed. *Enzyme Mechanisms*. London: Royal Society of Chemistry Burlington House; 241–258.

Auld DS. 1992 Astacin family of zinc proteases. *Faraday Discuss* **93**, 117–120.

Auld DS. 1997 Zinc catalysis in metalloproteases. *Structure and Bonding* **89**, 29–50.

Auld DS. 1998a Carboxypeptidase A. In: Barrett AJ, Rawlings ND, Woessner JF, eds. *Handbook of Proteolytic Enzymes*. London: Academic Press; 1321–1326.

Auld DS. 1998b Carboxypeptidase A2. In: Barrett AJ, Rawlings ND, Woessner JF, eds. *Handbook of Proteolytic Enzymes*. London: Academic Press; 1326–1328.

Auld DS. 2001 Zinc Sites in Metalloenzymes and Related Proteins. In: Bertini I, Sigel A, Sigel H, eds. *Handbook on Metalloproteins*. New York: M. Dekker; 881–959.

Auld DS, Vallee BL. 1987 Carboxypeptidase-A. In: Neuberger H, Brocklehurst K, ed. *Hydrolytic Enzymes*. Amsterdam: Elsevier; 201–255.

Aviles FX, Vendrel J. 1998 Carboxypeptidase B. In: Barrett AJ, Rawlings ND, Woessner JF, eds. *Handbook of Proteolytic Enzymes*. London: Academic Press; 1333–1335.

Avvakumov GV, Muller YA, Hammond GL. 2000 Steroid-binding specificity of human sex hormone-binding globulin is influenced by occupancy of a zinc-binding site. *J Biol Chem* **275**, 25920–25925.

Baldwin GS, Galdes A, Hill HA, Smith BE, Waley SG, Abraham EP. 1978 Histidine residues of zinc ligands in beta-lactamase II. *Biochem J* **175**, 441–447.

Banbula A, Potempa J, Travis J, Fernandez-Catalan C, Mann K, Huber R, Bode W, Medrano F. 1998 Amino-acid sequence and three-dimensional structure of the *Staphylococcus aureus* metalloproteinase at 1.72 Å resolution. *Structure* **6**, 1185–1193.

Bannister JV, Bannister WH, Rotilio G. 1987 Aspects of the structure, function, and applications of superoxide dismutase. *CRC Crit Rev Biochem* **22**, 111–180.

Barbato G, Cicero DO, Nardi MC, Steinkuhler C, Cortese R, De Francesco R, Bazzo R. 1999 The solution structure of the N-terminal proteinase domain of the hepatitis C virus (HCV) NS3 protein provides new insights into its activation and catalytic mechanism. *J Mol Biol* **289**, 371–384.

Barrett AJ, Rawlings ND. 2001 MEROPS the Peptidase Database. http://www.merops.co.uk.

Barrett AJ, Rawlings ND, Woessner JF. 1998 Introduction: Clan MC containing metallocarboxypeptidases. In: Barrett AJ, Rawlings ND, Woessner JF, eds. *Handbook of Proteolytic Enzymes*. London: Academic Press; 1318–1320.

Baumann U. 1994 Crystal structure of the 50 kDa metallo protease from *Serratia marcescens*. *J Mol Biol* **242**, 244–251.

Baumann U, Bauer M, Letoffe S, Delepelaire P, Wandersman C. 1995 Crystal structure of a complex between *Serratia*

marcescens metallo-protease and an inhibitor from *Erwinia chrysanthemi*. *J Mol Biol* **248**, 653–661.

Baumann U, Wu S, Flaherty KM, McKay DB. 1993 Three-dimensional structure of the alkaline protease of *Pseudomonas aeruginosa*: a two-domain protein with a calcium binding parallel beta roll motif. *EMBO J* **12**, 3357–3364.

Bax B, Blundell TL, Murray-Rust J, McDonald NQ. 1997 Structure of mouse 7S NGF: a complex of nerve growth factor with four binding proteins. *Structure* **5**, 1275–1285.

Becker A, Schlichting I, Kabsch W, Groche D, Schultz S, Wagner AF. 1998 Iron center, substrate recognition and mechanism of peptide deformylase. *Nat Struct Biol* **5**, 1053–1058.

Becker JW, Marcy AI, Rokosz LL, Axel MG, Burbaum JJ, Fitzgerald PM, Cameron PM, Esser CK, Hagmann WK, Hermes JD, Springer JP. 1995 Stromelysin-1: three-dimensional structure of the inhibited catalytic domain and of the C-truncated proenzyme. *Protein Sci* **4**, 1966–1976.

Benning MM, Kuo JM, Raushel FM, Holden HM. 1994 Three-dimensional structure of phosphotriesterase: an enzyme capable of detoxifying organophosphate nerve agents. *Biochemistry* **33**, 15001–15007.

Berg JM, Shi Y. 1996 The galvanization of biology: a growing appreciation for the roles of zinc. *Science* **271**, 1081–1085.

Berry MB, Phillips GN, Jr. 1998 Crystal structures of *Bacillus stearothermophilus* adenylate kinase with bound Ap5A, Mg^{2+} Ap5A, and Mn^{2+} Ap5A reveal an intermediate lid position and six coordinate octahedral geometry for bound Mg^{2+} and Mn^{2+}. *Proteins* **32**, 276–288.

Bertini I, Lanini G, Luchinat C, Haas C, Maret W, Zeppezauer M. 1987 The influence of anions and inhibitors on the catalytic metal ion in Co(II)-substituted horse liver alcohol dehydrogenase. *Eur Biophys J* **14**, 431–439.

Betts L, Xiang S, Short SA, Wolfenden R, Carter CW, Jr. 1994 Cytidine deaminase. The 2.3 Å crystal structure of an enzyme: transition–state analog complex. *J Mol Biol* **235**, 635–656.

Betz M, Huxley P, Davies SJ, Mushtaq Y, Pieper M, Tschesche H, Bode W, Gomis-Ruth FX. 1997 1.8-Å crystal structure of the catalytic domain of human neutrophil collagenase (matrix metalloproteinase-8) complexed with a peptidomimetic hydroxamate primed-side inhibitor with a distinct selectivity profile. *Eur J Biochem* **247**, 356–363.

Bixby KA, Nanao MH, Shen NV, Kreusch A, Bellamy H, Pfaffinger PJ, Choe S. 1999 Zn^{2+}-binding and molecular determinants of tetramerization in voltage-gated K^+ channels. *Nat Struct Biol* **6**, 38–43.

Bode W, Gomis-Ruth FX, Huber R, Zwilling R, Stocker W. 1992 Structure of astacin and implications for activation of astacins and zinc-ligation of collagenases. *Nature* **358**, 164–167.

Bode W, Reinemer P, Huber R, Kleine T, Schnierer S, Tschesche H. 1994 The X-ray crystal structure of the catalytic domain of human neutrophil collagenase inhibited by a substrate analogue reveals the essentials for catalysis and specificity. *EMBO J* **13**, 1263–1269.

Borden KL, Lally JM, Martin SR, O'Reilly NJ, Etkin LD, Freemont PS. 1995 Novel topology of a zinc-binding domain from a protein involved in regulating early *Xenopus* development. *EMBO J* **14**, 5947–5956.

Boriack-Sjodin PA, Heck RW, Laipis PJ, Silverman DN, Christianson DW. 1995 Structure determination of murine mitochondrial carbonic anhydrase V at 2.45-Å resolution: implications for catalytic proton transfer and inhibitor design. *Proc Natl Acad Sci USA* **92**, 10949–10953.

Botos I, Meyer E, Swanson SM, Lemaitre V, Eeckhout Y, Meyer EF. 1999 Structure of recombinant mouse collagenase-3 (MMP-13). *J Mol Biol* **292**, 837–844.

Bourne Y, Redford SM, Steinman HM, Lepock JR, Tainer JA, Getzoff ED. 1996 Novel dimeric interface and electrostatic recognition in bacterial Cu,Zn superoxide dismutase. *Proc Natl Acad Sci USA* **93**, 12774–12779.

Bracey MH, Christiansen J, Tovar P, Cramer SP, Bartlett SG. 1994 Spinach carbonic anhydrase: investigation of the zinc-binding ligands by site-directed mutagenesis, elemental analysis, and EXAFS. *Biochemistry* **33**, 13126–13131.

Brodersen DE, Nyborg J, Kjeldgaard M. 1999 Zinc-binding site of an S100 protein revealed. Two crystal structures of Ca^{2+}-bound human psoriasin (S100A7) in the Zn^{2+}-loaded and Zn^{2+}-free states. *Biochemistry* **38**, 1695–1704.

Browner MF, Smith WW, Castelhano AL. 1995 Matrilysin-inhibitor complexes: common themes among metalloproteases. *Biochemistry* **34**, 6602–6610.

Buchbinder JL, Stephenson RC, Dresser MJ, Pitera JW, Scanlan TS, Fletterick RJ. 1998 Biochemical characterization and crystallographic structure of an *Escherichia coli* protein from the phosphotriesterase gene family [published erratum appears in Biochemistry 1998 Jul 28;**37**(30):10860]. *Biochemistry* **37**, 5096–5106.

Bukrinsky JT, Bjerrum MJ, Kadziola A. 1998 Native carboxypeptidase A in a new crystal environment reveals a different conformation of the important tyrosine 248. *Biochemistry* **37**, 16555–16564.

Burgisser DM, Thony B, Redweik U, Hess D, Heizmann CW, Huber R, Nar H. 1995 6-Pyruvoyl tetrahydropterin synthase, an enzyme with a novel type of active site involving both zinc binding and an intersubunit catalytic triad motif; site-directed mutagenesis of the proposed active center, characterization of the metal binding site and modelling of substrate binding. *J Mol Biol* **253**, 358–369.

Burley SK, David PR, Sweet RM, Taylor A, Lipscomb WN. 1992 Structure determination and refinement of bovine lens leucine aminopeptidase and its complex with bestatin. *J Mol Biol* **224**, 113–140.

Bussiere DE, Pratt SD, Katz L, Severin JM, Holzman T, Park CH. 1998 The structure of VanX reveals a novel amino-dipeptidase involved in mediating transposon-based vancomycin resistance. *Mol Cell* **2**, 75–84.

Cai M, Zheng R, Caffrey M, Craigie R, Clore GM, Gronenborn AM. 1997 Solution structure of the N-terminal zinc binding domain of HIV-1 integrase [published erratum appears in Nat Struct Biol 1997 Oct; **4**(10): 839–840]. *Nat Struct Biol* **4**, 567–577.

Cameron AD, Olin B, Ridderstrom M, Mannervik B, Jones TA. 1997 Crystal structure of human glyoxalase I–evidence for gene duplication and 3D domain swapping. *EMBO J* **16**, 3386–3395.

Cameron AD, Ridderstrom M, Olin B, Kavarana MJ, Creighton DJ, Mannervik B. 1999a Reaction mechanism of glyoxalase I explored by an X-ray crystallographic analysis of the human enzyme in complex with a transition state analogue. *Biochemistry* **38**, 13480–13490.

Cameron AD, Ridderstrom M, Olin B, Mannervik B. 1999b Crystal structure of human glyoxalase II and its complex with a glutathione thiolester substrate analogue. *Structure Fold Des* **7**, 1067–1078.

Carfi A, Duee E, Galleni M, Frere JM, Dideberg O. 1998a 1.85 Å resolution structure of the zinc (II) beta-lactamase from *Bacillus cereus*. *Acta Cryst D* **54**, 313–323.

Carfi A, Duee E, Paul-Soto R, Galleni M, Frere JM, Dideberg O. 1998b X-ray structure of the ZnII beta-lactamase from *Bac-*

teroides fragilis in an orthorhombic crystal form. *Acta Cryst D Biol Cryst* **54**, 45–57.

Carfi A, Pares S, Duee E, Galleni M, Duez C, Frere JM, Dideberg O. 1995 The 3-D structure of a zinc metallo-beta-lactamase from *Bacillus cereus* reveals a new type of protein fold. *EMBO J* **14**, 4914–4921.

Carlow DC, Carter CW, Jr., Mejlhede N, Neuhard J, Wolfenden R. 1999 Cytidine Deaminases from *B. subtilis* and *E. coli*: Compensating effects of changing zinc coordination and quaternary structure. *Biochemistry* **38**, 12258–12265.

Carugo KD, Battistoni A, Carri MT, Polticelli F, Desideri A, Rotilio G, Coda A, Bolognesi M. 1994 Crystal structure of the cyanide-inhibited *Xenopus laevis* Cu,Zn superoxide dismutase at 98 K. *FEBS Lett* **349**, 93–98.

Cha J, Auld DS. 1997 Site-directed mutagenesis of the active site glutamate in human matrilysin: investigation of its role in catalysis. *Biochemistry* **36**, 16019–16024.

Chan MK, Gong W, Rajagopalan PT, Hao B, Tsai CM, Pei D. 1997 Crystal structure of the *Escherichia coli* peptide deformylase [published erratum appears in Biochemistry 1998 Sep 15; **37**(37): 13042]. *Biochemistry* **36**, 13904–13909.

Chantalat L, Leroy D, Filhol O, Nueda A, Benitez MJ, Chambaz EM, Cochet C, Dideberg O. 1999 Crystal structure of the human protein kinase CK2 regulatory subunit reveals its zinc finger-mediated dimerization. *EMBO J* **18**, 2930–2940.

Chen L, Rydel TJ, Gu F, Dunaway CM, Pikul S, Dunham KM, Barnett BL. 1999 Crystal structure of the stromelysin catalytic domain at 2.0 Å resolution: inhibitor-induced conformational changes. *J Mol Biol* **293**, 545–557.

Chen YL, Park S, Thornburg RW, Tabatabai LB, Kintanar A. 1995 Structural characterization of the active site of *Brucella abortus* Cu-Zn superoxide dismutase: a 15N and 1H NMR investigation. *Biochemistry* **34**, 12265–12275.

Cheng X, Zhang X, Pflugrath JW, Studier FW. 1994 The structure of bacteriophage T7 lysozyme, a zinc amidase and an inhibitor of T7 RNA polymerase. *Proc Natl Acad Sci USA* **91**, 4034–4038.

Chevrier B, D'Orchymont H, Schalk C, Tarnus C, Moras D. 1996 The structure of the *Aeromonas proteolytica* aminopeptidase complexed with a hydroxamate inhibitor. Involvement in catalysis of Glu151 and two zinc ions of the co–catalytic unit. *Eur J Biochem* **237**, 393–398.

Chevrier B, Schalk C, D'Orchymont H, Rondeau JM, Moras D, Tarnus C. 1994 Crystal structure of *Aeromonas proteolytica* aminopeptidase: a prototypical member of the co-catalytic zinc enzyme family. *Structure* **2**, 283–291.

Cho H, Ramaswamy S, Plapp BV. 1997 Flexibility of liver alcohol dehydrogenase in stereoselective binding of 3-butylthiolane 1-oxides. *Biochemistry* **36**, 382–389.

Chong CR, Auld DS. 2000 Inhibition of carboxypeptidase A by D-pencillamine: Mechanism and implications for drug design. *Biochemistry* **39**, 7580–7588.

Christianson DW, Cox JD. 1999 Catalysis by metal-activated hydroxide in zinc and manganese metalloenzymes. *Annu Rev Biochem* **68**, 33–57.

Christianson DW, Fierke CA. 1996 Carbonic anhydrase: Evolution of the design of the zinc binding site by nature and by design. *Acc Chem Res* **29**, 331–339.

Christianson DW, Lipscomb WN. 1989 Carboxypeptidase A. *Acc Chem Res* **22**, 62–69.

Cleasby A, Wonacott A, Skarzynski T, Hubbard RE, Davies GJ, Proudfoot AE, Bernard AR, Payton MA, Wells TN. 1996 The X-ray crystal structure of phosphomannose isomerase from *Candida albicans* at 1.7 angstrom resolution. *Nat Struct Biol* **3**, 470–479.

Clugston SL, Barnard JF, Kinach R, Miedema D, Ruman R, Daub E, Honek JF. 1998 Overproduction and characterization of a dimeric non-zinc glyoxalase I from *Escherichia coli*: evidence for optimal activation by nickel ions. *Biochemistry* **37**, 8754–8763.

Coleman JE. 1992 Structure and mechanism of alkaline phosphatase. *Annu Rev Biophys Biomol Struct* **21**, 441–483.

Coleman JE. 1998 Zinc enzymes. *Curr Opin Chem Biol* **2**, 222–234.

Coll M, Guasch A, Aviles FX, Huber R. 1991 Three-dimensional structure of porcine procarboxypeptidase B: a structural basis of its inactivity. *EMBO J* **10**, 1–9.

Colonna-Cesari F, Perahia D, Karplus M, Eklund H, Branden CI, Tapia O. 1986 Interdomain motion in liver alcohol dehydrogenase. Structural and energetic analysis of the hinge bending mode. *J Biol Chem* **261**, 15273–15280.

Concha NO, Janson CA, Rowling P, Pearson S, Cheever CA, Clarke BP, Lewis C, Galleni M, Frere JM, Payne DJ, Bateson JH, Abdel-Meguid SS. 2000 Crystal structure of the IMP-1 metallo beta-lactamase from *Pseudomonas aeruginosa* and its complex with a mercaptocarboxylate inhibitor: binding determinants of a potent, broad-spectrum inhibitor. *Biochemistry* **39**, 4288–4298.

Concha NO, Rasmussen BA, Bush K, Herzberg O. 1996 Crystal structure of the wide-spectrum binuclear zinc beta-lactamase from *Bacteroides fragilis*. *Structure* **4**, 823–836.

Crane BR, Arvai AS, Ghosh DK, Wu C, Getzoff ED, Stuehr DJ, Tainer JA. 1998 Structure of nitric oxide synthase oxygenase dimer with pterin and substrate. *Science* **279**, 2121–2126.

Daniels DS, Mol CD, Arvai AS, Kanugula S, Pegg AE, Tainer JA. 2000 Active and alkylated human AGT structures: a novel zinc site, inhibitor and extrahelical base binding. *EMBO J* **19**, 1719–1730.

Davis GJ, Bosron WF, Stone CL, Owusu-Dekyi K, Hurley TD. 1996 X-ray structure of human beta3beta3 alcohol dehydrogenase. The contribution of ionic interactions to coenzyme binding. *J Biol Chem* **271**, 17057–17061.

De Francesco R, Urbani A, Nardi MC, Tomei L, Steinkuhler C, Tramontano A. 1996 A zinc binding site in viral serine proteinases. *Biochemistry* **35**, 13282–13287.

Dhanaraj V, Ye QZ, Johnson LL, Hupe DJ, Ortwine DF, Dunbar JB, Jr., Rubin JR, Pavlovsky A, Humblet C, Blundell TL. 1996 X-ray structure of a hydroxamate inhibitor complex of stromelysin catalytic domain and its comparison with members of the zinc metalloproteinase superfamily. *Structure* **4**, 375–386.

Ding YH, Javaherian K, Lo KM, Chopra R, Boehm T, Lanciotti J, Harris BA, Li Y, Shapiro R, Hohenester E, Timpl R, Folkman J, Wiley DC. 1998 Zinc-dependent dimers observed in crystals of human endostatin. *Proc Natl Acad Sci USA* **95**, 10443–10448.

Djinovic K, Gatti G, Coda A, Antolini L, Pelosi G, Desideri A, Falconi M, Marmocchi F, Rotilio G, Bolognesi M. 1992 Crystal structure of yeast Cu,Zn superoxide dismutase. Crystallographic refinement at 2.5 Å resolution. *J Mol Biol* **225**, 791–809.

Doss M, von Tiepermann R, Schneider J, Schmid H. 1979 New type of hepatic porphyria with porphobilinogen synthase defect and intermittent acute clinical manifestation. *Klin Wochenschr* **57**, 1123–1127.

Dreyer MK, Schulz GE. 1993 The spatial structure of the class II L-fuculose-1-phosphate aldolase from *Escherichia coli*. *J Mol Biol* **231**, 549–553.

Dreyer MK, Schulz GE. 1996 Catalytic mechanism of the metal-dependent fuculose aldolase from *Escherichia coli* as derived from the structure. *J Mol Biol* **259**, 458–466.

D'Souza VM, Holz RC. 1999 The methionyl aminopeptidase from *Escherichia coli* can function as an iron(II) enzyme. *Biochemistry* **38**, 11079–11085.

Dumermuth E, Sterchi EE, Jiang WP, Wolz RL, Bond JS, Flannery AV, Beynon RJ. 1991 The astacin family of metalloendopeptidases. *J Biol Chem* **266**, 21381–21385.

Earhart CA, Vath GM, Roggiani M, Schlievert PM, Ohlendorf DH. 2000 Structure of streptococcal pyrogenic exotoxin A reveals a novel metal cluster. *Protein Sci* **9**, 1847–1851.

Egloff MP, Cohen PT, Reinemer P, Barford D. 1995 Crystal structure of the catalytic subunit of human protein phosphatase 1 and its complex with tungstate. *J Mol Biol* **254**, 942–959.

Eijkelenboom AP, van den Ent FM, Vos A, Doreleijers JF, Hard K, Tullius TD, Plasterk RH, Kaptein R, Boelens R. 1997 The solution structure of the amino-terminal HHCC domain of HIV-2 integrase: a three-helix bundle stabilized by zinc. *Curr Biol* **7**, 739–746.

Eijkelenboom AP, van den Ent FM, Wechselberger R, Plasterk RH, Kaptein R, Boelens R. 2000 Refined solution structure of the dimeric N-terminal HHCC domain of HIV-2 integrase. *J Biomol NMR* **18**, 119–128.

Eklund H. 1989 Coenzyme binding in alcohol dehydrogenase. *Biochem Soc Trans* **17**, 293–296.

Eklund H, Branden CI. 1987 Alcohol Dehydrogenase. In: Jurnak FA, McPherson A. eds. *Biological Macromolecules and Assemblies: Vol. 3, Active Sites of Enzumes*. New York: John Wiley & Sons, Inc; 73–143.

Eklund H, Nordstrom B, Zeppezauer E, Soderlund G, Ohlsson I, Boiwe T, Branden CI. 1974 The structure of horse liver alcohol dehydrogenase. *FEBS Lett.* **44**, 200–204.

Eklund H, Nordstrom B, Zeppezauer E, Soderlund G, Ohlsson I, Boiwe T, Soderberg BO, Tapia O, Branden CI, Akeson A. 1976 Three-dimensional structure of horse liver alcohol dehydrogenase at 2–4 Å resolution. *J Mol Biol* **102**, 27–59.

Eklund H, Samama JP, Wallen L, Branden CI, Akeson A, Jones TA. 1981 Structure of a triclinic ternary complex of horse liver alcohol dehydrogenase at 2.9 Å resolution. *J Mol Biol* **146**, 561–587.

Eriksson AE, Liljas A. 1993 Refined structure of bovine carbonic anhydrase III at 2.0 Å resolution. *Proteins* **16**, 29–42.

Erskine PT, Duke EM, Tickle IJ, Senior NM, Warren MJ, Cooper JB. 2000 MAD analyses of yeast 5-aminolaevulinate dehydratase: their use in structure determination and in defining the metal-binding sites. *Acta Cryst D* **56**, 421–430.

Erskine PT, Newbold R, Roper J, Coker A, Warren MJ, Shoolingin-Jordan PM, Wood SP, Cooper JB. 1999a The Schiff base complex of yeast 5-aminolaevulinic acid dehydratase with laevulinic acid. *Protein Sci* **8**, 1250–1256.

Erskine PT, Norton E, Cooper JB, Lambert R, Coker A, Lewis G, Spencer P, Sarwar M, Wood SP, Warren MJ, Shoolingin-Jordan PM. 1999b X-ray structure of 5-aminolevulinic acid dehydratase from *Escherichia coli* complexed with the inhibitor levulinic acid at 2.0 Å resolution. *Biochemistry* **38**, 4266–4276.

Erskine PT, Senior N, Awan S, Lambert R, Lewis G, Tickle IJ, Sarwar M, Spencer P, Thomas P, Warren MJ, Shoolingin-Jordan PM, Wood SP, Cooper JB. 1997 X-ray structure of 5-aminolaevulinate dehydratase, a hybrid aldolase. *Nat Struc Biol* **4**, 1025–1031.

Estevez AG, Crow JP, Sampson JB, Reiter C, Zhuang Y, Richardson GJ, Tarpey MM, Barbeito L, Beckman JS. 1999 Induction of nitric oxide-dependent apoptosis in motor neurons by zinc-deficient superoxide dismutase. *Science* **286**, 2498–2500.

Fabiane SM, Sohi MK, Wan T, Payne DJ, Bateson JH, Mitchell T, Sutton BJ. 1998 Crystal structure of the zinc-dependent beta-lactamase from *Bacillus cereus* at 1.9 Å resolution: binuclear active site with features of a mononuclear enzyme. *Biochemistry* **37**, 12404–12411.

Faming Z, Kobe B, Stewart CB, Rutter WJ, Goldsmith EJ. 1991 Structural evolution of an enzyme specificity. The structure of rat carboxypeptidase A2 at 1.9 Å- resolution. *J Biol Chem* **266**, 24606–24612.

Feese M, Pettigrew DW, Meadow ND, Roseman S, Remington SJ. 1994 Cation-promoted association of a regulatory and target protein is controlled by protein phosphorylation. *Proc Natl Acad Sci USA* **91**, 3544–3548.

Feese MD, Comolli L, Meadow ND, Roseman S, Remington SJ. 1997 Structural studies of the *Escherichia coli* signal transducing protein IIAGlc: implications for target recognition. *Biochemistry* **36**, 16087–16096.

Fischmann TO, Hruza A, Niu XD, Fossetta JD, Lunn CA, Dolphin E, Prongay AJ, Reichert P, Lundell DJ, Narula SK, Weber PC. 1999 Structural characterization of nitric oxide synthase isoforms reveals striking active-site conservation. *Nat Struct Biol* **6**, 233–242.

Forest KT, Langford PR, Kroll JS, Getzoff ED. 2000 Cu,Zn superoxide dismutase structure from a microbial pathogen establishes a class with a conserved dimer interface. *J Mol Biol* **296**, 145–153.

Fourmy D, Dardel F, Blanquet S. 1993a Methionyl-tRNA synthetase zinc binding domain. Three–dimensional structure and homology with rubredoxin and gag retroviral proteins. *J Mol Biol* **231**, 1078–1089.

Fourmy D, Meinnel T, Mechulam Y, Blanquet S. 1993b Mapping of the zinc binding domain of *Escherichia coli* methionyl-tRNA synthetase. *J Mol Biol* **231**, 1068–1077.

Frankenberg N, Jahn D, Jaffe EK. 1999 *Pseudomonas aeruginosa* contains a novel type V porphobilinogen synthase with no required catalytic metal ions. *Biochemistry* **38**, 13976–13982.

Fraser J, Arcus V, Kong P, Baker E, Proft T. 2000 Superantigens - powerful modifiers of the immune system. *Mol Med Today* **6**, 125–132.

Fraser JD, Urban RG, Strominger JL, Robinson H. 1992 Zinc regulates the function of two superantigens. *Proc Natl Acad Sci USA* **89**, 5507–5511.

Fujii T, Hata Y, Wakagi T, Tanaka N, Oshima T. 1996 Novel zinc-binding centre in thermoacidophilic archaeal ferredoxins [letter]. *Nat Struct Biol* **3**, 834–837.

Fujinaga M, James MN. 1987 Rat submaxillary gland serine protease, tonin. Structure solution and refinement at 1.8 Å resolution. *J Mol Biol* **195**, 373–396.

Fukai S, Nureki O, Sekine S, Shimada A, Tao J, Vassylyev DG, Yokoyama S. 2000 Structural basis for double-sieve discrimination of L-valine from L-isoleucine and L-threonine by the complex of tRNA(Val) and valyl-tRNA synthetase. *Cell* **103**, 793–803.

Garcia–Iniguez L, Powers L, Chance B, Sellin S, Mannervik B, Mildvan AS. 1984 X-ray absorption studies of the Zn^{2+} site of glyoxalase I. *Biochemistry* **23**, 685–689.

Garcia–Saez I, Reverter D, Vendrell J, Aviles FX, Coll M. 1997 The three-dimensional structure of human procarboxypeptidase A2. Deciphering the basis of the inhibition, activation and intrinsic activity of the zymogen. *EMBO J* **16**, 6906–6913.

Geeganage S, Frey PA. 1999 Significance of metal ions in galactose-1-phosphate uridylyltransferase: An essential structural zinc and a nonessential structural iron. *Biochemistry* **38**, 13398–133406.

Ghosh DK, Crane BR, Ghosh S, Wolan D, Gachhui R, Crooks C, Presta A, Tainer JA, Getzoff ED, Stuehr DJ. 1999 Inducible ni-

tric oxide synthase: role of the N-terminal beta-hairpin hook and pterin-binding segment in dimerization and tetrahydrobiopterin interaction. *EMBO J* **18**, 6260–6270.

Ghuysen JM. 1988 Evolution of DD-peptidases and beta-lactamases. In: Actor P, Daneo–Moore L, Higgens ML, Salton MRJ, Shockman GD, ed. *Antibiotic Inhibition of Bacterial Cell Surface Assembly and Function*. Washington DC: American Society for Microbiology; 268–284.

Gibbs JB, Oliff A. 1997 The potential of farnesyltransferase inhibitors as cancer chemotherapeutics. *Annu Rev Pharmacol Toxicol* **37**, 143–166.

Gilboa R, Greenblatt HM, Perach M, Spungin-Bialik A, Lessel U, Wohlfahrt G, Schomburg D, Blumberg S, Shoham G. 2000 Interactions of *Streptomyces griseus* aminopeptidase with a methionine product analogue: a structural study at 1.53 Å resolution. *Acta Cryst D* **56**, 551–558.

Gomis-Ruth FX, Companys V, Qian Y, Fricker LD, Vendrell J, Aviles FX, Coll M. 1999 Crystal structure of avian carboxypeptidase D domain II: a prototype for the regulatory metallocarboxypeptidase subfamily. *EMBO J* **18**, 5817–5826.

Gomis-Ruth FX, Gomez M, Bode W, Huber R, Aviles FX. 1995 The three-dimensional structure of the native ternary complex of bovine pancreatic procarboxypeptidase A with proproteinase E and chymotrypsinogen C. *EMBO J* **14**, 4387–4394.

Gomis-Ruth FX, Kress LF, Bode W. 1993a First structure of a snake venom metalloproteinase: a prototype for matrix metalloproteinases/collagenases. *EMBO J* **12**, 4151–4157.

Gomis-Ruth FX, Kress LF, Kellermann J, Mayr I, Lee X, Huber R, Bode W. 1994 Refined 2.0 Å X-ray crystal structure of the snake venom zinc-endopeptidase adamalysin II. Primary and tertiary structure determination, refinement, molecular structure and comparison with astacin, collagenase and thermolysin. *J Mol Biol* **239**, 513–544.

Gomis-Ruth FX, Stocker W, Huber R, Zwilling R, Bode W. 1993b Refined 1.8 Å X-ray crystal structure of astacin, a zinc-endopeptidase from the crayfish *Astacus astacus* L. Structure determination, refinement, molecular structure and comparison with thermolysin. *J Mol Biol* **229**, 945–968.

Gong W, Zhu X, Liu S, Teng M, Niu L. 1998 Crystal structures of acutolysin A, a three-disulfide hemorrhagic zinc metalloproteinase from the snake venom of *Agkistrodon acutus*. *J Mol Biol* **283**, 657–668.

Gooley PR, O'Connell JF, Marcy AI, Cuca GC, Salowe SP, Bush BL, Hermes JD, Esser CK, Hagmann WK, Springer JP, Johnson BA. 1994 The NMR structure of the inhibited catalytic domain of human stromelysin-1. *Nat Struct Biol* **1**, 111–118.

Grams F, Dive V, Yiotakis A, Yiallouros I, Vassiliou S, Zwilling R, Bode W, Stocker W. 1996 Structure of astacin with a transition-state analogue inhibitor [letter]. *Nat Struct Biol* **3**, 671–675.

Greenblatt HM, Almog O, Maras B, Spungin-Bialik A, Barra D, Blumberg S, Shoham G. 1997 *Streptomyces griseus* aminopeptidase: X-ray crystallographic structure at 1.75 Å resolution. *J Mol Biol* **265**, 620–636.

Griffith JP, Kim JL, Kim EE, Sintchak MD, Thomson JA, Fitzgibbon MJ, Fleming MA, Caron PR, Hsiao K, Navia MA. 1995 X-ray structure of calcineurin inhibited by the immunophilin-immunosuppressant FKBP12-FK506 complex. *Cell* **82**, 507–522.

Guasch A, Coll M, Aviles FX, Huber R. 1992 Three-dimensional structure of porcine pancreatic procarboxypeptidase A. A comparison of the A and B zymogens and their determinants for inhibition and activation. *J Mol Biol* **224**, 141–157.

Guddat LW, McAlpine AS, Hume D, Hamilton S, de Jersey J, Martin JL. 1999 Crystal structure of mammalian purple acid phosphatase. *Structure Fold Des* **7**, 757–767.

Guenther B, Onrust R, Sali A, O'Donnell M, Kuriyan J. 1997 Crystal structure of the delta' subunit of the clamp–loader complex of *E. coli* DNA polymerase III. *Cell* **91**, 335–345.

Haeggstrom JZ, Wetterholm A, Shapiro R, Vallee BL, Samuelsson B. 1990 Leukotriene A4 hydrolase: a zinc metalloenzyme. *Biochem Biophys Res Commun* **172**, 965–700.

Hakansson M, Petersson K, Nilsson H, Forsberg G, Bjork P, Antonsson P, Svensson LA. 2000 The crystal structure of staphylococcal enterotoxin H: implications for binding properties to MHC class II and TcR molecules. *J Mol Biol* **302**, 527–537.

Hall TM, Porter JA, Beachy PA, Leahy DJ. 1995 A potential catalytic site revealed by the 1.7-Å crystal structure of the amino-terminal signalling domain of Sonic hedgehog. *Nature* **378**, 212–216.

Hamada K, Hata Y, Katsuya Y, Hiramatsu H, Fujiwara T, Katsube Y. 1996 Crystal structure of Serratia protease, a zinc-dependent proteinase from *Serratia sp.* E-15, containing a beta-sheet coil motif at 2.0 Å resolution. *J Biochem (Tokyo)* **119**, 844–851.

Hard T, Rak A, Allard P, Kloo L, Garber M. 2000 The solution structure of ribosomal protein L36 from *Thermus thermophilus* reveals a zinc-ribbon-like fold. *J Mol Biol* **296**, 169–180.

He MM, Clugston SL, Honek JF, Matthews BW. 2000 Determination of the structure of *Escherichia coli* glyoxalase I suggests a structural basis for differential metal activation. *Biochemistry* **39**, 8719–8727.

Hernandez Valladares M, Felici A, Weber G, Adolph HW, Zeppezauer M, Rossolini GM, Amicosante G, Frere JM, Galleni M. 1997 Zn(II) dependence of the *Aeromonas hydrophila* AE036 metallo-beta-lactamase activity and stability. *Biochemistry* **36**, 11534–11541.

Hewett-Emmett D, Tashian RE. 1996 Functional diversity, conservation, and convergence in the evolution of the alpha-, beta-, and gamma-carbonic anhydrase gene families. *Mol Phylogenet Evol* **5**, 50–77.

Hohenester E, Sasaki T, Mann K, Timpl R. 2000 Variable zinc coordination in endostatin. *J Mol Biol* **297**, 1–6.

Holland DR, Hausrath AC, Juers D, Matthews BW. 1995 Structural analysis of zinc substitutions in the active site of thermolysin. *Protein Sci* **4**, 1955–1965.

Holtz KM, Stec B, Kantrowitz ER. 1999 A model of the transition state in the alkaline phosphatase reaction. *J Biol Chem* **274**, 8351–8354.

Hommel U, Zurini M, Luyten M. 1994 Solution structure of a cysteine rich domain of rat protein kinase C. *Nat Struct Biol* **1**, 383–387.

Honzatko RB, Crawford JL, Monaco HL, Ladner JE, Ewards BF, Evans DR, Warren SG, Wiley DC, Ladner RC, Lipscomb WN. 1982 Crystal and molecular structures of native and CTP-liganded aspartate carbamoyltransferase from *Escherichia coli*. *J Mol Biol* **160**, 219–263.

Hosfield DJ, Guan Y, Haas BJ, Cunningham RP, Tainer JA. 1999 Structure of the DNA repair enzyme endonuclease IV and its DNA complex: double-nucleotide flipping at abasic sites and three-metal-ion catalysis. *Cell* **98**, 397–408.

Hough E, Hansen LK, Birknes B, Jynge K, Hansen S, Hordvik A, Little C, Dodson E, Derewenda Z. 1989 High-resolution (1.5 Å) crystal structure of phospholipase C from *Bacillus cereus*. *Nature* **338**, 357–360.

Huang CC, Casey PJ, Fierke CA. 1997 Evidence for a catalytic role of zinc in protein farnesyltransferase. Spectroscopy of Co^{2+}-

farnesyltransferase indicates metal coordination of the substrate thiolate. *J Biol Chem* **272**, 20–23.

Huang S, Xue Y, Sauer-Eriksson E, Chirica L, Lindskog S, Jonsson BH. 1998 Crystal structure of carbonic anhydrase from *Neisseria gonorrhoeae* and its complex with the inhibitor acetazolamide. *J Mol Biol* **283**, 301–310.

Hubbard SR, Bishop WR, Kirschmeier P, George SJ, Cramer SP, Hendrickson WA. 1991 Identification and characterization of zinc binding sites in protein kinase C. *Science* **254**, 1776–1179.

Hunt JA, Ahmed M, Fierke CA. 1999 Metal binding specificity in carbonic anhydrase is influenced by conserved hydrophobic core residues. *Biochemistry* **38**, 9054–9062.

Hurley JH, Newton AC, Parker PJ, Blumberg PM, Nishizuka Y. 1997 Taxonomy and function of C1 protein kinase C homology domains. *Protein Sci* **6**, 477–480.

Hurley TD, Bosron WF, Hamilton JA, Amzel LM. 1991 Structure of human beta 1 beta 1 alcohol dehydrogenase: catalytic effects of non-active-site substitutions. *Proc Natl Acad Sci USA* **88**, 8149–8153.

Hurley TD, Bosron WF, Stone CL, Amzel LM. 1994 Structures of three human beta alcohol dehydrogenase variants. Correlations with their functional differences. *J Mol Biol* **239**, 415–429.

Hymowitz SG, O'Connell MP, Ultsch MH, Hurst A, Totpal K, Ashkenazi A, de Vos AM, Kelley RF. 2000 A unique zinc-binding site revealed by a high-resolution X-ray structure of homotrimeric Apo2L/TRAIL. *Biochemistry* **39**, 633–640.

Hyvonen M, Saraste M. 1997 Structure of the PH domain and Btk motif from Bruton's tyrosine kinase: molecular explanations for X-linked agammaglobulinaemia. *EMBO J* **16**, 3396–3404.

Ichikawa S, Hatanaka H, Takeuchi Y, Ohno S, Inagaki F. 1995 Solution structure of cysteine-rich domain of protein kinase C alpha. *J Biochem (Tokyo)* **117**, 566–574.

Iverson TM, Alber BE, Kisker C, Ferry JG, Rees DC. 2000 A closer look at the active site of gamma-class carbonic anhydrases: high-resolution crystallographic studies of the carbonic anhydrase from *Methanosarcina thermophila*. *Biochemistry* **39**, 9222–9231.

Iwasaki T, Suzuki T, Kon T, Imai T, Urushiyama A, Ohmori D, Oshima T. 1997 Novel zinc-containing ferredoxin family in *thermoacidophilic archaea*. *J Biol Chem* **272**, 3453–3458.

Jaffe EK. 2000 The porphobilinogen synthase family of metalloenzymes. *Acta Cryst D* **56**, 115–128.

Joerger AC, Mueller-Dieckmann C, Schulz GE. 2000 Structures of l-fuculose-1-phosphate aldolase mutants outlining motions during catalysis. *J Mol Biol* **303**, 531–543.

Jornvall H, Hoog JO. 1995 Nomenclature of alcohol dehydrogenases. *Alcohol Alcohol* **30**, 153–161.

Jornvall H, Hoog JO, von Bahr-Lindstrom H, Vallee BL. 1987 Mammalian alcohol dehydrogenases of separate classes: intermediates between different enzymes and intraclass isozymes. *Proc Natl Acad Sci USA* **84**, 2580–2584.

Kannan KK, Notstrand B, Fridborg K, Lovgren S, Ohlsson A, Petef M. 1975 Crystal structure of human erythrocyte carbonic anhydrase B. Three-dimensional structure at a nominal 2.2-Å resolution. *Proc Natl Acad Sci USA* **72**, 51–55.

Karlin S, Zhu ZY, Karlin KD. 1998 Extended metal environments of cytochrome c oxidase structures. *Biochemistry* **37**, 17726–17734.

Karp DR, Long EO. 1992 Identification of HLA–DR1 beta chain residues critical for binding staphylococcal enterotoxins A and E. *J Exp Med* **175**, 415–424.

Karpusas M, Nolte M, Benton CB, Meier W, Lipscomb WN, Goelz S. 1997 The crystal structure of human interferon beta at 2.2-Å resolution. *Proc Natl Acad Sci USA* **94**, 11813–11818.

Kim EE, Wyckoff HW. 1991 Reaction mechanism of alkaline phosphatase based on crystal structures. Two-metal ion catalysis. *J Mol Biol* **218**, 449–464.

Kim H, Lipscomb WN. 1994 Structure and mechanism of bovine lens leucine aminopeptidase. *Adv Enzymol Relat Areas Mol Biol* **68**, 153–213.

Kimber MS, Pai EF. 2000 The active site architecture of *Pisum sativum* beta-carbonic anhydrase is a mirror image of that of alpha-carbonic anhydrases. *EMBO J* **19**, 1407–1418.

Kisker C, Schindelin H, Alber BE, Ferry JG, Rees DC. 1996 A left-hand beta-helix revealed by the crystal structure of a carbonic anhydrase from the archaeon *Methanosarcina thermophila*. *EMBO J* **15**, 2323–2330.

Kissinger CR, Parge HE, Knighton DR, Lewis CT, Pelletier LA, Tempczyk A, Kalish VJ, Tucker KD, Showalter RE, Moomaw EW, Gastinel LN, Habuka N, Chen X, Maldonado F, Baker JE, Bacquet R, Villefranco JE. 1995 Crystal structures of human calcineurin and the human FKBP12-FK506-calcineurin complex. *Nature* **378**, 641–644.

Kitagawa Y, Tanaka N, Hata Y, Kusunoki M, Lee GP, Katsube Y, Asada K, Aibara S, Morita Y. 1991 Three-dimensional structure of Cu,Zn-superoxide dismutase from spinach at 2.0 Å resolution. *J Biochem (Tokyo)* **109**, 477–485.

Klabunde T, Krebs B. 1997 The dimetal centre in purple acid phosphatases. *Structure and Bonding* **89**, 177–198.

Klabunde T, Strater N, Frohlich R, Witzel H, Krebs B. 1996 Mechanism of Fe(III)-Zn(II) purple acid phosphatase based on crystal structures. *J Mol Biol* **259**, 737–748.

Klinman JP. 1981 Probes of mechanism and transition-state structure in the alcohol dehydrogenase reaction. *CRC Crit Rev Biochem* **10**, 39–78.

Klug A. 1999 Zinc finger peptides for the regulation of gene expression. *J Mol Biol* **293**, 215–218.

Knofel T, Strater N. 1999 X-ray structure of the *Escherichia coli* periplasmic 5'-nucleotidase containing a dimetal catalytic site. *Nat Struct Biol* **6**, 448–453.

Ko TP, Liao CC, Ku WY, Chak KF, Yuan HS. 1999 The crystal structure of the DNase domain of colicin E7 in complex with its inhibitor Im7 protein. *Structure* **7**, 91–102.

Korkhin Y, Kalb AJ, Peretz M, Bogin O, Burstein Y, Frolow F. 1998 NADP-dependent bacterial alcohol dehydrogenases: crystal structure, cofactor-binding and cofactor specificity of the ADHs of *Clostridium beijerinckii* and *Thermoanaerobacter brockii*. *J Mol Biol* **278**, 967–981.

Korndorfer IP, Fessner WD, Matthews BW. 2000 The structure of rhamnose isomerase from *Escherichia coli* and its relation with xylose isomerase illustrates a change between inter and intra-subunit complementation during evolution. *J Mol Biol* **300**, 917–933.

Kumasaka T, Yamamoto M, Moriyama H, Tanaka N, Sato M, Katsube Y, Yamakawa Y, Omori-Satoh T, Iwanaga S, Ueki T. 1996 Crystal structure of H2-proteinase from the venom of *Trimeresurus flavoviridis*. *J Biochem (Tokyo)* **119**, 49–57.

Kurisu G, Kinoshita T, Sugimoto A, Nagara A, Kai Y, Kasai N, Harada S. 1997 Structure of the zinc endoprotease from *Streptomyces caespitosus*. *J Biochem (Tokyo)* **121**, 304–308.

Lacy DB, Stevens RC. 1999 Sequence homology and structural analysis of the clostridial neurotoxins. *J Mol Biol* **291**, 1091–1104.

Lacy DB, Tepp W, Cohen AC, DasGupta BR, Stevens RC. 1998 Crystal structure of botulinum neurotoxin type A and implications for toxicity. *Nat Struct Biol* **5**, 898–902.

Laity JH, Lee BM, Wright PE. 2001 Zinc finger proteins: new insights into structural and functional diversity. *Curr Opin Struct Biol* **11**, 39–46.

Lawrence MC, Pilling PA, Epa VC, Berry AM, Ogunniyi AD, Paton JC. 1998 The crystal structure of pneumococcal surface antigen PsaA reveals a metal-binding site and a novel structure for a putative ABC-type binding protein. *Structure* **6**, 1553–1561.

LeBrun LA, Plapp BV. 1999 Control of coenzyme binding to horse liver alcohol dehydrogenase. *Biochemistry* **38**, 12387–12393.

Lee JY, Chang C, Song HK, Moon J, Yang JK, Kim HK, Kwon ST, Suh SW. 2000 Crystal structure of NAD(+)-dependent DNA ligase: modular architecture and functional implications. *EMBO J* **19**, 1119–1129.

Lee YH, Deka RK, Norgard MV, Radolf JD, Hasemann CA. 1999 *Treponema pallidum* TroA is a periplasmic zinc-binding protein with a helical backbone. *Nat Struct Biol* **6**, 628–633.

Li C, Zhao D, Djebli A, Shoham M. 1999a Crystal structure of colicin E3 immunity protein: an inhibitor of a ribosome-inactivating RNase. *Structure Fold Des* **7**, 1365–1372.

Li H, Raman CS, Glaser CB, Blasko E, Young TA, Parkinson JF, Whitlow M, Poulos TL. 1999b Crystal structures of zinc-free and -bound heme domain of human inducible nitric-oxide synthase. Implications for dimer stability and comparison with endothelial nitric-oxide synthase. *J Biol Chem* **274**, 21276–21284.

Li YC, Zhang X, Melton R, Ganu V, Gonnella NC. 1998 Solution structure of the catalytic domain of human stromelysin-1 complexed to a potent, nonpeptidic inhibitor. *Biochemistry* **37**, 14048–14056.

Li Z, Rasmussen BA, Herzberg O. 1999c Structural consequences of the active site substitution Cys181 $\Longrightarrow$ Ser in metallo-beta-lactamase from *Bacteroides fragilis*. *Protein Sci* **8**, 249–252.

Liljas A, Kannan KK, Bergsten PC, Waara I, Fridborg K, Strandberg B, Carlbom U, Jarup L, Lovgren S, Petef M. 1972 Crystal structure of human carbonic anhydrase C. *Nat New Biol* **235**, 131–137.

Lindahl T. 1993 Instability and decay of the primary structure of DNA. *Nature* **362**, 709–715.

Lindqvist Y, Johansson E, Kaija H, Vihko P, Schneider G. 1999 Three-dimensional structure of a mammalian purple acid phosphatase at 2.2 Å resolution with a mu-(hydr)oxo bridged di-iron center. *J Mol Biol* **291**, 135–147.

Lindskog S, Liljas A. 1993 Carbonic anhydrose and the role of orientation in catalysis. *Cur Opin Struct Biol* **3**, 915–920.

Lipscomb WN, Strater N. 1996 Recent advances in zinc enzymology. *Chem Rev* **96**, 2375–2433.

Liu L, Hausladen A, Zeng M, Que L, Heitman J, Stamler JS. 2001 A metabolic enzyme for S-nitrosothiol conserved from bacteria to humans. *Nature* **410**, 490–494.

Liu S, Widom J, Kemp CW, Crews CM, Clardy J. 1998 Structure of human methionine aminopeptidase-2 complexed with fumagillin. *Science* **282**, 1324–1327.

Love RA, Parge HE, Wickersham JA, Hostomsky Z, Habuka N, Moomaw EW, Adachi T, Hostomska Z. 1996 The crystal structure of hepatitis C virus NS3 proteinase reveals a trypsin-like fold and a structural zinc binding site. *Cell* **87**, 331–342.

Lovejoy B, Cleasby A, Hassell AM, Longley K, Luther MA, Weigl D, McGeehan G, McElroy AB, Drewry D, Lambert MH, Jordan SR. 1994a Structure of the catalytic domain of fibroblast collagenase complexed with an inhibitor. *Science* **263**, 375–377.

Lovejoy B, Hassell AM, Luther MA, Weigl D, Jordan SR. 1994b Crystal structures of recombinant 19-kDa human fibroblast collagenase complexed to itself. *Biochemistry* **33**, 8207–8217.

Lovejoy B, Welch AR, Carr S, Luong C, Broka C, Hendricks RT, Campbell JA, Walker KA, Martin R, Van Wart H, Browner MF. 1999 Crystal structures of MMP-1 and -13 reveal the structural basis for selectivity of collagenase inhibitors. *Nat Struct Biol* **6**, 217–221.

Lowther WT, Zhang Y, Sampson PB, Honek JF, Matthews BW. 1999 Insights into the mechanism of *Escherichia coli* methionine aminopeptidase from the structural analysis of reaction products and phosphorus-based transition-state analogues. *Biochemistry* **38**, 14810–14819.

Mackay JP, Crossley M. 1998 Zinc fingers are sticking together. *Trends Biochem Sci* **23**, 1–4.

Mackereth CD, Arrowsmith CH, Edwards AM, McIntosh LP. 2000 Zinc-bundle structure of the essential RNA polymerase subunit RPB10 from *Methanobacterium thermoautotrophicum*. *Proc Natl Acad Sci USA* **97**, 6316–6321.

Mallis RJ, Poland BW, Chatterjee TK, Fisher RA, Darmawan S, Honzatko RB, Thomas JA. 2000 Crystal structure of S-glutathiolated carbonic anhydrase III. *FEBS Lett* **482**, 237–241.

Mandiyan V, Andreev J, Schlessinger J, Hubbard SR. 1999 Crystal structure of the ARF-GAP domain and ankyrin repeats of PYK2-associated protein beta. *EMBO J* **18**, 6890–6898.

Maret W. 1989 Cobalt(II)-substituted class III alcohol and sorbitol dehydrogenases from human liver. *Biochemistry* **28**, 9944–9949.

Maret W, Jacob C, Vallee BL, Fischer EH. 1999 Inhibitory sites in enzymes: zinc removal and reactivation by thionein. *Proc Natl Acad Sci USA* **96**, 1936–1940.

Maret W, Vallee BL. 1998 Thiolate ligands in metallothionein confer redox activity on zinc clusters. *Proc Natl Acad Sci USA* **95**, 3478–3482.

Maret W, Zeppezauer M. 1986 Influence of anions and pH on the conformational change of horse liver alcohol dehydrogenase induced by binding of oxidized nicotinamide adenine dinucleotide: binding of chloride to the catalytic metal ion. *Biochemistry* **25**, 1584–1588.

Mariani SM, Matiba B, Armandola EA, Krammer PH. 1997 Interleukin 1 beta-converting enzyme related proteases/caspases are involved in TRAIL-induced apoptosis of myeloma and leukemia cells. *J Cell Biol* **137**, 221–229.

Martinez-Yamout M, Legge GB, Zhang O, Wright PE, Dyson HJ. 2000 Solution structure of the cysteine-rich domain of the *Escherichia coli* chaperone protein DnaJ. *J Mol Biol* **300**, 805–818.

Maskos K, Fernandez-Catalan C, Huber R, Bourenkov GP, Bartunik H, Ellestad GA, Reddy P, Wolfson MF, Rauch CT, Castner BJ, Davis R, Clarke HR, Petersen M, Fitzner JN, Cerretti DP, March CJ, Paxton RJ, Black RA, Bode W. 1998 Crystal structure of the catalytic domain of human tumor necrosis factor-alpha-converting enzyme. *Proc Natl Acad Sci USA* **95**, 3408–3412.

Matthews BW. 1988 Structural basis of the action of thermolysin and related zinc proteases. *Acc Chem Res* **21**, 333–340.

Matthews BW, Weaver LH, Kester WR. 1974 The conformation of thermolysin. *J Biol Chem* **249**, 8030–8044.

Mechulam Y, Schmitt E, Maveyraud L, Zelwer C, Nureki O, Yokoyama S, Konno M, Blanquet S. 1999 Crystal structure of *Escherichia coli* methionyl-tRNA synthetase highlights species-specific features. *J Mol Biol* **294**, 1287–1297.

Medina JF, Wetterholm A, Radmark O, Shapiro R, Haeggstrom JZ, Vallee BL, Samuelsson B. 1991 Leukotriene A4 hydrolase: determination of the three zinc-binding ligands by site-directed

mutagenesis and zinc analysis. *Proc Natl Acad Sci USA* **88**, 7620–7624.

Meijers R, Morris RJ, Adolph HW, Merli A, Lamzin VS, Cedergren-Zeppezauer ES. 2001 On the enzymatic activation of NADH. *J Biol Chem* **276**, 9316–9321.

Meinnel T, Blanquet S, Dardel F. 1996 A new subclass of the zinc metalloproteases superfamily revealed by the solution structure of peptide deformylase. *J Mol Biol* **262**, 375–386.

Mitsuhashi S, Mizushima T, Yamashita E, Yamamoto M, Kumasaka T, Moriyama H, Ueki T, Miyachi S, Tsukihara T. 2000 X-ray structure of beta-carbonic anhydrase from the red alga, *Porphyridium purpureum*, reveals a novel catalytic site for CO(2) hydration. *J Biol Chem* **275**, 5521–5526.

Miyatake H, Hata Y, Fujii T, Hamada K, Morihara K, Katsube Y. 1995 Crystal structure of the unliganded alkaline protease from *Pseudomonas aeruginosa* IFO3080 and its conformational changes on ligand binding. *J Biochem (Tokyo)* **118**, 474–479.

Morgunova E, Tuuttila A, Bergmann U, Isupov M, Lindqvist Y, Schneider G, Tryggvason K. 1999 Structure of human pro-matrix metalloproteinase-2: activation mechanism revealed [see comments]. *Science* **284**, 1667–1670.

Mott HR, Carpenter JW, Zhong S, Ghosh S, Bell RM, Campbell SL. 1996 The solution structure of the Raf-1 cysteine-rich domain: a novel ras and phospholipid binding site. *Proc Natl Acad Sci USA* **93**, 8312–8317.

Moy FJ, Chanda PK, Chen JM, Cosmi S, Edris W, Skotnicki JS, Wilhelm J, Powers R. 1999 NMR solution structure of the catalytic fragment of human fibroblast collagenase complexed with a sulfonamide derivative of a hydroxamic acid compound. *Biochemistry* **38**, 7085–7096.

Moy FJ, Chanda PK, Cosmi S, Pisano MR, Urbano C, Wilhelm J, Powers R. 1998 High-resolution solution structure of the inhibitor-free catalytic fragment of human fibroblast collagenase determined by multidimensional NMR. *Biochemistry* **37**, 1495–1504.

Muchmore SW, Chen J, Jakob C, Zakula D, Matayoshi ED, Wu W, Zhang H, Li F, Ng SC, Altieri DC. 2000 Crystal structure and mutagenic analysis of the inhibitor-of-apoptosis protein survivin. *Mol Cell* **6**, 173–182.

Murphy JE, Stec B, Ma L, Kantrowitz ER. 1997 Trapping and visualization of a covalent enzyme-phosphate intermediate [letter]. *Nat Struct Biol* **4**, 618–622.

Myers LC, Cushing TD, Wagner G, Verdine GL. 1994 Metal-coordination sphere in the methylated Ada protein-DNA co-complex. *Chem Biol* **1**, 91–97.

Naylor CE, Jepson M, Crane DT, Titball RW, Miller J, Basak AK, Bolgiano B. 1999 Characterisation of the calcium-binding C-terminal domain of *Clostridium perfringens* alpha-toxin. *J Mol Biol* **294**, 757–770.

Nureki O, Vassylyev DG, Tateno M, Shimada A, Nakama T, Fukai S, Konno M, Hendrickson TL, Schimmel P, Yokoyama S. 1998 Enzyme structure with two catalytic sites for double-sieve selection of substrate [see comments]. *Science* **280**, 578–582.

Oefner C, D'Arcy A, Hennig M, Winkler FK, Dale GE. 2000 Structure of human neutral endopeptidase (Neprilysin) complexed with phosphoramidon. *J Mol Biol* **296**, 341–349.

Ogihara NL, Parge HE, Hart PJ, Weiss MS, Goto JJ, Crane BR, Tsang J, Slater K, Roe JA, Valentine JS, Eisenberg D, Tainer JA. 1996 Unusual trigonal-planar copper configuration revealed in the atomic structure of yeast copper-zinc superoxide dismutase. *Biochemistry* **35**, 2316–2321.

Pan H, Wigley DB. 2000 Structure of the zinc-binding domain of *Bacillus stearothermophilus* DNA primase. *Structure* **8**, 231–239.

Papageorgiou AC, Acharya KR. 1997 Superantigens as immunomodulators: recent structural insights. *Structure* **5**, 991–996.

Papageorgiou AC, Acharya KR, Shapiro R, Passalacqua EF, Brehm RD, Tranter HS. 1995 Crystal structure of the superantigen enterotoxin C2 from *Staphylococcus aureus* reveals a zinc-binding site. *Structure* **3**, 769–779.

Papageorgiou AC, Collins CM, Gutman DM, Kline JB, O'Brien SM, Tranter HS, Acharya KR. 1999 Structural basis for the recognition of superantigen streptococcal pyrogenic exotoxin A (SpeA1) by MHC class II molecules and T-cell receptors. *EMBO J* **18**, 9–21.

Parge HE, Hallewell RA, Tainer JA. 1992 Atomic structures of wild-type and thermostable mutant recombinant human Cu,Zn superoxide dismutase [published erratum appears in Proc Natl Acad Sci USA 1992 Nov 15; **89**(22):11106]. *Proc Nat Acad Sci USA* **89**, 6109–6113.

Park HW, Boduluri SR, Moomaw JF, Casey PJ, Beese LS. 1997 Crystal structure of protein farnesyltransferase at 2.25 angstrom resolution [see comments] [published erratum appears in Science 1997 Apr 4; **276**(5309):21]. *Science* **275**, 1800–1804.

Paul-Soto R, Bauer R, Frere JM, Galleni M, Meyer-Klaucke W, Nolting H, Rossolini GM, de Seny D, Hernandez-Valladares M, Zeppezauer M, Adolph HW. 1999 Mono- and binuclear Zn^{2+}-beta-lactamase. Role of the conserved cysteine in the catalytic mechanism. *J Biol Chem* **274**, 13242–13249.

Paul-Soto R, Hernandez-Valladares M, Galleni M, Bauer R, Zeppezauer M, Frere JM, Adolph HW. 1998 Mono- and binuclear Zn-beta-lactamase from *Bacteroides fragilis*: catalytic and structural roles of the zinc ions. *FEBS Lett* **438**, 137–140.

Pauptit RA, Karlsson R, Picot D, Jenkins JA, Niklaus-Reimer AS, Jansonius JN. 1988 Crystal structure of neutral protease from *Bacillus cereus* refined at 3.0 Å resolution and comparison with the homologous but more thermostable enzyme thermolysin. *J Mol Biol 199*, 525–537.

Perrier V, Burlacu-Miron S, Bourgeois S, Surewicz WK, Gilles AM. 1998 Genetically engineered zinc-chelating adenylate kinase from *Escherichia coli* with enhanced thermal stability. *J Biol Chem* **273**, 19097–19101.

Perrier V, Surewicz WK, Glaser P, Martineau L, Craescu CT, Fabian H, Mantsch HH, Barzu O, Gilles AM. 1994 Zinc chelation and structural stability of adenylate kinase from *Bacillus subtilis*. *Biochemistry* **33**, 9960–9967.

Pesce A, Battistoni A, Stroppolo ME, Polizio F, Nardini M, Kroll JS, Langford PR, O'Neill P, Sette M, Desideri A, Bolognesi M. 2000 Functional and Crystallographic Characterization of *Salmonella typhimurium* Cu,Zn Superoxide Dismutase Coded by the sodCI Virulence Gene. *J Mol Biol* **302**, 465–478.

Pesce A, Capasso C, Battistoni A, Folcarelli S, Rotilio G, Desideri A, Bolognesi M. 1997 Unique structural features of the monomeric Cu,Zn superoxide dismutase from *Escherichia coli*, revealed by X-ray crystallography. *J Mol Biol* **274**, 408–420.

Petersen JF, Cherney MM, Liebig HD, Skern T, Kuechler E, James MN. 1999 The structure of the 2A proteinase from a common cold virus: a proteinase responsible for the shut-off of host-cell protein synthesis. *EMBO J* **18**, 5463–5475.

Pieroni L, Santolini E, Fipaldini C, Pacini L, Migliaccio G, La Monica N. 1997 In vitro study of the NS2–3 protease of hepatitis C virus. *J Virol* **71**, 6373–6380.

Ploom T, Thony B, Yim J, Lee S, Nar H, Leimbacher W, Richardson J, Huber R, Auerbach G. 1999 Crystallographic and kinetic investigations on the mechanism of 6-pyruvoyl tetrahydropterin synthase. *J Mol Biol* **286**, 851–860.

Poland BW, Xu MQ, Quiocho FA. 2000 Structural insights into the protein splicing mechanism of PI-SceI. *J Biol Chem* **275**, 16408–16413.

Prasad GS, Radhakrishnan R, Mitchell DT, Earhart CA, Dinges MM, Cook WJ, Schlievert PM, Ohlendorf DH. 1997 Refined structures of three crystal forms of toxic shock syndrome toxin-1 and of a tetramutant with reduced activity. *Protein Sci* **6**, 1220–1227.

Proft T, Moffatt SL, Berkahn CJ, Fraser JD. 1999 Identification and characterization of novel superantigens from *Streptococcus pyogenes*. *J Exp Med* **189**, 89–102.

Quest AF, Bloomenthal J, Bardes ES, Bell RM. 1992 The regulatory domain of protein kinase C coordinates four atoms of zinc. *J Biol Chem* **267**, 10193–10197.

Quiocho FA, Lipscomb WN. 1971 Carboxypeptidase A: a protein and an enzyme. *Adv Protein Chem* **25**, 1–78.

Raaijmakers H, Vix O, Toro I, Golz S, Kemper B, Suck D. 1999 X-ray structure of T4 endonuclease VII: a DNA junction resolvase with a novel fold and unusual domain-swapped dimer architecture. *EMBO J* **18**, 1447–1458.

Radhakrishnan R, Walter LJ, Hruza A, Reichert P, Trotta PP, Nagabhushan TL, Walter MR. 1996 Zinc mediated dimer of human interferon-alpha 2b revealed by X-ray crystallography. *Structure* **4**, 1453–1463.

Raman CS, Li H, Martasek P, Kral V, Masters BS, Poulos TL. 1998 Crystal structure of constitutive endothelial nitric oxide synthase: a paradigm for pterin function involving a novel metal center. *Cell* **95**, 939–950.

Ramaswamy S, el Ahmad M, Danielsson O, Jornvall H, Eklund H. 1996 Crystal structure of cod liver class I alcohol dehydrogenase: substrate pocket and structurally variable segments. *Protein Sci* **5**, 663–671.

Redlich PN, Grossberg SE. 1990 Immunochemical characterization of antigenic domains on human interferon-beta: spatially distinct epitopes are associated with both antiviral and antiproliferative activities. *Eur J Immunol* **20**, 1933–1939.

Rees DC, Lewis M, Lipscomb WN. 1983 Refined crystal structure of carboxypeptidase A at 1.54 Å resolution. *J Mol Biol* **168**, 367–387.

Reverter D, Fernandez-Catalan C, Baumgartner R, Pfander R, Huber R, Bode W, Vendrell J, Holak TA, Aviles FX. 2000 Structure of a novel leech carboxypeptidase inhibitor determined free in solution and in complex with human carboxypeptidase A2. *Nat Struct Biol* **7**, 322–328.

Ridderstrom M, Cameron AD, Jones TA, Mannervik B. 1998 Involvement of an active-site Zn^{2+} ligand in the catalytic mechanism of human glyoxalase I. *J Biol Chem* **273**, 21623–21628.

Riordan JF. 1974 Metal-containing exopeptidases. In: Whitaker JR, ed. *Food Related Enzymes*. Vol. 136. Washington DC: American Chemical Society; 220–240.

Roderick SL, Matthews BW. 1993 Structure of the cobalt-dependent methionine aminopeptidase from *Escherichia coli*: a new type of proteolytic enzyme. *Biochemistry* **32**, 3907–3912.

Roussel A, Anderson BF, Baker HM, Fraser JD, Baker EN. 1997 Crystal structure of the streptococcal superantigen SPE-C: dimerization and zinc binding suggest a novel mode of interaction with MHC class II molecules. *Nat Struct Biol* **4**, 635–643.

Rowlett RS, Chance MR, Wirt MD, Sidelinger DE, Royal JR, Woodroffe M, Wang YF, Saha RP, Lam MG. 1994 Kinetic and structural characterization of spinach carbonic anhydrase. *Biochemistry* **33**, 13967–13976.

Rowsell S, Pauptit RA, Tucker AD, Melton RG, Blow DM, Brick P. 1997 Crystal structure of carboxypeptidase G2, a bacterial enzyme with applications in cancer therapy. *Structure* **5**, 337–347.

Ryde U. 1995 On the role of Glu-68 in alcohol dehydrogenase. *Protein Sci* **4**, 1124–1132.

Sang QA, Douglas DA. 1996 Computational sequence analysis of matrix metalloproteinases. *J Protein Chem* **15**, 137–160.

Sankaranarayanan R, Dock-Bregeon AC, Rees B, Bovee M, Caillet J, Romby P, Francklyn CS, Moras D. 2000 Zinc ion mediated amino acid discrimination by threonyl-tRNA synthetase [see comments]. *Nat Struct Biol* **7**, 461–465.

Sankaranarayanan R, Dock-Bregeon AC, Romby P, Caillet J, Springer M, Rees B, Ehresmann C, Ehresmann B, Moras D. 1999 The structure of threonyl-tRNA synthetase-tRNA(Thr) complex enlightens its repressor activity and reveals an essential zinc ion in the active site. *Cell* **97**, 371–381.

Schad EM, Papageorgiou AC, Svensson LA, Acharya KR. 1997 A structural and functional comparison of staphylococcal enterotoxins A and C2 reveals remarkable similarity and dissimilarity. *J Mol Biol* **269**, 270–280.

Schad EM, Zaitseva I, Zaitsev VN, Dohlsten M, Kalland T, Schlievert PM, Ohlendorf DH, Svensson LA. 1995 Crystal structure of the superantigen staphylococcal enterotoxin type A. *EMBO J* **14**, 3292–3301.

Schlagenhauf E, Etges R, Metcalf P. 1998 The crystal structure of the *Leishmania major* surface proteinase leishmanolysin (gp63). *Structure* **6**, 1035–1046.

Schmid MF, Herriott JR. 1976 Structure of carboxypeptidase B at 2–8 Å resolution. *J Mol Biol* **103**, 175–190.

Sellin S, Eriksson LE, Aronsson AC, Mannervik B. 1983 Octahedral metal coordination in the active site of glyoxalase I as evidenced by the properties of Co(II)-glyoxalase I. *J Biol Chem* **258**, 2091–2093.

Sellin S, Mannervik B. 1984 Metal dissociation constants for glyoxalase I reconstituted with Zn^{2+}, Co^{2+}, Mn^{2+}, and Mg^{2+}. *J Biol Chem* **259**, 11426–11429.

Sideraki V, Mohamedali KA, Wilson DK, Chang Z, Kellems RE, Quiocho FA, Rudolph FB. 1996 Probing the functional role of two conserved active site aspartates in mouse adenosine deaminase. *Biochemistry* **35**, 7862–7872.

Silverman DN, Lindskog S. 1988 The catalytic mechanism of carbonic anhydrase: Implications of a rate limiting protolysis of water. *Acc Chem Res* **21**, 30–36.

Silvian LF, Wang J, Steitz TA. 1999 Insights into editing from an ile-tRNA synthetase structure with tRNAile and mupirocin. *Science* **285**, 1074–1077.

Simons TJ. 1995 The affinity of human erythrocyte porphobilinogen synthase for Zn^{2+} and Pb^{2+}. *Eur J Biochem* **234**, 178–183.

Smith KS, Ferry JG. 2000 Prokaryotic carbonic anhydrases. *FEMS Microbiol Rev* **24**, 335–366.

Soler D, Nomizu T, Brown WE, Chen M, Ye QZ, Van Wart HE, Auld DS. 1994 Zinc content of promatrilysin, matrilysin and the stromelysin catalytic domain. *Biochem Biophys Res Commun* **201**, 917–923.

Soler D, Nomizu T, Brown WE, Shibata Y, Auld DS. 1995 Matrilysin: expression, purification, and characterization. *J Protein Chem* **14**, 511–520.

Somers W, Ultsch M, De Vos AM, Kossiakoff AA. 1994 The X-ray structure of a growth hormone-prolactin receptor complex [see comments]. *Nature* **372**, 478–481.

Springman EB, Angleton EL, Birkedal-Hansen H, Van Wart HE. 1990 Multiple modes of activation of latent human fibroblast collagenase: evidence for the role of a Cys73 active-site zinc complex in latency and a 'cysteine switch' mechanism for activation. *Proc Natl Acad Sci USA* **87**, 364–368.

Stamler JS. 1994 Redox signaling: nitrosylation and related target interactions of nitric oxide. *Cell* **78**, 931–936.

Stams T, Chen Y, Boriack-Sjodin PA, Hurt JD, Liao J, May JA, Dean T, Laipis P, Silverman DN, Christianson DW. 1998 Structures of murine carbonic anhydrase IV and human carbonic anhydrase II complexed with brinzolamide: molecular basis of isozyme-drug discrimination. *Protein Sci* **7**, 556–563.

Stams T, Nair SK, Okuyama T, Waheed A, Sly WS, Christianson DW. 1996 Crystal structure of the secretory form of membrane-associated human carbonic anhydrase IV at 2.8-Å resolution. *Proc Natl Acad Sci USA* **93**, 13589–13594.

Stec B, Hehir MJ, Brennan C, Nolte M, Kantrowitz ER. 1998 Kinetic and X-ray structural studies of three mutant *E. coli* alkaline phosphatases: insights into the catalytic mechanism without the nucleophile Ser102. *J Mol Biol* **277**, 647-662.

Stec B, Holtz KM, Kantrowitz ER. 2000 A revised mechanism for the alkaline phosphatase reaction involving three metal ions. *J Mol Biol* **299**, 1303–1311.

Stocker W, Ng M, Auld DS. 1990 Fluorescent oligopeptide substrates for kinetic characterization of the specificity of Astacus protease. *Biochemistry* **29**, 10418–10425.

Stocker W, Wolz RL, Zwilling R, Strydom DJ, Auld DS. 1988 Astacus protease, a zinc metalloenzyme. *Biochemistry* **27**, 5026–5032.

Strater N, Klabunde T, Tucker P, Witzel H, Krebs B. 1995 Crystal structure of a purple acid phosphatase containing a dinuclear Fe(III)-Zn(II) active site. *Science* **268**, 1489–1492.

Strater N, Lipscomb WN. 1995 Transition state analogue L-leucinephosphonic acid bound to bovine lens leucine aminopeptidase: X-ray structure at 1.65 Å resolution in a new crystal form. *Biochemistry* **34**, 9200–9210.

Strickland CL, Windsor WT, Syto R, Wang L, Bond R, Wu Z, Schwartz J, Le HV, Beese LS, Weber PC. 1998 Crystal structure of farnesyl protein transferase complexed with a CaaX peptide and farnesyl diphosphate analogue. *Biochemistry* **37**, 16601–16611.

Strop P, Smith KS, Iverson TM, Ferry JG, Rees DC. 2001 Crystal structure of the 'cab type' beta class carbonic anhydrase from the archaeon *Methanobacterium thermoautotrophicum. J Biol Chem* **276**, 10299–10305.

Sugahara M, Mikawa T, Kumasaka T, Yamamoto M, Kato R, Fukuyama K, Inoue Y, Kuramitsu S. 2000 Crystal structure of a repair enzyme of oxidatively damaged DNA, MutM (Fpg), from an extreme thermophile, *Thermus thermophilus* HB8. *EMBO J* **19**, 3857–3869.

Sugiura I, Nureki O, Ugaji-Yoshikawa Y, Kuwabara S, Shimada A, Tateno M, Lorber B, Giege R, Moras D, Yokoyama S, Konno M. 2000 The 2.0 Å crystal structure of *Thermus thermophilus* methionyl-tRNA synthetase reveals two RNA-binding modules. *Structure Fold Des* **8**, 197–208.

Sundstrom M, Abrahmsen L, Antonsson P, Mehindate K, Mourad W, Dohlsten M. 1996a The crystal structure of staphylococcal enterotoxin type D reveals Zn^{2+}-mediated homodimerization. *EMBO J* **15**, 6832–6840.

Sundstrom M, Hallen D, Svensson A, Schad E, Dohlsten M, Abrahmsen L. 1996b The Co-crystal structure of staphylococcal enterotoxin type A with Zn^{2+} at 2.7 Å resolution. Implications for major histocompatibility complex class II binding. *J Biol Chem* **271**, 32212–32216.

Svensson S, Hoog JO, Schneider G, Sandalova T. 2000 Crystal Structures of mouse class II alcohol dehydrogenase reveal determinants of substrate specificity and catalytic efficiency. *J Mol Biol* **302**, 441–453.

Swaminathan S, Eswaramoorthy S. 2000 Structural analysis of the catalytic and binding sites of *Clostridium botulinum* neurotoxin B [see comments]. *Nat Struct Biol* **7**, 693–699.

Tahirov TH, Oki H, Tsukihara T, Ogasahara K, Yutani K, Libeu CP, Izu Y, Tsunasawa S, Kato I. 1998a High-resolution crystals of methionine aminopeptidase from *Pyrococcus furiosus* obtained by water-mediated transformation. *J Struct Biol* **121**, 68–72.

Tahirov TH, Oki H, Tsukihara T, Ogasahara K, Yutani K, Ogata K, Izu Y, Tsunasawa S, Kato I. 1998b Crystal structure of methionine aminopeptidase from hyperthermophile, *Pyrococcus furiosus. J Mol Biol* **284**, 101–124.

Tainer JA, Getzoff ED, Beem KM, Richardson JS, Richardson DC. 1982 Determination and analysis of the 2 Å-structure of copper, zinc superoxide dismutase. *J Mol Biol* **160**, 181–217.

Taylor A. 1993 Aminopeptidases: structure and function. *FASEB J* **7**, 290–298.

Teplyakov A, Polyakov K, Obmolova G, Strokopytov B, Kuranova I, Osterman A, Grishin N, Smulevitch S, Zagnitko O, Galperina O, Matz M, Stepanov V. 1992 Crystal structure of carboxypeptidase T from *Thermoactinomyces vulgaris. Eur J Biochem* **208**, 281–288.

Thayer MM, Flaherty KM, McKay DB. 1991 Three–dimensional structure of the elastase of *Pseudomonas aeruginosa* at 1.5-Å resolution. *J Biol Chem* **266**, 2864–2871.

Thoden JB, Ruzicka FJ, Frey PA, Rayment I, Holden HM. 1997 Structural analysis of the H166G site-directed mutant of galactose-1-phosphate uridylyltransferase complexed with either UDP-glucose or UDP-galactose: detailed description of the nucleotide sugar binding site. *Biochemistry* **36**, 1212–1222.

Thunnissen MM, Nordlund P, Haeggstrom JZ. 2001 Crystal structure of human leukotriene A(4) hydrolase, a bifunctional enzyme in inflammation. *Nat Struct Biol* **8**, 131–135.

Tsutakawa SE, Muto T, Kawate T, Jingami H, Kunishima N, Ariyoshi M, Kohda D, Nakagawa M, Morikawa K. 1999 Crystallographic and functional studies of very short patch repair endonuclease. *Mol Cell* **3**, 621–628.

Ullah JH, Walsh TR, Taylor IA, Emery DC, Verma CS, Gamblin SJ, Spencer J. 1998 The crystal structure of the L1 metallo–beta–lactamase from *Stenotrophomonas maltophilia* at 1.7 Å resolution. *J Mol Biol* **284**, 125–136.

Uppenberg J, Lindqvist F, Svensson C, Ek–Rylander B, Andersson G. 1999 Crystal structure of a mammalian purple acid phosphatase. *J Mol Biol* **290**, 201–211.

Urbani A, Bazzo R, Nardi MC, Cicero DO, De Francesco R, Steinkuhler C, Barbato G. 1998 The metal binding site of the hepatitis C virus NS3 protease. A spectroscopic investigation. *J Biol Chem* **273**, 18760–18769.

Vallee BL, Auld DS. 1990a Active-site zinc ligands and activated H_2O of zinc enzymes. *Proc Natl Acad Sci USA* **87**, 220–224.

Vallee BL, Auld DS. 1990b Zinc coordination, function, and structure of zinc enzymes and other proteins. *Biochemistry* **29**, 5647–5659.

Vallee BL, Auld DS. 1992a Active zinc binding sites of zinc metalloenzymes. *Matrix Suppl* **1**, 5–19.

Vallee BL, Auld DS. 1992b Functional zinc-binding motifs in enzymes and DNA-binding proteins. *Faraday Discuss* **93**, 47–65.

Vallee BL, Auld DS. 1993a New perspective on zinc biochemistry: cocatalytic sites in multi-zinc enzymes. *Biochemistry* **32**, 6493–6500.

Vallee BL, Auld DS. 1993b Zinc: Biological Functions and Coordination Motifs. *Acc Chem Res* **26**, 543–551.

Vallee BL, Coleman JE, Auld DS. 1991 Zinc fingers, zinc clusters, and zinc twists in DNA-binding protein domains. *Proc Natl Acad Sci USA* **88**, 999–1003.

Vallee BL, Falchuk KH. 1993 The biochemical basis of zinc physiology. *Physiol Rev* **73**, 79–118.

Vallee BL, Galdes A. 1984 The metallobiochemistry of zinc enzymes. *Adv Enzymol Relat Areas Mol Biol* **56**, 283–430.

Van Doren SR, Kurochkin AV, Hu W, Ye QZ, Johnson LL, Hupe DJ, Zuiderweg ER. 1995 Solution structure of the catalytic domain of human stromelysin complexed with a hydrophobic inhibitor. *Protein Sci* **4**, 2487–2498.

Vanhooke JL, Benning MM, Raushel FM, Holden HM. 1996 Three-dimensional structure of the zinc-containing phosphotriesterase with the bound substrate analog diethyl 4-methylbenzylphosphonate. *Biochemistry* **35**, 6020–6025.

Verdecia MA, Huang H, Dutil E, Kaiser DA, Hunter T, Noel JP. 2000 Structure of the human anti-apoptotic protein survivin reveals a dimeric arrangement [see comments]. *Nat Struct Biol* **7**, 602–608.

Volbeda A, Lahm A, Sakiyama F, Suck D. 1991 Crystal structure of *Penicillium citrinum* P1 nuclease at 2.8 Å resolution. *EMBO J* **10**, 1607–1618.

Walker KW, Bradshaw RA. 1998 Yeast methionine aminopeptidase I can utilize either Zn^{2+} or Co^{2+} as a cofactor: a case of mistaken identity? *Protein Sci* **7**, 2684–2687.

Wang B, Jones DN, Kaine BP, Weiss MA. 1998 High-resolution structure of an archaeal zinc ribbon defines a general architectural motif in eukaryotic RNA polymerases. *Structure* **6**, 555–569.

Wang Z, Quiocho FA. 1998 Complexes of adenosine deaminase with two potent inhibitors: X-ray structures in four independent molecules at pH of maximum activity. *Biochemistry* **37**, 8314–8324.

Whitlow M, Howard AJ, Finzel BC, Poulos TL, Winborne E, Gilliland GL. 1991 A metal-mediated hydride shift mechanism for xylose isomerase based on the 1.6 Å *Streptomyces rubiginosus* structures with xylitol and D-Xylose. *Proteins Struc Funct Genet* **9**, 153–173.

Wilson DK, Quiocho FA. 1993 A pre-transition-state mimic of an enzyme: X-ray structure of adenosine deaminase with bound 1-deazaadenosine and zinc-activated water. *Biochemistry* **32**, 1689–1694.

Wilson DK, Rudolph FB, Quiocho FA. 1991 Atomic structure of adenosine deaminase complexed with a transition-state analog: understanding catalysis and immunodeficiency mutations. *Science* **252**, 1278–1284.

Wimberly BT, Brodersen DE, Clemons WM, Jr., Morgan-Warren RJ, Carter AP, Vonrhein C, Hartsch T, Ramakrishnan V. 2000 Structure of the 30S ribosomal subunit [see comments]. *Nature* **407**, 327–339.

Xiang S, Short SA, Wolfenden R, Carter CW, Jr. 1995 Transition-state selectivity for a single hydroxyl group during catalysis by cytidine deaminase. *Biochemistry* **34**, 4516–4523.

Xie P, Parsons SH, Speckhard DC, Bosron WF, Hurley TD. 1997 X-ray structure of human class IV sigmasigma alcohol dehydrogenase. Structural basis for substrate specificity. *J Biol Chem* **272**, 18558–18563.

Yan Y, Li Y, Munshi S, Sardana V, Cole JL, Sardana M, Steinkuehler C, Tomei L, De Francesco R, Kuo LC, Chen Z. 1998 Complex of NS3 protease and NS4A peptide of BK strain hepatitis C virus: a 2.2 Å resolution structure in a hexagonal crystal form. *Protein Sci* **7**, 837–847.

Yang Y, Keeney D, Tang X, Canfield N, Rasmussen BA. 1999 Kinetic properties and metal content of the metallo-beta-lactamase CcrA harboring selective amino acid substitutions. *J Biol Chem* **274**, 15706–15711.

Yang ZN, Bosron WF, Hurley TD. 1997 Structure of human chi chi alcohol dehydrogenase: a glutathione-dependent formaldehyde dehydrogenase. *J Mol Biol* **265**, 330–343.

Yano JK, Koo LS, Schuller DJ, Li H, Ortiz De Montellano PR, Poulos TL. 2000 Crystal structure of a thermophilic cytochrome P450 from the archaeon *sulfolobus solfataricus*. *J Biol Chem* **275**, 31086–31092.

Yaremchuk A, Cusack S, Tukalo M. 2000 Crystal structure of a eukaryote/archaeon-like prolyl-tRNA synthetase and its complex with tRNA(Pro)(CGG). *EMBO J* **19**, 4745–4758.

Zhang FL, Casey PJ. 1996 Protein prenylation: molecular mechanisms and functional consequences. *Ann Rev Biochem* **65**, 241–269.

Zhang G, Campbell EA, Minakhin L, Richter C, Severinov K, Darst SA. 1999 Crystal structure of *Thermus aquaticus* core RNA polymerase at 3.3 Å resolution [see comments]. *Cell* **98**, 811–824.

Zhang G, Kazanietz MG, Blumberg PM, Hurley JH. 1995 Crystal structure of the cys2 activator-binding domain of protein kinase C delta in complex with phorbol ester. *Cell* **81**, 917–924.

Zhang H, Seabra MC, Deisenhofer J. 2000 Crystal structure of Rab geranylgeranyltransferase at 2.0 Å resolution. *Structure* **8**, 241–251.

Zhu X, Teng M, Niu L. 1999 Structure of acutolysin-C, a haemorrhagic toxin from the venom of *Agkistrodon acutus*, providing further evidence for the mechanism of the pH-dependent proteolytic reaction of zinc metalloproteinases. *Acta Crystallogr D Biol Cryst* **55**, 1834–1841.